ALLIGATOR RIVERS ANALOGUE PROJECT

FINAL REPORT

VOLUME 2

GEOLOGIC SETTING

A. A. Snelling[1]

[1]Consultant Geologist,
P.O. Box 302, Sunnybank, Qld, 4109, Australia

ALLIGATOR RIVERS ANALOGUE PROJECT

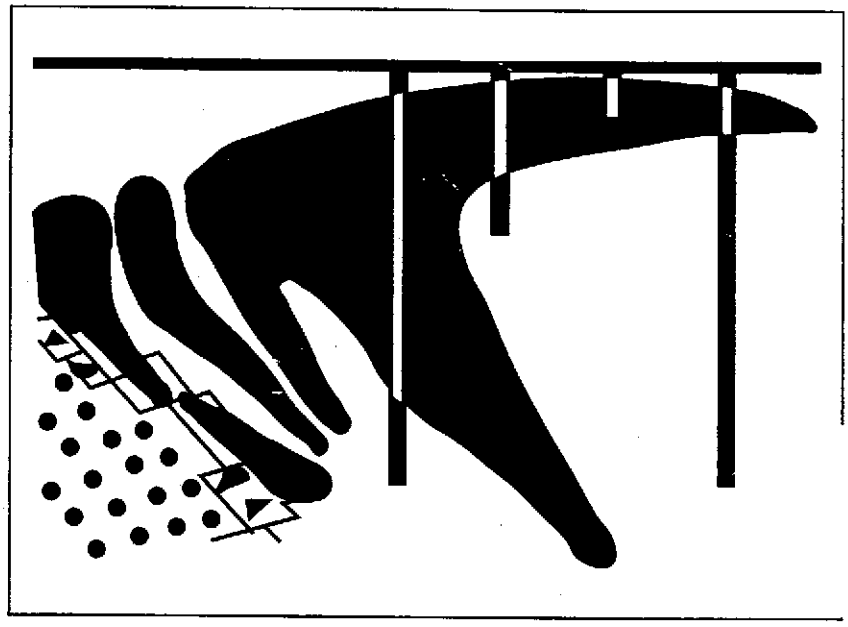

ISBN 0-642-59928-9

DOE/HMIP/RR/92/072

SKI TR 92:20-2 cy.1

FINAL REPORT
VOLUME 2

GEOLOGIC SETTING

1992

AN OECD/NEA INTERNATIONAL PROJECT MANAGED BY:
AUSTRALIAN NUCLEAR SCIENCE AND TECHNOLOGY ORGANISATION

PREFACE

The Koongarra uranium ore deposit is located in the Alligator Rivers Region of the Northern Territory of Australia. Many of the processes that have controlled the development of this natural system are relevant to the performance assessment of radioactive waste repositories. An Agreement was reached in 1987 by a number of agencies concerned with radioactive waste disposal, to set up the International Alligator Rivers Analogue Project (ARAP) to study relevant aspects of the hydrological and geochemical evolution of the site. The Project ran for five years.

The work was undertaken by ARAP through an Agreement sponsored by the OECD Nuclear Energy Agency (NEA). The Agreement was signed by the following organisations: the Australian Nuclear Science and Technology Organisation (ANSTO); the Japan Atomic Energy Research Institute (JAERI); the Power Reactor and Nuclear Fuel Development Corporation of Japan (PNC); the Swedish Nuclear Power Inspectorate (SKI); the UK Department of the Environment (UKDoE); and the US Nuclear Regulatory Commission (USNRC). ANSTO was the managing participant.

This report is one of a series of 16 describing the work of the Project; these are listed below:

No.	Title	Lead Author(s)
1	Summary of Findings	P Duerden, D A Lever, D A Sverjensky and L R Townley
2	Geologic Setting	A A Snelling
3	Geomorphology and Paleoclimatic History	K-H Wyrwoll
4	Geophysics, Petrophysics and Structure	D W Emerson
5	Hydrogeological Field Studies	S N Davis
6	Hydrogeological Modelling	L R Townley
7	Groundwater Chemistry	T E Payne
8	Chemistry and Mineralogy of Rocks and Soils	R Edis
9	Weathering and its Effects on Uranium Redistribution	T Murakami
10	Geochemical Data Bases	D G Bennett and D Read
11	Geochemical Modelling of Secondary Uranium Ore Formation	D A Sverjensky
12	Geochemical Modelling of Present-day Groundwaters	D A Sverjensky
13	Uranium Sorption	T D Waite
14	Radionuclide Transport	C Golian and D A Lever,
15	Geochemistry of ^{239}Pu, ^{129}I, ^{99}Tc and ^{36}Cl	J T Fabryka-Martin
16	Scenarios	K Skagius and S Wingefors

CONTENTS

EXECUTIVE SUMMARY

The Koongarra uranium deposit is 225 km east of Darwin, capital city of the Northern Territory, Australia, in the area known as the Alligator Rivers Region. It is one of four major uranium deposits discovered in the region.

In 1981 the US Nuclear Regulatory Commission (USNRC) began to sponsor research by the Australian Nuclear Science and Technology Organisation (ANSTO, then called the Australian Atomic Energy Commission) on aspects of all four uranium deposits in the region as natural analogues of radioactive waste repositories. As the USNRC-funded project progressed, efforts became almost entirely directed towards study of the Koongarra deposit, both because it has not yet been mined and so the ore is still in place, and because its No. 1 orebody comprises well-defined zones of primary, weathered primary and dispersion fan ore. Furthermore, results of extensive investigations by the mining companies, including hydrological data, and all the drill cores and samples, plus numerous vertical boreholes in and around the deposit, were also available. Thus the internationally sponsored Alligator Rivers Analogue Project (ARAP) focussed research on the dispersal of uranium from the weathered primary ore in the weathered rock zone to form the dispersion fan ore as the natural analogue most suitable for validation of models for radionuclide transport.

Discovered in July 1970, the Koongarra deposit was delineated by diamond and rotary percussion drilling between 1970 and 1973 and concluded to consist of two orebodies, designated as the Koongarra No. 1 and No. 2 orebodies. The host rocks to the mineralisation are schists of the Cahill Formation, rocks that were once shales and siltstones deposited on the flanks of domes of older crystalline granitic rocks (the Nanambu Complex) about 2200 million years ago. Multiple severe folding accompanied the 550°–630°C heat and 5-8 kb pressure of metamorphism between 1870 and 1800 million years ago. Subsequent uplift, weathering and erosion produced a new land surface on which thick layers of sandstone (the Kombolgie Formation) were then deposited probably between 1690 and 1600 million years ago. At Koongarra the host Cahill schists which dip at 55° to the south-east are now in reverse faulted contact with the younger Kombolgie sandstone, which is below the schists.

The uranium mineralisation consists of uraninite veins and veinlets in crosscutting fractures and brecciated zones within a 50 m thick quartz-chlorite schist unit. Associated with the ore are minor volumes of sulfides, which include galena, chalcopyrite, bornite and pyrite, with rare grains of gold, clausthalite, gersdorffite-cobaltite and mackinawite. The orebodies consist of partially coalescing lenses that are elongated and dip at 55° broadly parallel to the reverse fault breccia which forms the footwall to the ore zone. The strongest mineralisation with grades in excess of 1%U over several metres are just below a distinctive sheared graphite-quartz-chlorite schist unit that forms the hanging wall to the ore.

The No. 1 orebody is elongated over a distance of 450 m and persists to a depth of about 100 m. The width of the primary ore averages 30 m at the top of the

unweathered schist, tapering out at the extremities. Secondary uranium mineralisation in the weathered schist zone, derived from decomposition and leaching of former primary ore, is present from the surface down to the base of weathering at 25-30 m, and consists of uranyl phosphate minerals, primarily saleeite. A tongue-like body of ore in the weathered schist has formed by the dispersion of uranium down-slope for about 80 m to the south-east — the dispersion fan ore.

A distinct and extensive primary hydrothermal alteration halo has been observed about the mineralisation extending for up to 1.5 km from the ore. Uranium mineralisation is only present within the inner halo which extends to nearly 50 m from ore, and in which pervasive chlorite-dominant replacement of the schist fabric and removal of quartz has occurred. Consequently, chlorite (magnesium-rich) is the principal gangue mineral. The bulk rock geochemistry reflects this alteration and is characterised by magnesium enrichment and silicon depletion. The primary ore is enriched in copper, lead, sulfur, arsenic and vanadium, while nickel and cobalt form an enrichment halo about the deposit.

The Sm-Nd isotopic data on uraninite suggests a 1650–1550 million year age for the primary ore, consistent with the observation that the mineralisation occupies the breccia zones generated by the post-Kombolgie reverse faulting. However, the secondary ore in the weathered zone appears to only have formed in the last 3 million years or less.

The Koongarra deposit today is covered by sandstone debris talus and eluvial sand, broken and washed down from an escarpment of Kombolgie sandstone just behind the deposit. Beneath these surficial deposits is the weathered schist zone which is separated from the unweathered schists beneath by a transitional zone. The natural analogue that was the focus of ARAP is the formation of the dispersion fan from the weathered primary ore in the weathered schist.

The Koongarra mine reference grid coupled with elevations referenced to Australian Height Datum was used to locate all samples collected and analysed during ARAP. Core and crushed core samples were selected from the inclined diamond drill holes that were drilled on cross-sections 30.5 metres apart through the No.1 orebody. At the south-western end of the orebody particularly and beyond, vertical percussion holes also provided drill chips for study. All company records on the holes, including assay and geological data, were made available to the research effort. Some 32 of the vertical percussion holes were still open, allowing water sampling equipment to be lowered to desired depths and measurements of standing water levels. Additional monitoring holes for strategic samples and water sampling holes were also drilled by ARAP to fill in gaps in the sampling pattern and ensure a good coverage of the weathered schist zone, the site of the natural analogue. Subsequent volumes in this series report on the analytical and modelling results obtained from the large number of rock and water samples collected and various measurements made on samples, down holes and across the site.

ACKNOWLEDGMENTS

Without the full support and cooperation of Koongarra Mines Pty Ltd and its parent company Denison Australia Pty Ltd this internationally sponsored Alligator Rivers Analogue Project (ARAP) would not have been possible. The companies greatly encouraged the success of the research effort by giving full access to the Koongarra site and all the drill core and drill hole samples, plus providing their camp facilities for accommodation during field work. I am personally indebted to Denison and its staff for their allowing me to work on their behalf with the ARAP team. Their trust in me is greatly appreciated.

The financial support of the sponsors is of course acknowledged.

I have appreciated, and benefitted from, the interaction with the many other scientists participating in the project. I trust that they have learnt as much from me as I have learnt from each of them. In particular, I would acknowledge the contribution made by Geoff Prowse, formerly with the NT Power and Water Authority, to our understanding of the regional geologic setting. And of course, the strong leadership of Peter Duerden, ANSTO's ARAP Manager, in holding the research team together and firmly guiding our efforts, must also be acknowledged.

In my own office I have had the full support of my colleagues and staff. In particular, I wish to acknowledge my secretary Laurel Hemmings whose help and support has been invaluable, and many of the figures in this volume were drafted by Cathy Christiansen.

Finally, what appears in this volume is really a synthesis of the work of the many who have investigated the Koongarra area and its regional geologic setting over more than 20 years. Their contribution can be seen in the frequent references to their work, including their time framework for the geologic development of the area.

1 INTRODUCTION

1.1 The Locational Setting

The Koongarra uranium deposit lies 225 km east of the city of Darwin and 25 km south of the town of Jabiru at latitude 12°52'S, longitude 123°50'E in the Northern Territory of Australia (Figure 1.1). The geographical and geological area is known as the Alligator Rivers Region due to its being drained, and geographically dominated, by two major river systems — the South Alligator and East Alligator Rivers. The headwaters of these river systems are in the Arnhem Land Plateau, a rugged, elevated sandstone plateau which is deeply dissected by fractures and faults, and bounded by spectacular vertical cliffs or escarpments.

Koongarra is one of four major uranium deposits so far discovered in the region (Figure 1.1). The smallest deposit, Nabarlek, which had the highest ore grades, is now mined out, while Ranger with its two proven orebodies is currently a fully operational mining project. Both Jabiluka, the largest of the four deposits, and Koongarra, ranked third, are still undeveloped awaiting Australian Government approval. The four deposits are situated either in valleys between eroded outliers of the Arnhem Land Plateau or on the edges of the lowland floodplains in the lower reaches of the major river systems, but are all adjacent to prominent sandstone escarpments (Figure 1.1). Koongarra, for example, lies in the valley between the main Arnhem Land Plateau and the Mt Brockman Massif outlier adjacent to the escarpment, the position of which along the south-eastern margin of Mt Brockman is controlled by a prominent fault. The Koongarra area is within the Alligator River 1:250000 (SD 53–1) and Cahill 1:100000 (5472) map sheets.

Reserves in the Koongarra No. 1 orebody currently stand at 3.453 Mt of ore grading 0.44% U_3O_8 at a cutoff of 0.02% U_3O_8. Most of the uranium (94% of the mineralisation) is contained in 1.831 Mt of high grade ore, which averages 0.795% U_3O_8 (cutoff grade 0.09% U_3O_8).

1.2 Uranium Orebodies as Natural Analogues

A major problem confronting the nuclear industry with the safe disposal of radioactive waste is to be able to predict before the waste is buried how the contained radionuclides will behave/migrate in the surrounding natural environment in the long term. A useful approach is to study the cumulative effect of radionuclide transport over geological time on systems which are acceptable analogues of radioactive waste repositories (Birchard and Alexander, 1983). Although no single system can adequately reflect all the relevant properties down-gradient of a repository, well-chosen analogues have features which can contribute to the basis of long-term prediction. Chapman, McKinley and Smellie (1984), and Airey and Ivanovich (1986) deal with these issues and provide examples of useful natural analogues.

Amongst the suitable natural analogues, uranium orebodies provide the opportunity

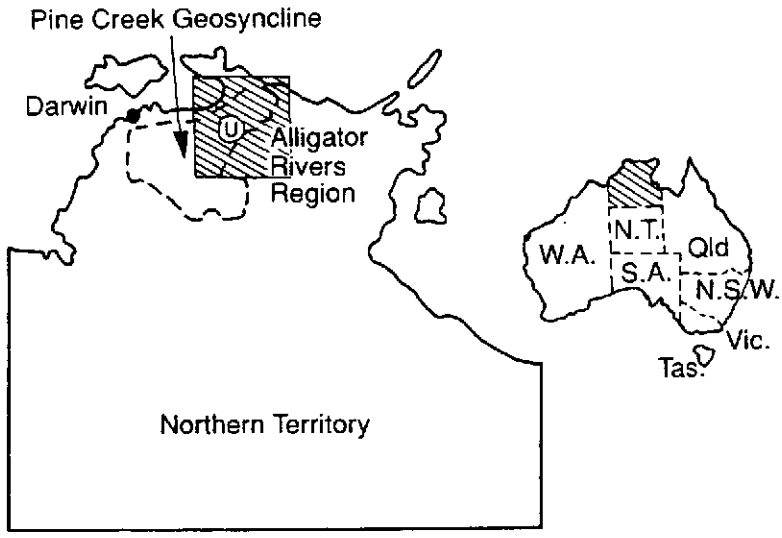

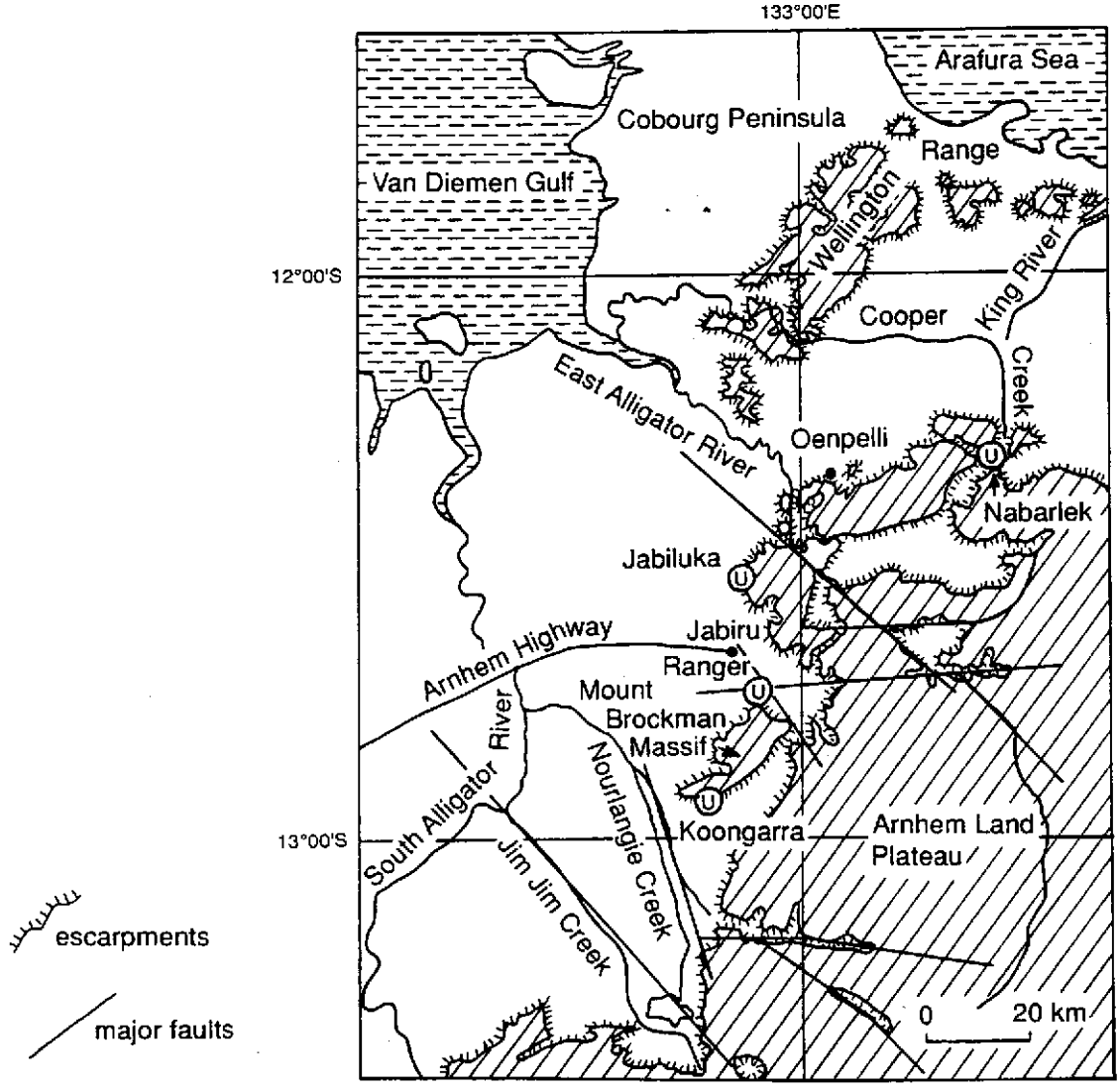

Figure 1.1 Location map showing the four uranium deposits of the Alligator Rivers Region, the sandstone escarpments and major faults. (Adapted from Needham and Stuart-Smith, 1976.)

for direct measurement of the migration of relevant radionuclides that has occurred over geological time, thus enabling the reduction of uncertainties in the prediction of long-term transport of these radionuclides. Uranium orebodies contain a wide range of radionuclides and heavy metals of direct interest, including actinides, radium isotopes, lead isotopes and rare earth elements, as well as ultra-low levels of significant transuranic elements (^{239}Pu, ^{237}Np) and fission products (^{99}Tc, ^{129}I). The accessible timescales range from <1 year to about 500000 or more years, depending on the process being studied. As uranium series elements are ubiquitous and can be measured at very low levels, there is a possibility of transferring information from the analogue to any proposed repository site.

For these reasons the US Nuclear Regulatory Commission (USNRC) in 1981 began to sponsor research by the Australian Atomic Energy Commission (now the Australian Nuclear Science and Technology Organisation — ANSTO), with sub-contractors, on the four uranium deposits of the Alligator Rivers Region. To ensure that generic rather than site-specific properties of uranium and radionuclides migration were being studied, the sites chosen for investigation included all four uranium deposits. The work involved both field and laboratory studies, the aims of which were under continuous review as the project progressed in response to the greater understanding of the scope and limitations of the natural analogue approach and the changing requirements of the potential users of the information being generated. The results of these research studies were reported by Airey et al. (1982, 1984, 1985, 1986a), Airey (1986), and Duerden et al. (1988).

However, as the USNRC-funded project progressed, efforts became almost entirely directed towards study of the Koongarra deposit, due to a greater refinement in the aims of the natural analogue study (in particular, the desirability to apply the results to the question of model validation), which required a much more detailed investigation of the geologically most suitable site. Also, the Koongarra deposit, being not mined as yet, is still in place and comprises well-defined zones of primary, weathered primary and dispersion fan ore. The results of extensive investigations by the mining companies, including hydrological data, and all the drill cores and samples, plus numerous open vertical boreholes in and around the deposit, were all also available to the project's research effort. Thus a number of reports concentrated on Koongarra (Airey et al., 1986b, 1987; Duerden et al., 1988) and specific aspects of the project (Airey, Golian and Lever, 1986). Additionally, beginning in 1986 a complementary collaborative study of colloids in groundwater at Koongarra was undertaken by ANSTO and Harwell (UKAEA) staff funded by the UK Department of the Environment (Ivanovich et al., 1988).

Even though there are two orebodies in the Koongarra deposit, most attention has focussed on the No. 1 orebody, the shallower of the two and the subject of development plans and technical investigations by the mining company. Within the objectives of the natural analogue studies the Koongarra No. 1 orebody has proven to be most suitable for validation of models for radionuclide transport, there being potentially two analogues because of its configuration. As previously stated, there are well-defined zones of primary, weathered primary and dispersion fan ore, and it is the processes of weathering of the primary ore to form the weathered primary

ore, then the dispersal of uranium from the weathered primary ore to form the dispersion fan ore, which provide the two potential analogues. A detailed description of the orebody follows and these processes and zones will be explained, but it is the latter of these two analogues, the dispersal of uranium from the weathered primary ore of the No. 1 orebody in the weathered rock zone to form the dispersion fan ore, that is the focus of this study.

2 GEOLOGIC DESCRIPTION

2.1 Exploration History

Exploration by Noranda Australia Ltd within the area commenced with an airborne spectrometer survey in October 1969. Systematic ground exploration of anomalies led to the discovery of the Koongarra Uranium Deposit (Anomaly G) by geologist J.A. Climie in July 1970. He first located the centre of the radiometric anomaly that had been detected from the air by doing a ground radiometric survey, and to confirm that the source was uranium mineralisation he dug a pit at the point where the count rate was highest (1300 cps). At a depth of 3.4 metres the count rate had increased to 5300 cps and he found secondary uranium minerals in weathered schist. The area was reflown in November/December 1970 when a magnetic as well as spectrometer survey was carried out.

During the latter part of 1970 and most of 1971, an intensive program of field work was completed at the discovery. This involved detailed geological and radiometric mapping on the ground, costeaning, and auger, rotary/percussion and diamond drilling:—

(a) The surveying of a mine grid orientated 46° east of true north which had its origin as an arbitrary datum located approximately at latitude 12° 52' 02" south, longitude 132°47' 50" east (see Figure 2.1). The mine grid was laid out in feet, the then current Australian distance measurement unit.

(b) The detailed geological mapping of approximately 160 acres (65 hectares).

(c) A large number of costeans and trenches were dug within the ground radiometric anomaly area so as to determine the strike and dip of the host strata, and the extent of the mineralisation, before proceeding with an expensive drilling program.

(d) Auger drilling of 184 holes totalling 1352.74 metres to complement the costeaning and trenching.

(e) Rotary percussion drilling of 62 holes totalling 3856.7 metres.

(f) Diamond drilling of 47 holes totalling 5372.87 metres.

It was concluded that the deposit was of economic significance. Although it was not yet clear that there were two orebodies, stepout drilling along strike beyond the

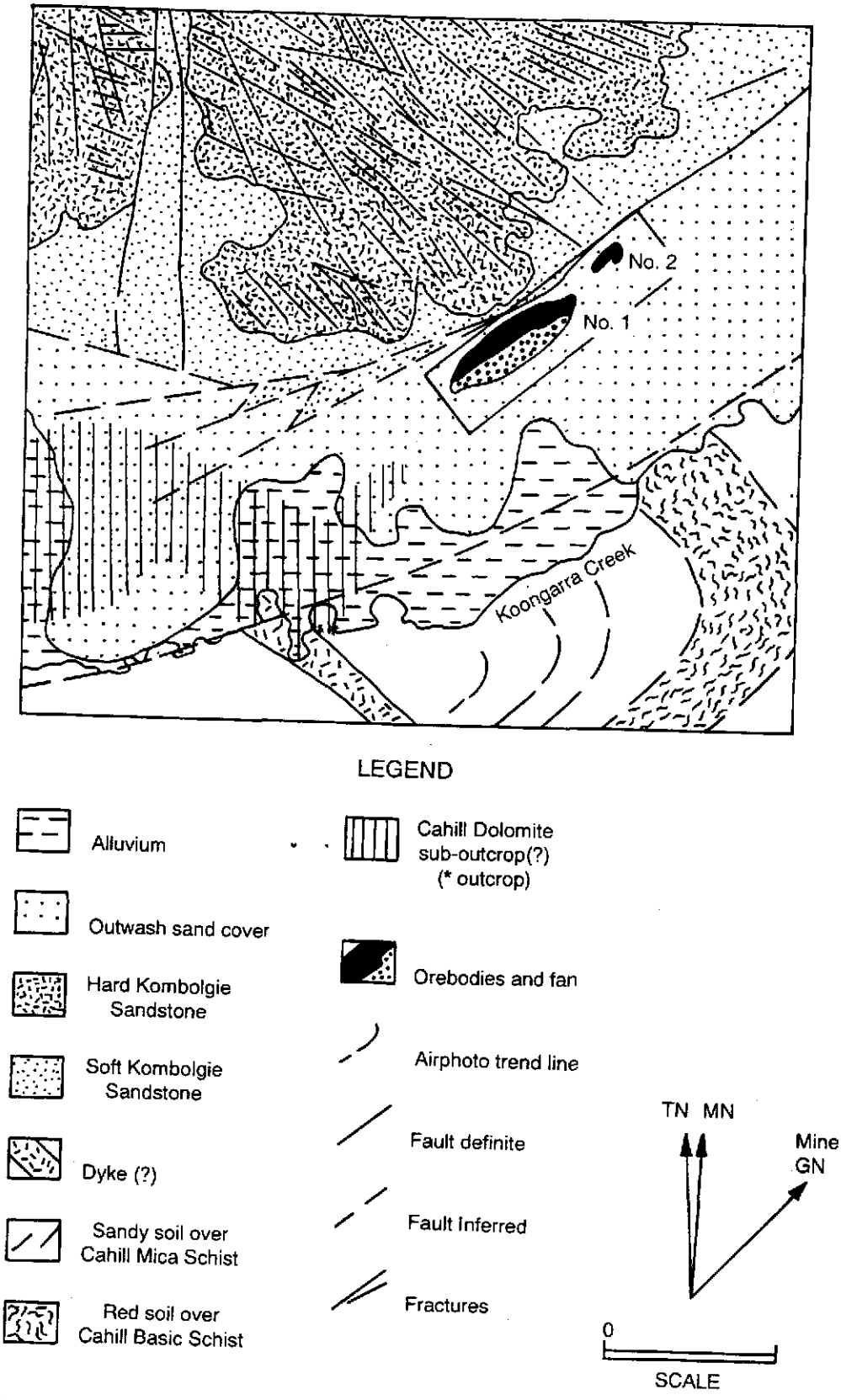

Figure 2.1 Koongarra area geology showing particularly the interpreted location of the Cahill dolomite to the south-west of the Koongarra No. 1 orebody (based on Australian Groundwater Consultants and McMahon Burgess and Yeates, 1978; Emerson et al. in Volume 4 of this series). The position and direction of the mine grid is also indicated.

ground radiometric anomaly had intersected what is now the No. 2 orebody (which has no surface radiometric 'expression').

During 1972, diamond drilling on lines intermediate to those drilled in 1971 confirmed the continuity of mineralisation and established the existence of the Koongarra No. 1 and No. 2 orebodies located between lines 9800N and 11300N, and 11300N and 11900N respectively. Thirty-six holes totalling 4872.1 metres were completed at the proposed mine area. Of these, twenty-eight holes totalling 3288.84 metres were drilled in the confirmatory program at the proposed open pit (the No.1 orebody), and a further eight holes totalling 1583.26 metres in the area just to the mine grid north (the No. 2 orebody). Percussion drilling to the mine grid north and south of Koongarra established extension of the Koongarra Reverse Fault.

An orientation Turam electromagnetic survey was also completed over the known mineralised zone during 1972. A strong Turam conductor axis appeared to coincide with the graphitic hanging wall unit associated with the mineralisation. A second, less conductive zone was located some 100-115 metres true south-east of and parallel to the former. Additionally, an orientation mercury vapour survey was carried out at Koongarra, while a track etch radon program was briefly trialled in the area to the true south-west of the No. 1 orebody.

During the 1973 field season fourteen diamond drill holes totalling 4508.78 metres were drilled, twelve of them to test for deep down-dip extensions of the Koongarra orebodies. The other two holes were designed to test for potential mineralisation immediately to the true north-east of the No. 2 orebody. In addition, five more vertical rotary percussion holes were drilled just to the true south-west of the No. 1 orebody and a further nine percussion were drilled along strike to the true north-east, all holes designed to test the extensions of the favourable Koongarra host quartz-chlorite schist.

During 1978 another ten cored holes and a number of vertical percussion holes were drilled in and around the orebodies, to assist with preparation of the Environmental Impact Statement (EIS) (Noranda Australia Limited, 1978). Investigations of some exploration techniques had also been undertaken (Pedersen, 1978), including stream sediment geochemistry (Foy and Gingrich, 1977) and soil geochemistry (Snelling, 1984).

In March 1980, the sale of the Koongarra project to Denison Mines Ltd of Canada was finalised, and the project placed in the hands of Denison's Australian subsidiary, Denison Australia Pty Ltd. The project was subsequently re-evaluated and redesigned in accord with changed concepts based on the latest technology.

Since then more exploration techniques have been tested in the Koongarra environment. These include hydrogeochemical methods (Giblin and Snelling, 1983), and sampling for lead isotopes in soils (Dickson, Gulson and Snelling, 1985, 1987), helium (Gole, Butt and Snelling, 1986), and mercury (Carr, Wilmshurst and Ryall, 1986).

During 1987 a check was made on the potential for economic gold mineralisation at Koongarra. A review of early Noranda assays confirmed the potential, and a full scale fire assay program on existing drill core samples was undertaken.

The Koongarra uranium deposit was first described in detail by Foy and Pedersen (1975), and subsequently in the Noranda Australia Ltd Environmental Impact Statement (Pedersen, 1978). Ewers and Ferguson (1980) briefly described the mineralogy. The deposit has also been the subject of several university research theses (Tucker, 1975; Snelling, 1980a; Johnston, 1984; Wilde, 1988), resulting in a number of published papers (Snelling and Dickson, 1979; Dickson and Snelling, 1980; Snelling, 1980b; Wilde, Wall and Bloom, 1985; Wilde, Mernagh, Bloom and Hoffmann, 1989). Snelling (1990) provides the most recent comprehensive description of the deposit.

2.2 Regional Geology

The regional geology (see Figure 2.2) has been described in detail by Needham and Stuart-Smith (1980), and by Needham (1982, 1984, 1988), while Hegge et al (1980) compared the similar geological settings of the four major uranium deposits of the Alligator Rivers Region — Ranger, Jabiluka, Koongarra and Nabarlek.

The uranium mineralisation at Koongarra occurs in a layered sequence of Lower Proterozoic schists, rocks that were once shales and siltstones (deposited about 2200 million years ago or My). Underneath the schists, and close to the uranium, are layers of dolomite, or metamorphosed limestone. These schist and dolomite layers (called the Cahill Formation) flank, and appear to have been deposited on the sides of a dome of crystalline Archaean granitic rocks (called the Nanambu Complex), that are thus obviously the oldest rocks in the area (estimated to be over 2500 My old), the nearest outcrop being 5 km to the north of Koongarra (see Figure 2.2 again). The shales, siltstones and limestones were metamorphosed or changed by heat and pressure to schists and dolomite between 1870 and 1800 My under temperature and pressure conditions of 550°–630°C and 5–8 kb respectively. Multiple severe folding accompanied metamorphism.

The Cahill Formation has been divided into two members. The lower member is dominated by the thick basal dolomite, which has been intersected in drilling immediately to the south-west of Koongarra (see Figure 2.1 again). The uranium mineralisation is associated with carbonaceous horizons within the immediately overlying chloritised quartz-mica (±feldspar ±garnet) schists (originally shales). The lower member passes transitionally upwards into the more psammitic (silty and sandy) upper member, which is largely feldspathic schist and quartzite.

A period of uplift, weathering and erosion over about 150 My followed, producing a new land surface on which thick layers of sandstone (the Kombolgie Formation) were then deposited (probably between 1690 and 1600 My), such that the tilted schist and dolomite layers are now at an angle to the overlying flat-lying layers of sandstone.

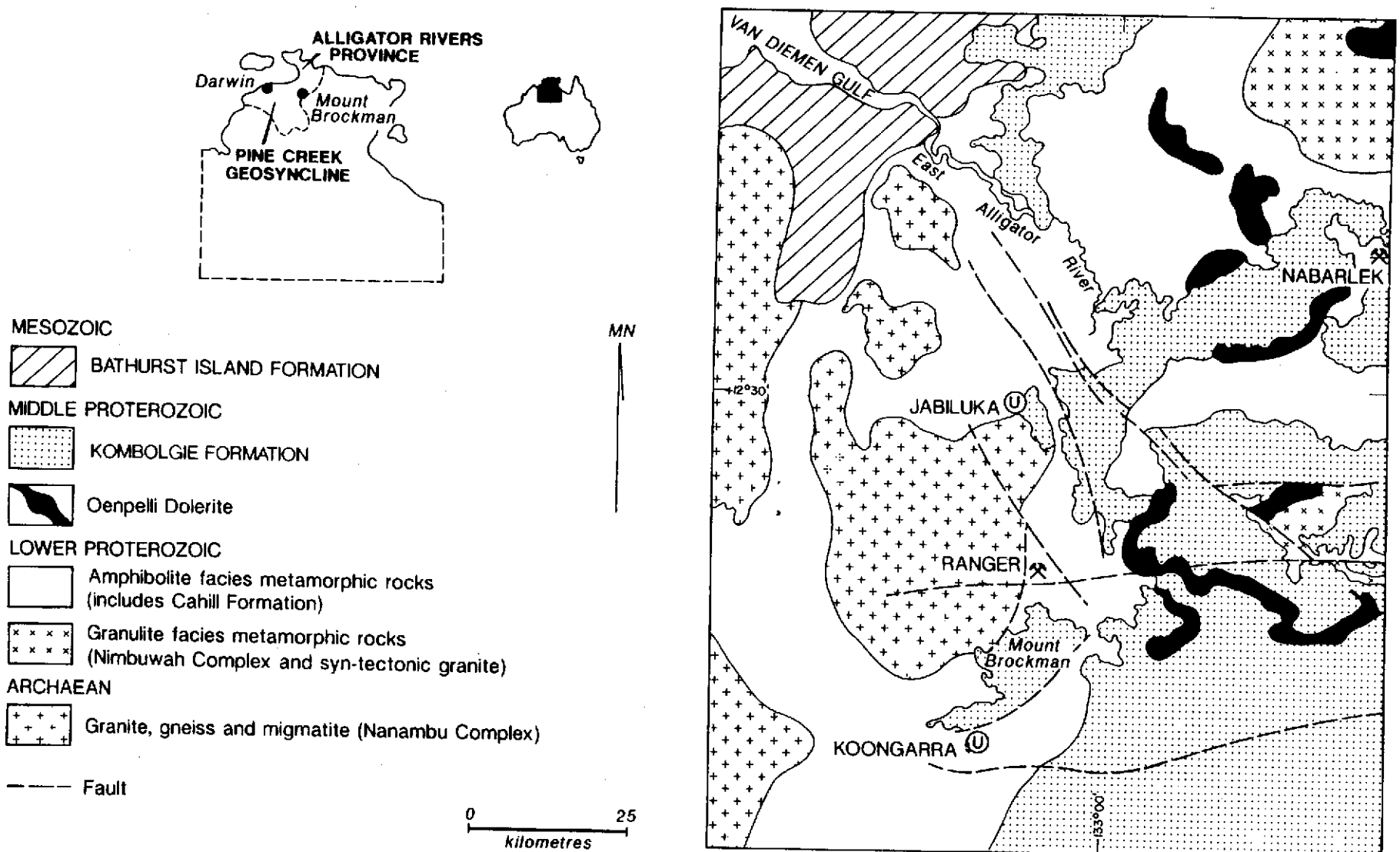

Figure 2.2 Regional geology map showing the location of the Koongarra uranium deposit (after Needham, 1984).

2.3 Local Geology

Owing to the folding over of the shales, siltstones and dolomite of the Cahill Formation during metamorphism and deformation, and the subsequent reverse faulting, the typical rock sequence encountered at Koongarra (with true thicknesses perpendicular to the schistosity indicated) is (Figures 2.1, 2.3 and 2.4):-

Hanging Wall (Above the Mineralised Zone)	— muscovite-biotite-quartz-feldspar schist (at least 180 m thick) — garnet-muscovite-biotite-quartz schist (90-100 m thick) — sulfide-rich graphite-mica-quartz schist (about 25 m thick) — distinctive basal graphite-quartz-chlorite schist marker unit (5 to 8 m thick)
Mineralised Zone	— quartz-chlorite schist (±illite, garnet, sillimanite, muscovite) (50 m thick)
Footwall (Below the Mineralised Zone)	— reverse fault breccia (5 to 7 m thick) — sandstone of the Kombolgie Formation

The uppermost muscovite-biotite-quartz-feldspar schist tends to be pale grey in colour and varies in composition from a quartz-biotite-muscovite schist to a feldspathic quartzite. Occasional large garnet grains have been chloritised, but otherwise any intense chloritic alteration is generally absent.

The garnet-muscovite-biotite-quartz schist is grey-green in colour, evenly banded, and with individual muscovite and chlorite bands up to 1 cm thick parallel to the well defined schistosity. Garnets are common within well defined bands up to 20 cm in width. Individual garnet grains are usually about 1 cm in diameter and are almost invariably altered to, and sheathed in, chlorite and muscovite elongated parallel to the schistosity, giving the rock an augen(eye)-like appearance. In places, however, garnets are wholly replaced by chlorite. Areas with disseminated pyrite are common, the garnets in particular being frequently associated with increased pyrite content, but overall sulfide content is low (<1%). Typical percentage mineral compositions of this schist are listed in Table 2.1.

The sulfide-rich graphite-mica-quartz schist is similar to the garnet-muscovite-biotite-quartz schist above it, except that garnet is not so prevalent and disseminated pyrite is common. Also, there are graphitic bands within this schist, the graphite usually occurring as thin films on schistosity planes.

At the base of the sulfide-rich graphite-mica-quartz schist is a distinctive graphite-quartz-chlorite schist that because of its position immediately adjacent to the mineralised zone below, and because it is easily identified, acts as a market unit. It ranges in width between 1 m and 10 m, but is generally 5 to 8 m thick. It is normally highly sheared with contorted fold structures and brecciation. Thin bands of graphite parallel the schistosity and often coat shear surfaces. Composition of this schist varies from almost pure graphite to inter-mixtures of quartz, chlorite

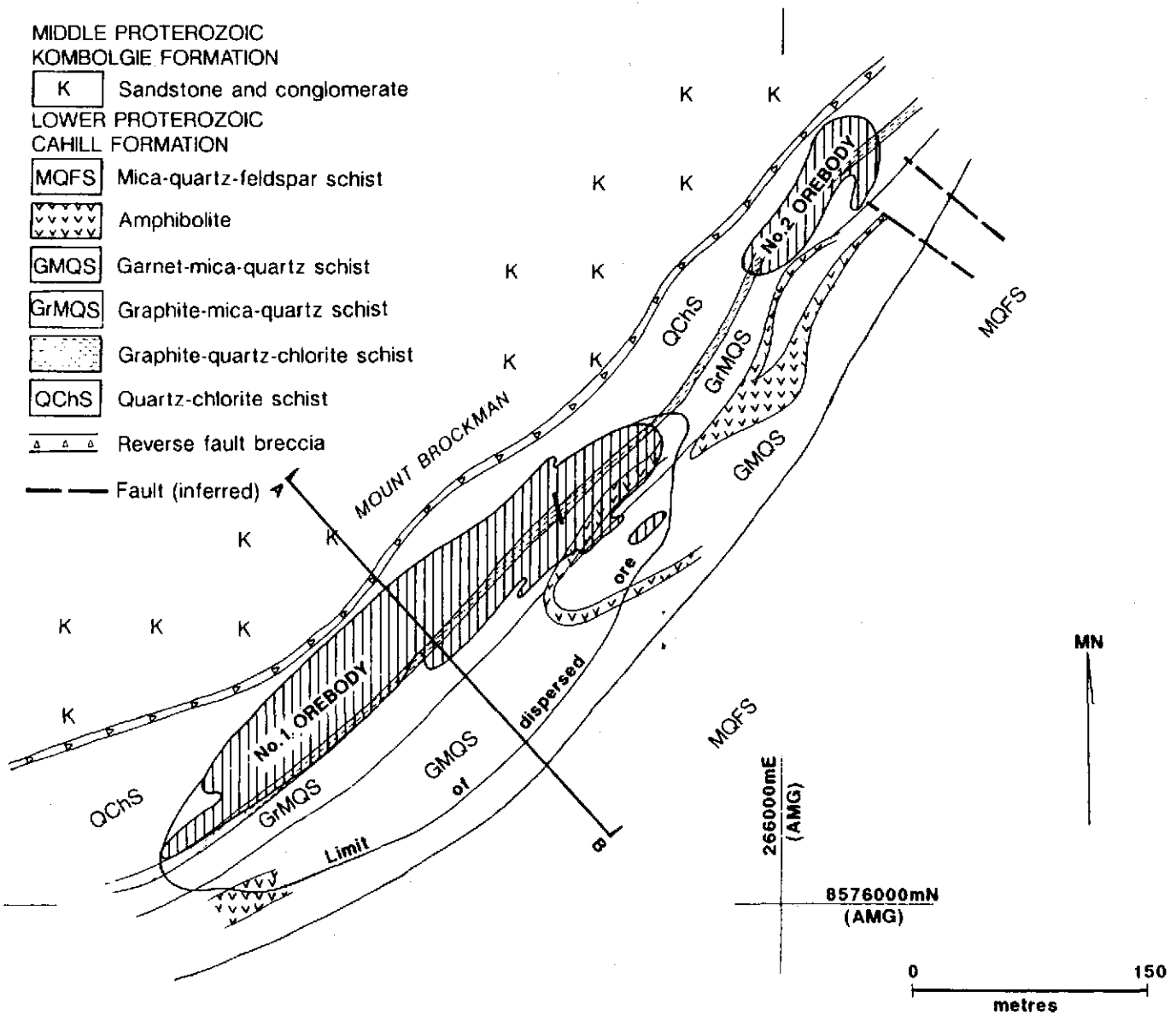

Figure 2.3 Local geology map of the Koongarra No. 1 and No. 2 orebodies. Because of the surficial cover the geological units and the outline of the mineralisation are projected to the surface from the base of weathering (after Pedersen, 1978).

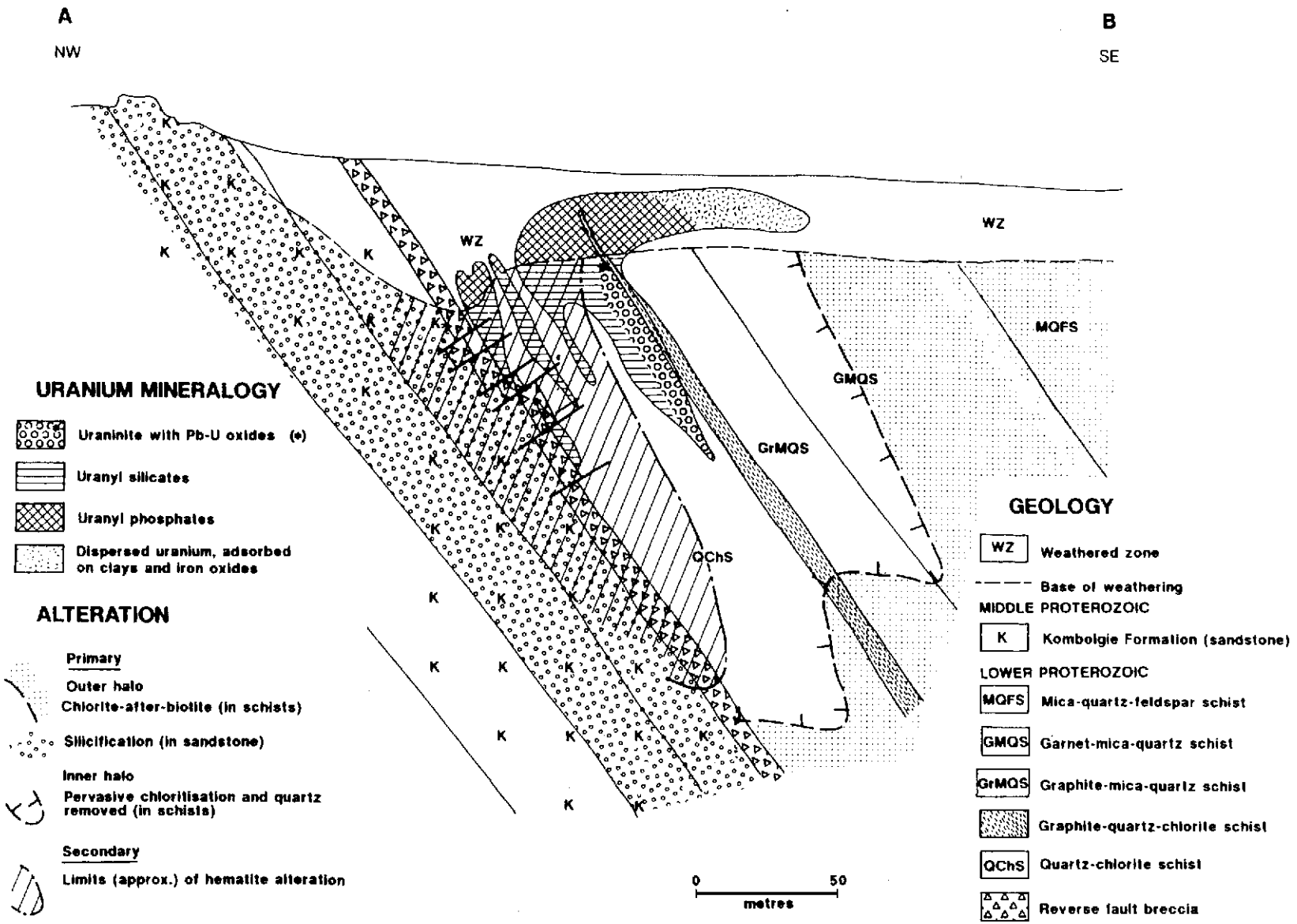

Figure 2.4 Simplified cross-section through the Koongarra No. 1 orebody showing the geology and the distribution of uranium minerals and alteration (after Snelling, 1990).

TABLE 2.1

TYPICAL PERCENTAGE MINERAL COMPOSITIONS (MODAL) OF THE GARNET-MUSCOVITE-BIOTITE-QUARTZ SCHIST

quartz	10	40	1
chlorite	5	15	8
muscovite	50	-	40
biotite (partly chloritised)	25	35	30
garnet	10	7	20
sulfide (mainly pyrite)	-	3	-
magnetite	-	-	1

and graphite, with highly variable quantities of pyrite and traces of other sulfides, notably chalcopyrite and galena. Some typical percentage mineral compositions are listed in Table 2.2.

TABLE 2.2

TYPICAL PERCENTAGE MINERAL COMPOSITIONS (MODAL) OF THE GRAPHITE-QUARTZ-CHLORITE SCHIST

quartz	70	50	20
chlorite	22	47	70
graphite	7	3	3
pyrite	1	-	-
chalcopyrite	trace	-	-
galena	trace	-	-
biotite (chloritised)	-	-	7

The quartz-chlorite schist that hosts most of the mineralisation is normally light grey in colour and finely banded with a well defined schistosity. The typical rock comprises thin alternating bands of quartz and chlorite with some quartz grains, while muscovite is often present as veneers on schistosity surfaces. Locally there has been massive replacement of virtually the entire rock by chlorite. Elsewhere

small "blobs" of chlorite up to 5 mm in diameter are common, usually representing replacement of garnets. Other minerals such as apatite, sillimanite and ilmenite are present in trace amounts that can only be detected with a microscope. Typical percentage mineral compositions are listed in Table 2.3.

TABLE 2.3

TYPICAL PERCENTAGE MINERAL COMPOSITIONS (MODAL)
OF THE QUARTZ-CHLORITE SCHIST

quartz	35	43	48
chlorite	45	50	35
muscovite	10	trace	5
biotite (chloritised)	10	7	10
apatite	trace	-	2
leucoxenised ilmenite	trace	-	-

The reverse fault breccia has been formed along the contact where the older Cahill Formation schists have been thrust over down-faulted Kombolgie Formation sandstone. Rock textures vary from coarse angular fragments of schist and/or sandstone through to almost completely pulverised rock flour, often heavily hematite stained. In a few places small fragments of dolomite have also been found in the fault breccia, perhaps suggesting that this fault movement which produced the breccia zone may have been close to, or along, the boundary between the Cahill Formation schists and dolomite. The Kombolgie Formation sandstone just below the fault zone is frequently highly silicified and hematite stained, sometimes with fractures infilled by chlorite. The schist just above is broken and fragmented or highly contorted, and is often very siliceous or heavily chloritised with strong hematite staining.

The Kombolgie Formation outcrops as a prominent scarp to the Mount Brockman Massif immediately north of the orebodies and comprises indurated, slightly micaceous, quartz sandstone of variable grain size. Further to the west along the scarp edge, quartz cobble conglomerate that is lower down in the Kombolgie Formation succession has been exposed, and several of the deeper drill holes at Koongarra terminated in that rock type.

Within the schist units of the hanging wall, several layers of amphibolite up to 15 m thick, probably repeated due to folding, have been intersected in a number of drill holes, particularly to the north-east of the No. 1 orebody and above the No. 2 orebody, and to a lesser extent above the south-western half of the No.1 orebody. In Figure 2.3 some of these drill hole intersections of interpreted amphibolite are shown as semi-continuous layers, both conformably to and cross-cutting the

schistosity, although it is possible that the intersections may only represent lenses or pods that have survived retrogressive metamorphism and hydrothermal alteration. Bands of altered amphibolite are also tentatively recognisable on textural grounds within the quartz-chlorite schist. Where recognisable, the amphibolites are finely foliated and dark green because chlorite has largely replaced the parent amphiboles. The whole-rock chemistry of all these amphibolites, though changed by alteration, does suggest that they were originally tholeiitic dolerite or basalt (rocks that cooled from molten magma or lava).

In the course of ARAP site investigations, the possibility that weathering of these amphibolites in the schist sequence may have produced a low conductivity barrier to groundwater flow was suggested. Consequently, further field studies on the amphibolites were undertaken (see Volume 4 of this series).

Pegmatites, composed of coarse grains of quartz, sericitised feldspar, muscovite, chlorite, and occasionally accessory tourmaline, form thin veins to 10 cm width which cut the schists. In the mineralised zone these pegmatites are largely obliterated by alteration.

Some well banded siliceous (microcrystalline quartz) lenses up to 5 m thick, and commonly brecciated (fragmented), are present in the quartz-chlorite schists of the mineralised zone, normally 10 to 20 m below the distinctive graphitic schist unit. Along the elongation of the strata (or strike) 750 m to the north-east, drilling has intersected dolomite lenses in the same stratigraphic position, and so these siliceous lenses in the mineralised zone have been interpreted as silicified dolomite.

To the south-west of the No.1 orebody, and to a lesser extent north-east of the No. 2 orebody, dolomite has been intersected in a number of drill holes. It is a massive grey-white to pink rock whose precise extent and thicknesses are still unknown. In some drill holes it was interbedded with schist as an integral part of the schist sequence, while in others only dolomite was intersected. The only known outcrops of what is now silicified dolomite in the area are in Koongarra Creek and adjacent to its south bank. These, plus the interpreted extent of the dolomite in the subsurface, are shown on Figure 2.1.

2.4 Structure

Multiple deformation (folding, fracturing and faulting) accompanied the mineralogical changes during metamorphism of the original sediments. Johnston (1984) suggested that it was the second deformation event in a series which was responsible for the dominant metamorphic layering (foliation) of the schist sequence at Koongarra, which strikes north-east and dips at 55° to the south-east.

The dominant structural feature at Koongarra is the reverse fault system that trends north-east along almost the entire south-east side of the Mount Brockman outlier of the Kombolgie Formation, and dips at about 60° south-east, subparallel to the dominant foliation and rock-type boundaries. The fault system extends 70 m into the schists above and about 100 m into the sandstone below. Individual fault

surfaces are defined by breccias (rocks made up of broken rock and mineral fragments), and brecciation (crushing and fragmentation of the rocks) is most intense at the sandstone-schist interface, where the breccia is generally 5 to 7 m thick but can exceed 15 m. Many parallel and subparallel fault structures of a few metres width occur in the mineralised zone above the main reverse fault breccia, and persist well into the sulfide-rich graphite-mica-quartz schist of the hanging wall. The distinctive graphite-quartz-chlorite schist marker unit itself is one such structure, slickensides (scratches and grooves) therein being evidence of shearing. Total vertical displacement along the reverse fault has been estimated to be a minimum of 50 m, possibly 100–200 m, but maybe up to 600 m.

Several north-west trending subvertical faults transect both the Kombolgie Formation and the adjacent ore zones, where only minor displacement can be interpreted from diamond drill intersections. Some minor offsetting of the reverse fault breccia along low angle faults has also been interpreted from drill core. Further investigations of folding, faulting and fracturing in the Koongarra area and the host schists are reported in Volume 4 of this series.

2.5 Distribution of the Mineralisation

Within the schist layers, probably within 100 m above the dolomite, the uranium ore occurs in two distinct but clearly related bodies, separated by about 100 m of barren schists (see Figure 2.3). Both orebodies are elongated and dip at 55° broadly parallel to the reverse fault (the Koongarra Reverse Fault), the movement along which has reversed the normal sequence of strata by bringing the overlying younger sandstone down underneath the older tilted schist layers (see Figure 2.4). This fault zone forms the lower boundary (or footwall) to the uranium ore zone. The primary mineralisation is largely confined to a schist layer consisting almost exclusively of grains and flakes of the minerals quartz and chlorite (quartz-chlorite schist) immediately above the fault zone, and a thin layer of similar schist that also contains large amounts of graphite forms a distinctive upper boundary or hanging wall unit (see Figure 2.4). At the northern end of the No. 1 orebody, and in the No. 2 orebody, mineralisation persists into the overlying schists that contain graphite, garnet and mica, as well as quartz and chlorite.

The more south-westerly of the two orebodies, the No. 1 orebody (Figure 2.3), is elongated over a distance of 450 m and persists to a depth of about 100 m. Secondary uranium mineralisation, derived from decomposition and leaching of the primary mineralised zone, is present from the surface down to the base of weathering over some 25–30 m and forms a tongue-like body of ore-grade material dispersed down-slope for about 80 m to the south-east. There is also some dispersion of secondary uranium mineralisation within the main fault zone. In cross-section the primary ore zone consists of a series of partially coalescing lenses that have the appearance of being stratabound, that is, they are confined within and parallel to the host schist layer (see Figure 2.4). The width of the primary ore zone averages 30 m at the top of the unweathered schist, tapering out at the extremities of the elongation, and down dip to about 100 m below surface. The strongest mineralisation, with most assay values in excess of 1% uranium, is over a thickness

of several metres just below the graphite-bearing hanging wall schist layer. This high grade ore is persistent both along the elongation and down dip. However, mineralisation of varying grades occurs down through the host schist layer and along minor fractures. Closer to the footwall fault breccia (crushed rock) zone the ore is of lower grade, is more sporadic, and tends to fade more rapidly with depth. Figure 2.5 depicts the three dimensional geometry of the No. 1 orebody based on four cross-sections.

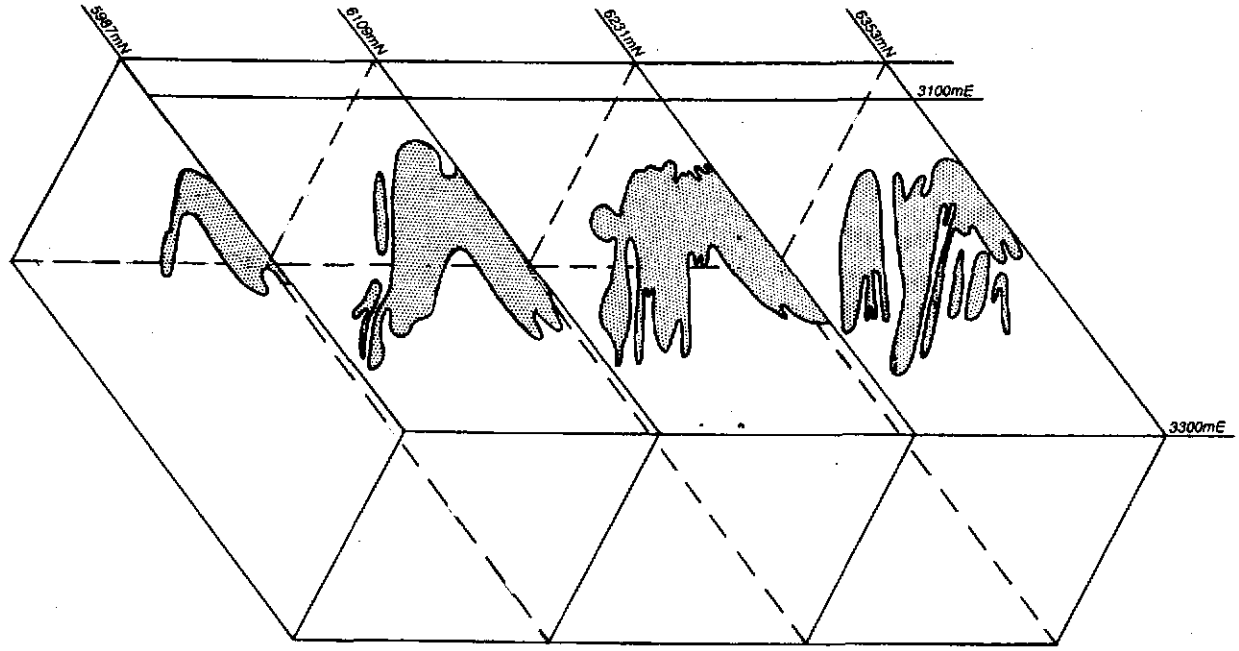

Figure 2.5 The three dimensional geometry of the Koongarra No. 1 orebody based on mine grid sections 5987 mN, 6109 mN, 6231 mN and 6353 mN.

In the No. 2 orebody, the mineralisation is elongated over a distance of about 100 m (see Figure 2.3) and persists down dip at 55° to at least 250 m. Because the top of the commercial grade mineralisation is at 50 m depth, no secondary uranium mineralisation has been identified in the weathered schists. In cross-section the ore zone tends to be oval in shape, narrow at the top, thickening with depth and then thinning again, and is made up of a series of partially coalescing lenses. Ore grades are generally lower than in the No. 1 orebody, but the mineralisation is present over greater widths. The hanging wall graphitic schist unit is less well developed and seems to have exerted a lesser degree of control on mineralisation, which also persists up into the hanging wall schists. However, the No. 2 orebody has not yet been as thoroughly investigated.

2.6 Hydrothermal Alteration

A distinct and extensive primary alteration halo has been observed about the mineralisation at Koongarra, which extends for up to 1.5 km from the ore in a direction perpendicular to the reverse fault zone. An inner and an outer halo have been identified (Figure 2.4). The outer zone is manifested by the pseudomorphous (look-alike) replacement of certain metamorphic minerals, while the inner zone involves pervasive chlorite-dominant replacement of the metamorphic rock fabric, and removal of quartz.

Outer halo alteration is most extensively developed in the schists that were originally shales. Biotite is replaced by chlorite, rutile and quartz, while feldspar is replaced by sericite. Metamorphic muscovite, garnet, tourmaline, magnetite, pyrite and apatite were preserved. Less than 200 m from the orebody, hornblende in amphibolite is replaced by chlorite and phengitic mica. Rare epidote, calcite and quartz veins have been observed in this zone, and these are associated with albitisation (Na-enrichment) of pre-existing plagioclase. Another feature of the outer halo is silicification, which occurred in fault planes and within the Kombolgie Formation sandstone. Silicification in the sandstone is best developed adjacent to the reverse fault, but may also occur in layers parallel to bedding. Association of this outer halo alteration with mineralisation is demonstrated by the apparent symmetrical distribution of this alteration about the deposit.

In the inner alteration zone, less than 50 m from the ore, the metamorphic rock fabric is disrupted, and quartz is replaced by pervasive chlorite and phengitic mica, and garnet by chlorite. Relict metamorphic minerals, mainly muscovitic mica, preserve the foliation (metamorphic layering). Quartz remains as rounded to ovoid grains "floating" in a conspicuously finer matrix of chlorite. Coarse chlorite after biotite may also be preserved. Uranium mineralisation is only present where this alteration has taken place.

Chlorite thus occurs ubiquitously throughout the unweathered host rocks at Koongarra, in proximity to the ore due to hydrothermal alteration, but also more generally due to retrogression of the schists. Chlorite is found replacing most metamorphic minerals, as cementing and fracture/breccia filling material and veins, and as groundmass (Ewers and Ferguson, 1980; Snelling 1980a). Consequently, both the compositions of the chlorite and the distribution of the different compositions are very variable (see Appendix 1 for electron microprobe analyses from Snelling, 1980a).

Snelling (1980a) found that chlorite associated with uraninite is distinctly and uniformly Mg-rich, and often also Al-rich, whereas chlorite in the host schists, whether in the ore zone below the graphitic hanging wall unit or above, shows a wide variation from Fe-rich to Mg-rich compositions. Some Fe-rich chlorite is found replacing biotite and immediately adjacent to garnet, pyrite and iron oxides. Otherwise, Snelling (1980a) found that in most cases the groundmass chlorite and chlorite after biotite are decidedly Mg-rich. Likewise, garnet is replaced by Mg-rich

chlorite, although in some cases patches of Fe-rich chlorite are found in proximity to the replaced garnet, the Fe probably having come from the garnet.

Ewers and Ferguson (1980) also found that generally the fracture/breccia filling and groundmass chlorite (in the ore) is more Mg- and Al-rich than replacement chlorite. However, they only recognised chlorite replacing biotite grains as tending to be more Fe-rich. In Volume 8 of this series it is suggested that in the unweathered zone schists, bulk rock Mg/Fe ratios indicate Mg-rich chlorite is most abundant in the primary ore zone and Fe-rich chlorite may become more dominant with distance away from the primary ore zone. This supports the findings of Snelling (1980a) that chlorite associated with uraninite is Mg-rich, whereas in the schists generally the chlorite varies more widely in Mg and Fe contents, the occasional Fe-rich chlorite being in Fe-rich 'micro-environments' or replacing an Fe-rich mineral such as biotite, particularly outside the ore zone.

The work of Murakami and others, reported in Volume 9 of this series, which considers the weathering of host rock minerals, has found that the Fe-rich chlorite is tens to hundreds of μm in size whereas the Mg-rich chlorite is less than tens of μm in size. This work has also found that the Fe-rich chlorite is predominant over the Mg-rich chlorite in the secondary ore zone and the dispersion fan. The effect of the weathering of the Fe-rich chlorite on uranium migration at Koongarra is discussed in detail in Volume 9.

2.7 Primary Ore Mineralogy and Chemistry

The primary ore consists of uraninite (or pitchblende, that is, uranium oxide) veins and veinlets (1 to 10 mm thick) that crosscut the foliation of the brecciated and hydrothermally altered host schist. Groups of uraninite veinlets are intimately intergrown with chlorite, which forms the matrix to the host breccias within the schist. Small (10–100 μm) euhedral and sub-euhedral uraninite grains (that is, grains bounded by crystal faces) are finely disseminated in the chloritic alteration adjacent to veins, but these grains may coalesce to form clusters, strings and massive uraninite. Coarse colloform and botryoidal uraninite masses, and uraninite spherules with internal lacework textures, have also been noted, but the bulk of the ore appears to be of the disseminated type, with thin (less than 0.5 mm) discontinuous wisps and streaks of uraninite, and continuous strings both parallel and discordant to the foliation, and parallel to mica cleavage planes. Appendix 2 lists representative analyses of uraninite at Koongarra.

Associated with the ore are minor volumes (up to 5%) of sulfides, which include galena (PbS) and lesser chalcopyrite ($CuFeS_2$), bornite (Cu_5FeS_4) and pyrite (FeS_2), with rare grains of native gold, clausthalite (PbSe), gersdorffite-cobaltite (Ni,Co,Fe)AsS and mackinawite $(Fe,Ni)_{1.1}S$. Galena is the most abundant, commonly occurring as cubes (5 to 10 μm wide) disseminated in uraninite or gangue, and as stringers and veinlets particularly filling thin fractures within uraninite. Galena may also overgrow clausthalite, and replace pyrite and chalcopyrite. Chalcopyrite occurs as irregular to rounded grains 10 to 100 μm in diameter, frequently with other sulfides, but occasionally as small inclusions within

uraninite itself or in chlorite-filled fractures within uraninite. Some chalcopyrite has clearly post-dated uraninite, for transgressive veins of carbonate or quartz carry chalcopyrite. Occasionally chalcopyrite grains have been altered to covellite (CuS) and chalcocite (Cu_2S). Pyrite is ubiquitous in the host schist but occurs more sparsely in the primary ore, where small rounded grains are disseminated in the gangue in proximity to uraninite. Occasionally there are larger crystals, grains and masses. Appendix 3 lists some representative analyses of these sulfide minerals.

To date the only gold mineral observed has been native gold in clusters of rounded grains (less than 5 μm diameter) in uraninite. Analyses show that gold is present at Koongarra, some of it occurring in conjunction with the uranium mineralisation, but not enough information is yet available on gold mineralogy.

Chlorite, predominantly Mg-rich chlorite, is the principal gangue, and its intimate association with the uraninite indicates that the two minerals formed together. Rutile (TiO_2) may comprise up to 5% by volume of ore (Gasparrini, 1978). On the other hand, hematite is not a common gangue phase, but may occur as a selvage (less than 2 mm thick) to some of the thicker (more than 3 mm) uraninite veins in the high grade ore zone immediately below the hanging wall graphitic unit. There is commonly a slight bleaching of the schist immediately adjacent to this hematite selvage.

Hematite is also present in the breccia in the reverse fault at Koongarra, and in the schist immediately above. It occurs as specks disseminated through the schist, as selective reddish staining of quartz-rich bands within the schist, or as bright red hematite-impregnated clay along joints and fractures. In the fault breccia and the Kombolgie Formation sandstone beneath, the hematite appears to be the product of oxidation of chlorite. Hematite is also present in the transitional zone to the weathered schist as an alteration product where secondary uranium minerals have formed in situ from uraninite, and in the schist between the fault breccia and the high grade ore zone. Hence, it is attributed to later alteration associated with deep oxidising groundwater movement down the fault system and into the schist (Figure 2.4).

In close proximity to the primary ore, the alteration in the host schists is characterised by magnesium enrichment and silicon depletion. Besides uranium, the primary ore is enriched in copper, lead, sulfur, arsenic and vanadium (Carson, 1978; Gasparrini, 1978) (see Appendix 4). Copper, lead and sulfur enrichment reflects the presence of chalcopyrite and galena, while lead is also present in uraninite (up to 13% PbO (Snelling, 1980b)) (see Appendices 2 and 3). Arsenic is a minor component of chalcopyrite (generally 0.2 to 0.5%). Nickel and cobalt form a minor enrichment halo about the deposit (Tucker, 1975). The presence of rare gersdorffite-cobaltite grains alone would not account for the nickel, cobalt and arsenic enrichment, but Snelling (1980b) also reported finding cobalt and nickel in pyrite. These would certainly account for the nickel and cobalt enrichment, since whole-rock values are seldom in excess of 100 ppm nickel and 50 ppm cobalt (Tucker, 1975; Noranda, unpublished data, 1971). Electron microprobe analyses of pyrite show that it is both normal and reverse zoned with respect to nickel and

cobalt (see Appendix 3). Some grains are found to be homogenous in the two elements, either individually or together. Maximum nickel content is 3%, while cobalt reaches 7.5%. Nickel:cobalt ratios vary, but in most samples cobalt exceeds nickel. The analyses also reveal that some pyrite may contain up to 6% copper or up to 4% lead, while most pyrite contains between 0.25 and 0.4% arsenic (maximum 1.8%). The source of the vanadium enrichment is enigmatic, but Carson (1978) and Gasparrini (1978) both suggest vanadium is present in rare unidentified uranium-manganese and silicon-titanium-iron-manganese minerals.

2.8 Age and Genesis of the Primary Ore

The age of the uranium-gold mineralisation is problematical. U-Pb isotope data on uraninites indicate crystallisation of some of the uranium at 870 My, but discordant results and Pb-Pb ages suggest the presence of radiogenic lead derived from considerably older uranium mineralisation, perhaps as old as 1800–1700 My (Hills and Richards, 1976). The mineralisation, however, must post-date both the Kombolgie Formation and the reverse fault at Koongarra, since it occupies the breccia zones generated by the post-Kombolgie reverse faulting. The pattern of alteration confirms this. Page, Compston and Needham (1980) determined the timing of Kombolgie Formation deposition as 1688 to 1600 My. The Sm-Nd isotopic data on uraninites of Maas (1987, 1989), which narrow down the timing of mineralisation to 1650 to 1550 My, are consistent with this.

Maas's data also indicate some Sm-Nd redistribution at 420 My. Coupled with Hills and Richards' (1976) 870 My concordant U-Pb data, this suggests a three-stage development for the primary uranium ore. The weathering of the primary ore to produce the secondary dispersion fan above the No. 1 orebody seems to have begun only in the last 1 to 3 My (Airey, Golian and Lever, 1986).

Views on the genesis of the deposit differ. Ferguson, Ewers and Donnelly (1980) suggested that the ore developed within collapsed dolines (sinkholes) during weathering and erosion of the Lower Proterozoic landscape after the 1870–1800 My regional metamorphism. In this concept, meteoric water (rainfall) percolated along bedding planes and fracture systems, scavenging uranium from the metasediments and depositing it where schist debris, clay and carbonaceous matter had accumulated in the dolines. They suggest that high heat flows due to pre-Kombolgie igneous activity remobilised the uranium in situ to form the primary ore lenses.

Wilde (1988) favoured a post-Kombolgie genesis, since the mineralisation occupies the breccia zones generated by the post-Kombolgie reverse faulting and fluid inclusion data (Wilde, 1988) also require ore genesis under a 6 km sediment cover. Therefore Wilde (1988) suggested a diagenetic (sedimentary)-hydrothermal genetic model, akin to the prevailing model for the comparable Canadian unconformity-related deposits, whereby the metals were scavenged by circulating saline diagenetic fluids from the thick Kombolgie sediment pile with its interbedded volcanic flows (the postulated source of gold and base metals), at temperatures around 270°C. The fluids were then transported down brecciated fault zones into

the Lower Proterozoic basement metasedimentary units, where mixing with resident fluids of contrasting oxidation state and changes in ligand concentration, temperature and pH resulted in precipitation in brecciated basement fault zones near the unconformity. Donnelly and Ferguson (1980) found that $\delta^{13}C$ values for Koongarra graphite indicated reactions involving organic matter, and this is consistent with the suggestion that the graphite via reducing reactions has exerted control on the localisation of the primary uranium mineralisation.

2.9 The Secondary Mineralisation

One of the most important features of the uranium mineralisation at Koongarra is the occurrence of abundant secondary uranium minerals, principally within the dispersion fan above the No. 1 orebody, but also to a lesser extent within the top of the primary ore zones just below the weathered zone, and at the bottom of the primary zones along and just above the fault. These secondary uranium minerals are noted for their variety of brilliant colours, so their presence is easily recognised both in subsurface samples and in drill core.

Oxidation and alteration of uraninite within the primary ore zone have produced a variety of secondary uranium minerals, particularly the uranyl silicates kasolite ($Pb(UO_2)SiO_4.H_2O$), sklodowskite ($Mg(UO_2)_2\ Si_2O_7.6H_2O$) and uranophane ($Ca(UO_2)_2Si_2O_7.6H_2O$). Uraninite veins, even veins over 1 cm wide, have been completely altered in situ. Some uraninite veins are concentrically sheathed outwards by the uranium-lead oxides vandendriesscheite ($PbO.7UO_3.12H_2O$), fourmarierite ($PbO.4UO_3.4H_2O$) and then curite ($2PbO.5UO_3.4H_2O$), and then sklodowskite. Other veins are partially or totally replaced by intergrown uranyl silicates. In most cases the physical positions and shapes of the replaced uraninite veins and masses, even euhedra (crystal shapes), are preserved. Uranophane and sklodowskite, remote from any parent uraninite, are also found as veins and stringers within fractures, between grain boundaries and within mica cleavage planes. Within fractures sklodowskite has also crystallised as aggregates of radiating acicular (needle-like) crystals, with chlorite as the infilling matrix. Within the primary ore zone this in situ replacement of uraninite is most pronounced immediately above the reverse fault breccia, and this alteration and oxidation diminish upwards toward the high grade ore beneath the hanging wall graphitic schist unit (Figure 2.4). Extensive in situ replacement of uraninite by uranyl silicates has also occurred where the high grade ore is intersected by the transitional zone to the weathered schists. Appendix 5 lists representative analyses of these uranyl oxide and silicate minerals.

The secondary mineralisation of the dispersion fan in the weathered schists above the No. 1 orebody is characterised by uranyl phosphates, particularly saleeite ($Mg(UO_2)_2(PO_4)_2.8H_2O$), metatorbernite ($Cu(UO_2)_2(PO_4)_2.8H_2O$) and renardite ($Pb(UO_2)(PO_4)_2(OH)_4.7H_20$), found exclusively in the "tail" of the fan. Much of this phosphate-bearing "tail" has been shown to be weathered and leached primary ore, and was originally, before weathering, the up-dip continuation of the present primary ore lenses. The uranyl phosphates of this "tail" occur as veins, stringers, euhedral grains, intergrowths and rosettes amongst the clay-mica-quartz mixtures of the

weathered schists. Appendix 6 lists representative analyses of these uranyl phosphate minerals. Away from the "tail" of the dispersion fan uranium is dispersed in the weathered schists and apparently adsorbed onto the surfaces of clay and iron oxide minerals.

Because much of the secondary mineralisation is derived from in situ oxidation and alteration of grains and veins of the primary uranium mineral, uraninite, and by the dissolving and retransporting of the uranium, these processes therefore represent the latest stage in the genesis of the deposit as we know it today, processes which may still be in operation. In the top of the No. 2 orebody, where no secondary dispersion fan has been identified, only uranyl silicates have been found. This contrasts with the pattern in the No. 1 orebody, where uranyl phosphate minerals are found in the "tail" of the secondary dispersion fan in, and down-slope from, what was the upwards extension of the primary ore zone, while uranyl silicates are either in the primary ore zone below or at the interface between the two (see Figure 2.4 again).

The differences in distribution and style between the uranyl silicates and phosphates strongly suggests a two-stage process for their development under different physico-chemical conditions. The first stage was the in situ alteration of uraninite to form uranyl silicates associated with chlorite veining at depth within the primary ore zones of both the No. 1 and No. 2 orebodies. Subsequent intersection of the zone of surface weathering with the top of the primary ore zone of the No. 1 orebody only, has resulted in the leaching and decomposition of both uraninite and uranyl silicates to form the uranyl phosphates within the secondary dispersion fan (see Volume 11 of this series).

In the primary ore zones at Koongarra, where the mineral apatite (the apparent main source of phosphorus) is stable, the soluble uranyl silicates precipitated under slightly reducing and weakly acidic conditions with negligible to zero concentration of phosphate and vanadate in the groundwaters (Snelling, 1980a). In the weathered zone, however, the precipitation of relatively insoluble uranyl phosphates has been favoured by oxidising conditions and much higher phosphate concentrations (due to weathering of apatite) in the groundwaters. It is also possible to conclude that vanadium concentrations in the circulating fluids at Koongarra were very low compared to phosphorus, because carnotite is sparse in its occurrence in the weathered zone.

This was the interpreted scenario prior to ARAP for the development of the secondary mineralisation in the weathered zone. An essential part of ARAP was to further investigate this scenario and further qualify and quantify how mobilisation/movement of uranium has occurred in the weathered zone. Details are thus dealt with in following volumes in this series.

3 THE DEVELOPMENT OF THE SOLID GEOLOGY

Because the main focus of the Alligator Rivers Analogue Project has been to model the development — mineralogically, geochemically, hydrogeologically — of the

secondary dispersion fan above the Koongarra No. 1 orebody, and determine the timescales for these processes, it is important to understand the overall geological development/history of the deposit and its geology. Some details of the timescales and processes have already been touched upon in the above geological description of the deposit, but a step-wise presentation of the geological history of development stage by stage is warranted here, particularly for those without a geological background who may have difficulty in visualising the processes that have led up to, and resulted in, the formation of the secondary dispersion fan.

The method chosen here is pictorial — a time series of idealised diagrams — with accompanying commentary. The focus is particularly on the Koongarra deposit and its environs, rather than on the regional scale, since the latter is too broad in the context of this analogue project and so is virtually irrelevant. Hopefully, this pictorial presentation will provide an adequate context in which to view the data and modelling studies generated by this analogue project and presented in the subsequent volumes of this report.

3.1 The Archaean Nanambu Complex Basement (2500–2200 My)

While the mineralisation is hosted by the schists of the Cahill Formation, the basement complex on which those metamorphosed sediments lie had to form first. The Nanambu basement rocks consist of a suite of granitic rocks that intruded previous sediment layers (now completely eroded away) and give a crystallisation age of around 2500 My, and a suite of metamorphosed granites with schists and gneisses (metamorphosed sediments) that yield an isotopic age of 1870–1800 My (Page, Compston and Needham, 1980). The isotopic data also indicate that these latter rocks had an earlier history, originally being granites overlain by later sediments, the granites crystallising with the unmetamorphosed granites around 2500 My, and the sediments being deposited on the granitic basement subsequent to that. The regional 1870–1800 My metamorphic event effectively reworked some of the granites and some of the sediment layers resting on the granites, physically incorporating them into the basement complex.

Figure 3.1 depicts three time "slices" in the development of the Nanambu Complex basement — the intrusion of the granites into previous (older) sediments and crystallisation around 2500 My (Figure 3.1a), the subsequent erosion of the older sediments and granites (Figure 3.1b), to leave by about 2200 My a new eroded land surface (Figure 3.1c), that was the basement surface or unconformity on which the later sediments that now host the uranium were deposited.

3.2 Sedimentation — The Cahill Formation (2200–1900 My)

Between 2200 and 1900 My a sequence of sediment layers, including the Cahill Formation that hosts the uranium mineralisation, was deposited unconformably on the eroded Nanambu Complex basement. First were the sands of the Kakadu Group, layers that were reworked with the Nanambu Complex granites by the later metamorphism so that they now appear to be an integral part of the Nanambu Complex. After deposition of the Kakadu Group sands came the limestones,

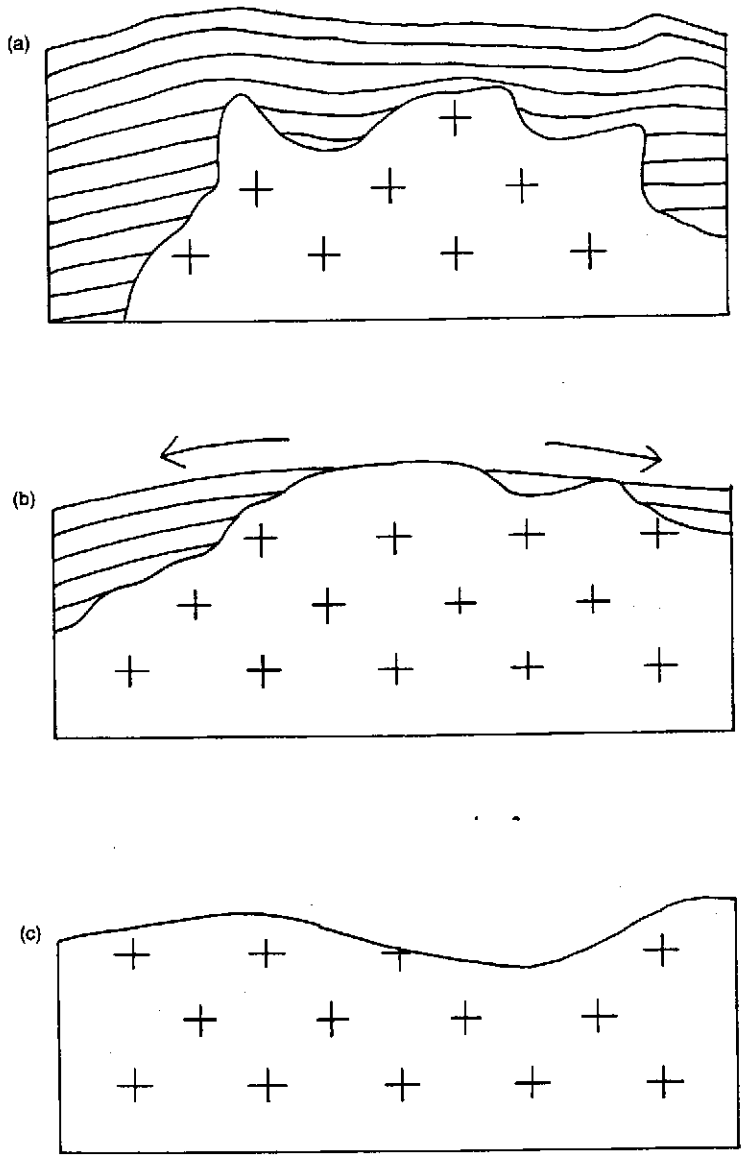

Figure 3.1 Development of the Archaean Nanambu Complex Basement between 2500 and 2200 My (see text).

probably with evaporites (largely being precipitated), muds and organic-rich muds of the lower Cahill Formation, followed by the silts and muds of the upper Cahill Formation (see Figure 3.2). In surrounding areas of the region other laterally equivalent sediments were being deposited at the same time. In the Koongarra area the muddy silts, that were the forerunner to the Nourlangie Schist, were then deposited on the Cahill Formation. Sedimentation throughout the region appears to have been completed by about 1900 My.

3.3 Dolerite Intrusion (1900–1885 My)

At or near the close of sedimentation, probably between 1900 and 1885 My, sills of the igneous Zamu Dolerite were intruded along the bedding of the sediments, and even into the Nanambu Complex (see Figure 3.3).

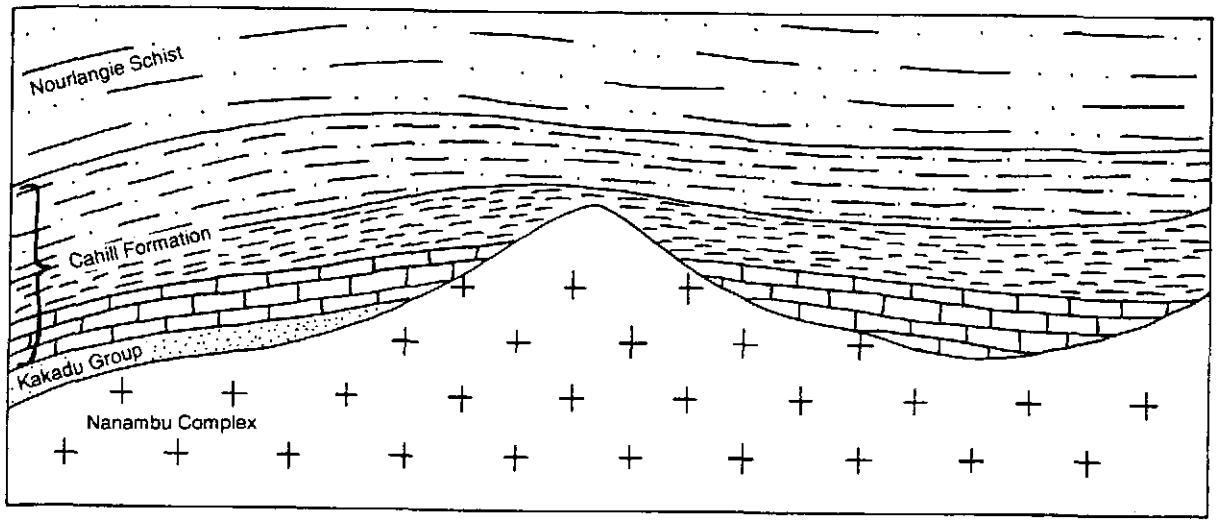

Figure 3.2 Deposition of a sequence of sediment layers (Kakadu Group, Cahill Formation and Nourlangie Schist) unconformably on the Nanambu Complex basement between 2200 and 1900 My.

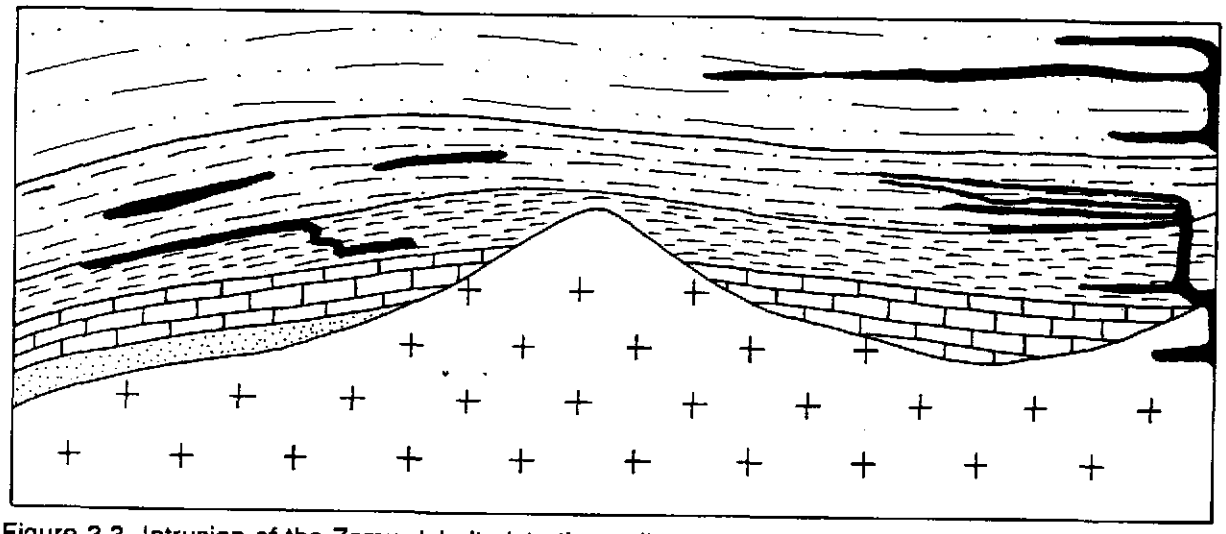

Figure 3.3 Intrusion of the Zamu dolerite into the sediments between 1900 and 1885 My.

3.4 Metamorphism and Deformation (1870–1800 My)

Following cessation of sedimentation and intrusion of the Zamu Dolerite, an intense mountain-building episode or orogeny commenced, in which the sediments were folded, faulted, metamorphosed, and intruded by granites (see Figure 3.4).

Burial of the sediments, in this case the Cahill Formation, to a depth of at least several kilometres produced the temperature and pressure gradients to attain amphibolite facies metamorphism. Intrusion of granite to the north-east (north of Nabarlek), at about 1870 My, probably initiated the regional polyphase folding and metamorphism, which was most intense in the north-east, reaching granulite facies. Most of the quartz-feldspar sands of the Kakadu Group (beneath the Cahill formation) and some of the Archaean granite were transformed to the gneisses of the Nanambu Complex. Deformation involved early, bedding-parallel folding and perhaps some bedding-parallel faulting. Later folding was isoclinal in the

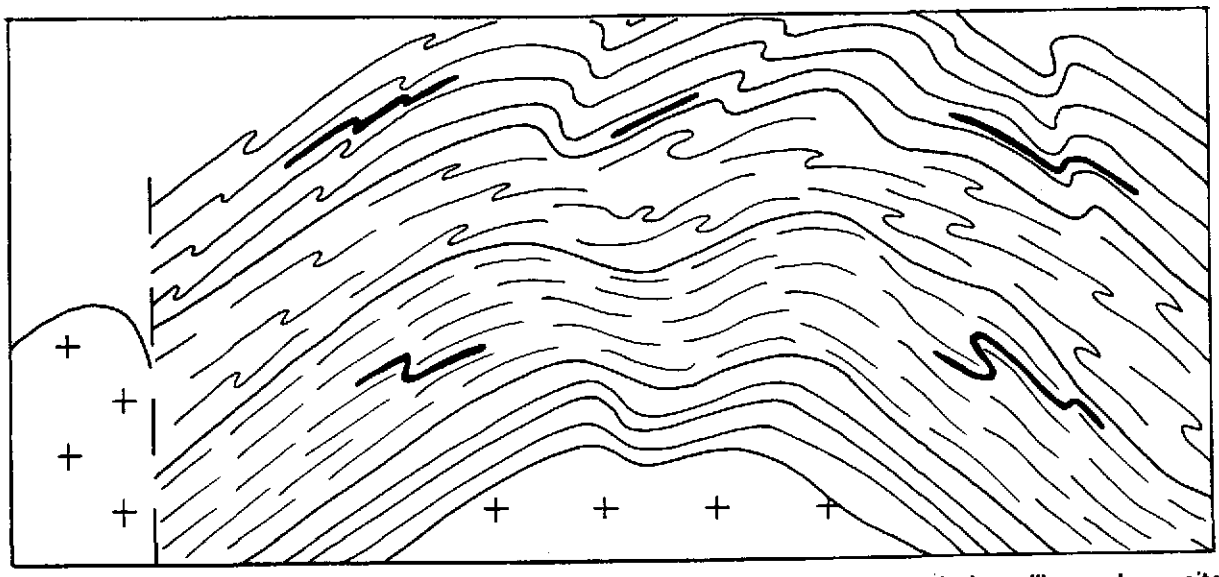

Figure 3.4 Metamorphism and deformation of the sediment layers, dolerite sills and granite basement between 1870 and 1800 My.

north-east, but dominantly upright in the Koongarra area, and to the south and west. More granite was emplaced soon after folding and metamorphism ceased around 1800 My.

3.5 Erosion (1800–1650 My)

An erosional period of 150 My followed the close of metamorphism and deformation (see Figure 3.5). Initially erosion must have been rapid, because airfall tuff deposits (of the Edith River Group), derived from material extruded from vents to the south at about 1803 My, were deposited unconformably on the high-grade metamorphic rocks. The region continued to undergo weathering and denudation for 150 My, and during this time lopoliths (large basin-shaped intrusions) of Oenpelli Dolerite were emplaced in the north-east at 1–2 km depth at about 1690 My. By 1650 My continued erosion had removed that 1–2 km of country rock to exhume parts of these lopoliths.

The present coastal lowlands of the Kakadu area, to the north-west of Koongarra, are in part this exhumed regional (pre-Kombolgie) unconformity land surface, and their topography is very similar to the exposed unconformity surface at the base of the Kombolgie Formation, with local relief up to 20 m and isolated hills up to 120 m above the general surface.

3.6 Sedimentation — The Kombolgie Formation (1650–1610 My)

Deposition of the Kombolgie Formation sediments, mainly medium to coarse-grained sandstones with minor conglomerates, occurred right across the area as, by inference, a braided alluvial fan (see Figures 3.6 and 3.7). The major lower and upper sandstone units of the Kombolgie formation (300 m and 350 m thick respectively are separated by up to 170 m of volcanic rocks (principally basalt)

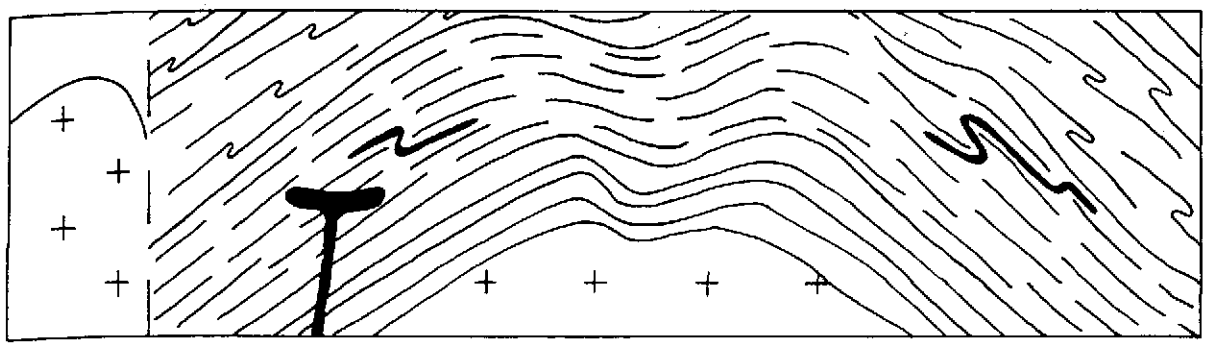

Figure 3.5 Erosion of the metamorphosed and deformed sediment layers to form another new land surface between 1800 and 1650 My.

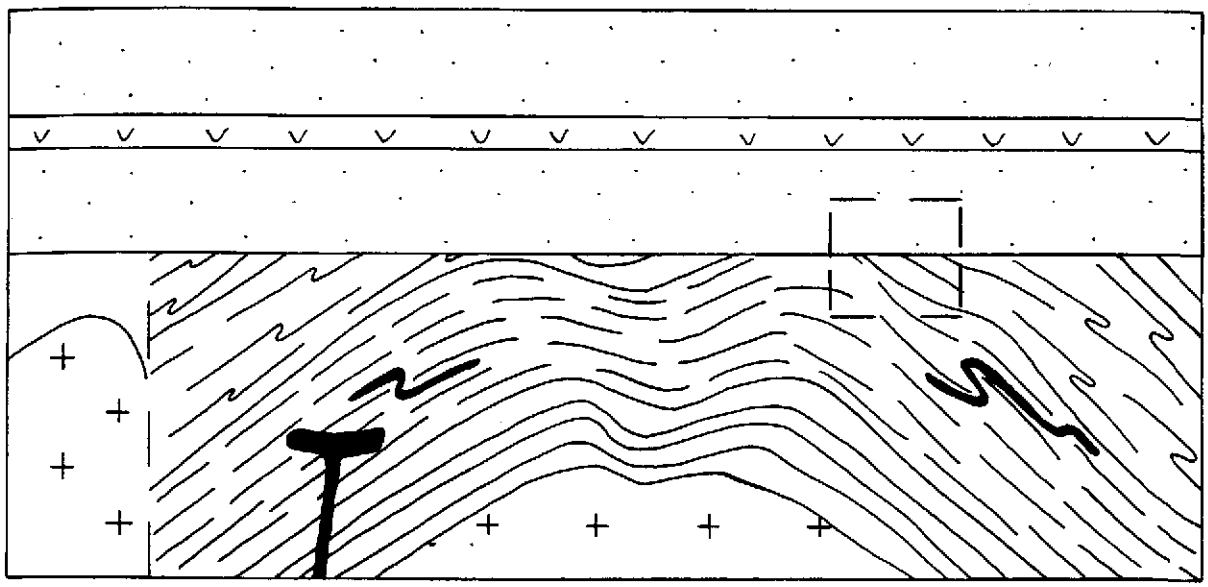

Figure 3.6 Deposition of the Kombolgie Formation sandstones and interbedded volcanics unconformably on the eroded land surface between 1650 and 1610 My. The "boxed" area is enlarged in Figure 3.7.

which have been radiometrically dated at 1648 My (Needham, 1988). The Kombolgie Formation once extended right across the Koongarra area, the present Mt Brockman Massif behind Koongarra and the Arnhem Land Plateau on the other side of the Koongarra Valley being noted for the 50–200 m high sandstone scarps that mark their edges.

3.7 Faulting (Approximately 1600 My)

Soon after deposition of the Kombolgie Formation sandstones, at approximately 1600 My, compressional tectonic forces generated major faults along which earth movements took place. A horst block of strata was uplifted with margins defined by the Koongarra Reverse Fault, the Sawcut and the western Nourlangie Fault systems (see Figures 3.8 and 3.9). The extent of vertical movement of this block has been difficult to determine, with estimates varying from as little as 50 m, to as much as 600 m, but 100–200 m is more likely.

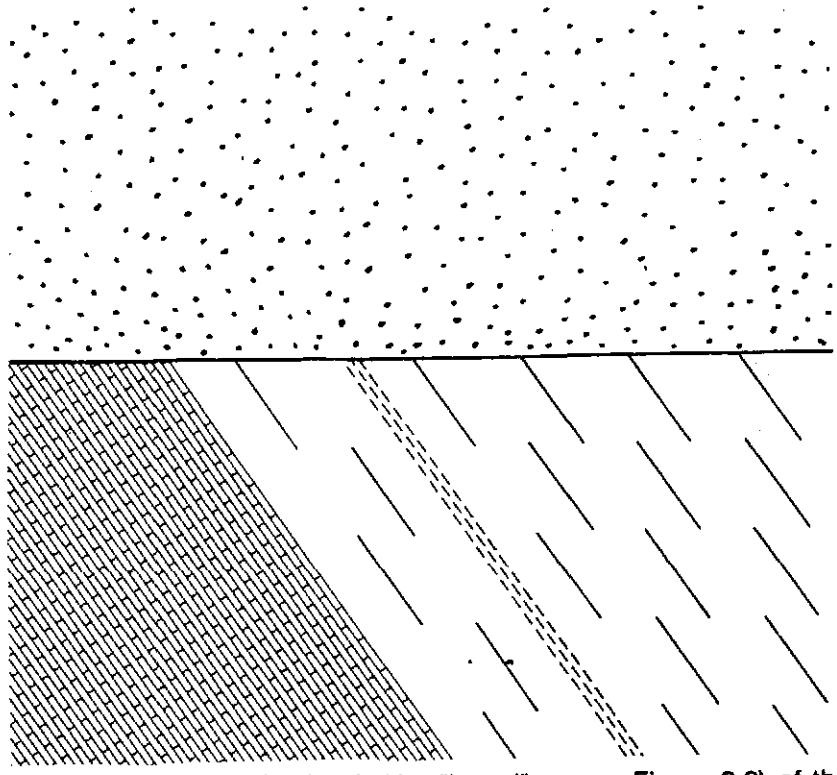

Figure 3.7 A "close-up" diagrammatic sketch (the "boxed" are on Figure 3.6) of the host strata at Koongarra at 1610 My with the Kombolgie Formation sandstone deposited unconformably on the eroded metamorphosed and tilted earlier sediment (Cahill Formation) layers (from left to right: dolomite, quartz-chlorite schist, graphitic schists, etc.)

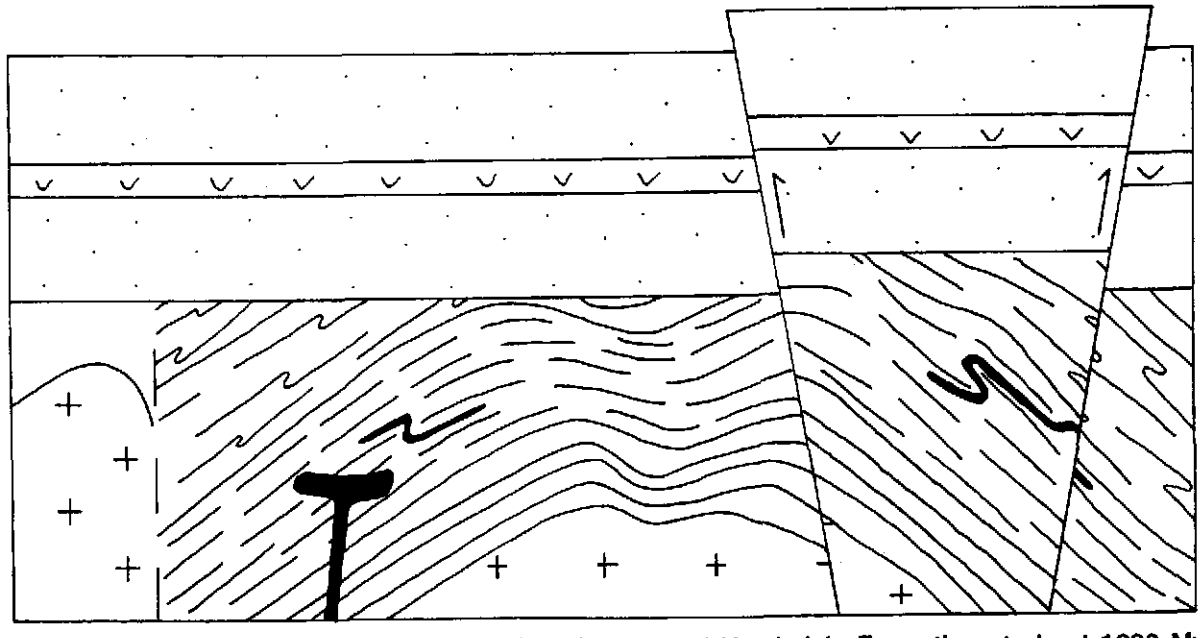

Figure 3.8 Faulting of the metamorphosed sediments and Kombolgie Formation at about 1600 My. The faults shown are the Koongarra Reverse Fault (left) and the Sawcut Fault (right), and the uplifted horst block between them was later eroded away to form the Koongarra Valley.

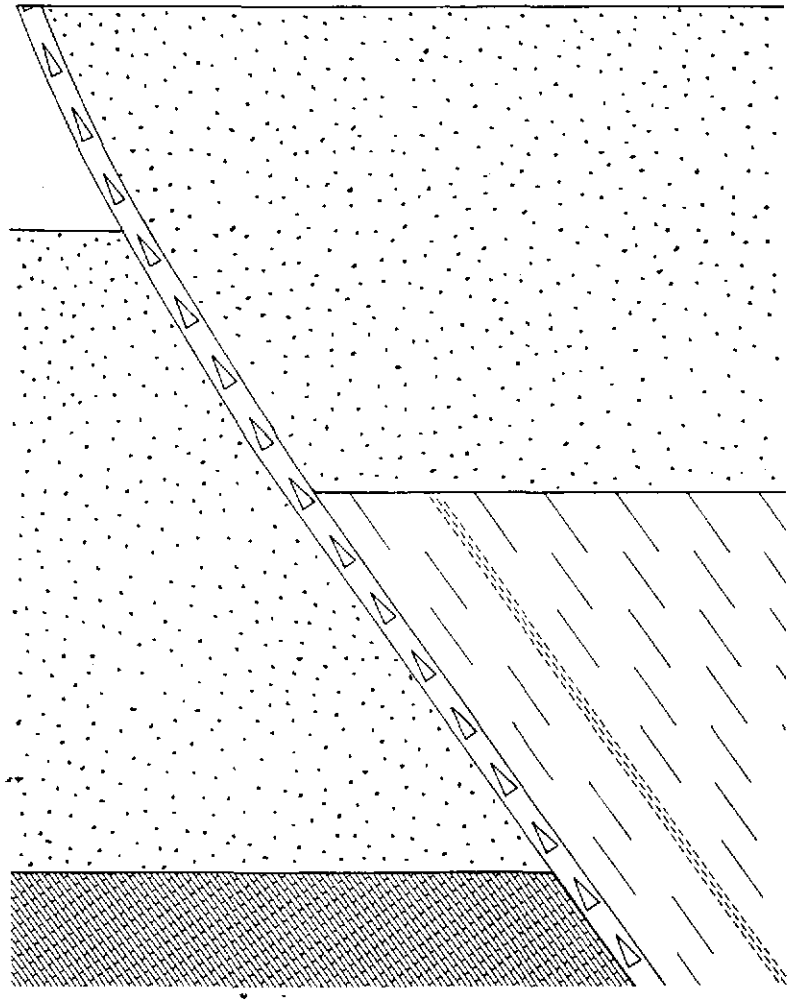

Figure 3.9 A "close-up" of the Koongarra Reverse Fault (schematic and not to scale) at about 1600 My showing how the Kombolgie sandstone has been "downfaulted" relative to the host Cahill schists at Koongarra.

The faulting has displaced the Nanambu granite basement and the Cahill Formation with respect to the overlying Nourlangie Schist. At Koongarra the reverse faulting, due to the compressional forces involved, has moved the older Cahill Formation rocks up the inclined fault plane over the younger Kombolgie Formation sandstone (see Figure 3.9 again). It would appear that the plane of the reverse fault probably coincides with the boundary between the lower Cahill dolomite and the overlying schist, as that change in rock type would have provided a plane of weakness which the compressional forces would then have exploited. The wide zone of brecciation along the Koongarra Reverse Fault plane is evidence of the intensity of the compressional forces involved in these earth movements. Related parallel fracturing of the uplifted horst block, across to the Sawcut Fault on the eastern margin, probably facilitated the subsequent erosion of this block, which later became the present Koongarra Valley.

3.8 Mineralisation — The Formation of the Koongarra Primary Ore (1600–1550 My)

While opinions have differed over the source of the uranium and the timing of primary ore formation in the Alligator Rivers uranium deposits (that is, Jabiluka, Ranger, Koongarra and Nabarlek), a number of important observations at Koongarra clearly delineate this 1600–1550 My interval as the time for primary ore formation at Koongarra (see Figure 3.10).

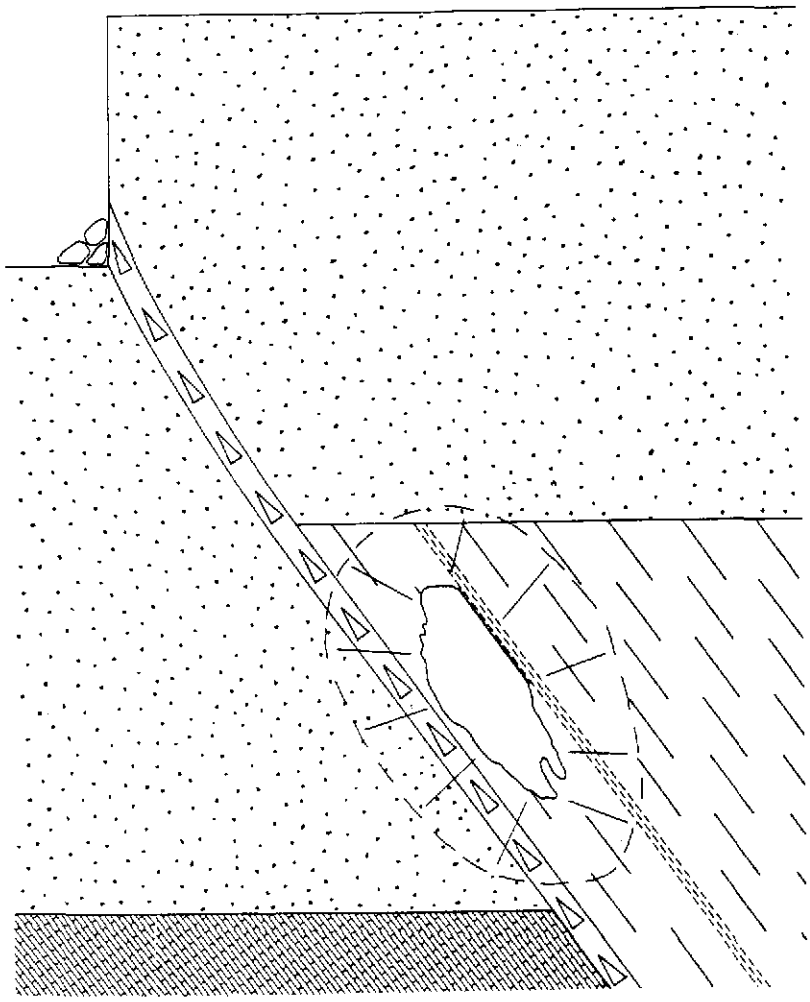

Figure 3.10 Schematic "close-up" (not to scale) of the setting for deposition of the Koongarra orebody mineralisation and associated alteration halo at 1600–1500 My.

First, the bulk of the primary ore uraninite has precipitated in the breccia zones in the host schists parallel to, and generated by, the post-Kombolgie 1600 My reverse faulting. Second, the pattern of alteration around the mineralisation confirms this, as the alteration halo continues across the reverse fault symmetrically around the mineralisation (see Figures 2.4 and 3.10). Third, the Sm-Nd isotopic data on the uraninite also coincide with the 1600–1550 My interval. Thus, whatever the source of the uranium, whether already in dispersed accumulations in the schists or

introduced by circulating fluids from the overlying Kombolgie Formation, these three observations clearly indicate that this 1600–1550 My interval was when the primary ore at Koongarra was formed, taking on the basic pattern in which it occurs today.

3.9 Erosion with Geological Stability (1500–135 My)

The region was then tectonically stable for over 1400 My, from 1550–135 My, with only gradual erosion of the Kombolgie sandstone that covered the schists containing the mineralisation (see Figures 3.11 and 3.12). Minor phonolite and dolerite (intrusive sub-volcanic rocks akin to basalt) were emplaced as dykes (generally vertical cross-cutting thin sheets intruded into fracture or fault planes) at about 1370, 1320 and 1200 My (Needham, 1988).

In the uranium deposits of the region other minor events have been recorded by some resetting of the isotopic clocks, but there appears to be no other readily apparent geological activity with which these isotopic resettings can be correlated. At Koongarra there was a resetting of the U-Pb isotopes at 870 My (Hills and Richards, 1976) and a redistribution of Sm-Nd at 420 My (Maas, 1989). On textural evidence it would appear that the U-Pb isotopes were reset by a major remobilisation of the uranium mineralisation, probably involving low temperature groundwaters dissolving uraninite and then re-precipitating it. The minor element

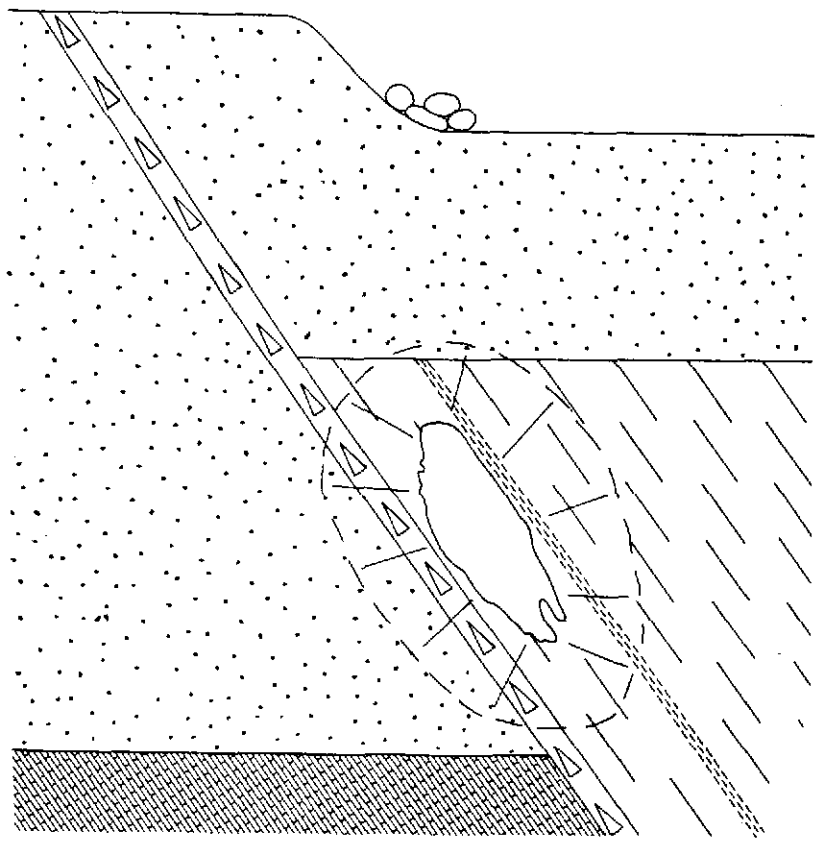

Figure 3.11 Erosion of the Kombolgie sandstone from above the Koongarra orebody 1550–135 My — Stage 1. Note the greater erosion on the "proto" Koongarra Valley side of the fault, due to the deep fracturing of the sandstone.

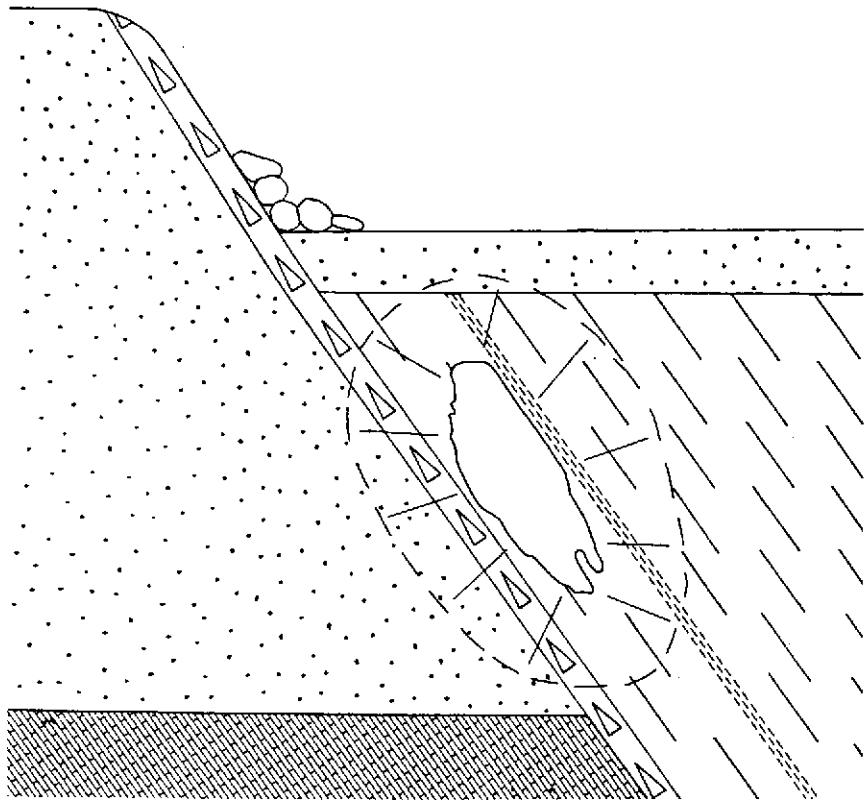

Figure 3.12 Erosion of the Kombolgie sandstone from above the Koongarra orebody, 1550–135 My — Stage 2. The Koongarra Valley and escarpment have now formed, but sandstone still covers the host schist on the valley floor.

chemistry of the uraninite also reflects this (Snelling, 1980a). However, the scale of movement would not have been great, the re-precipitated uraninite being confined to the same zone and basic disposition within the host schists as in the original mineralisation event.

During this extended 1400 My erosional period the Kombolgie sandstones and interbedded volcanic units were gradually stripped away, as shown in Figures 3.11 and 3.12. As mentioned previously the compressional tectonic forces responsible for the Koongarra and Sawcut Faults, and the uplifting of the horst block between them, also probably heavily fractured the sandstones within the horst block, thus facilitating more rapid and much deeper erosion of the horst block to open up the Koongarra Valley (see Figures 3.13 and 3.14). By the beginning of the Cretaceous at 135 My, it is envisaged that the Kombolgie sandstones had been cut back close to the present margin, and that the bulk of the erosion was completed.

3.10 The Site Today

From the beginning of the Cretaceous through to the present there has probably been only minor modification of the landscape, compared to the geological processes and quantity of erosion that previously shaped the development of the area's solid geology. Nevertheless, the geomorphological development of the area up to the present was critical to the initiation of the weathering processes that have

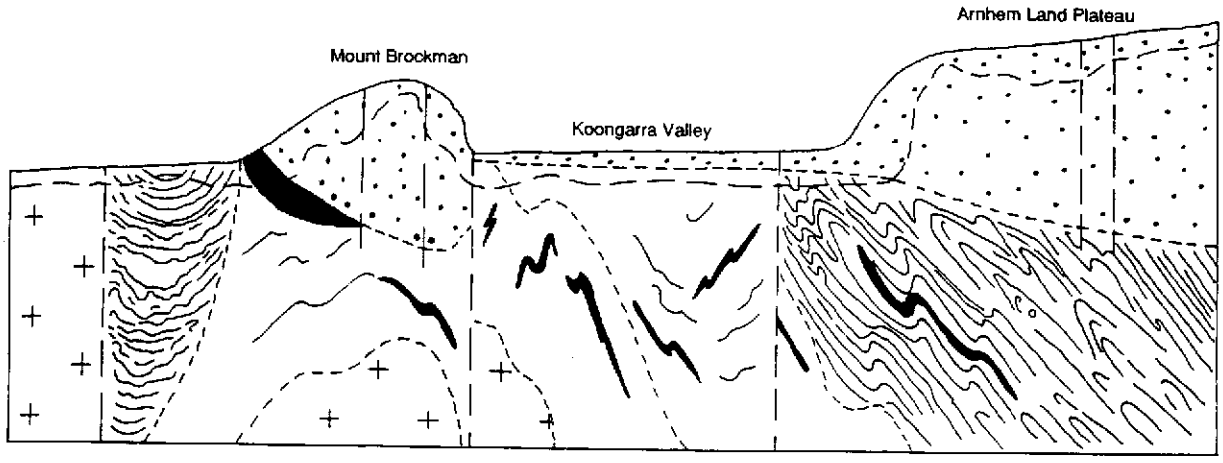

Figure 3.13 Wider view of the Koongarra Valley at 135 My, largely eroded (redrawn from Needham, 1982). The present landscape surface is shown as a dashed line.

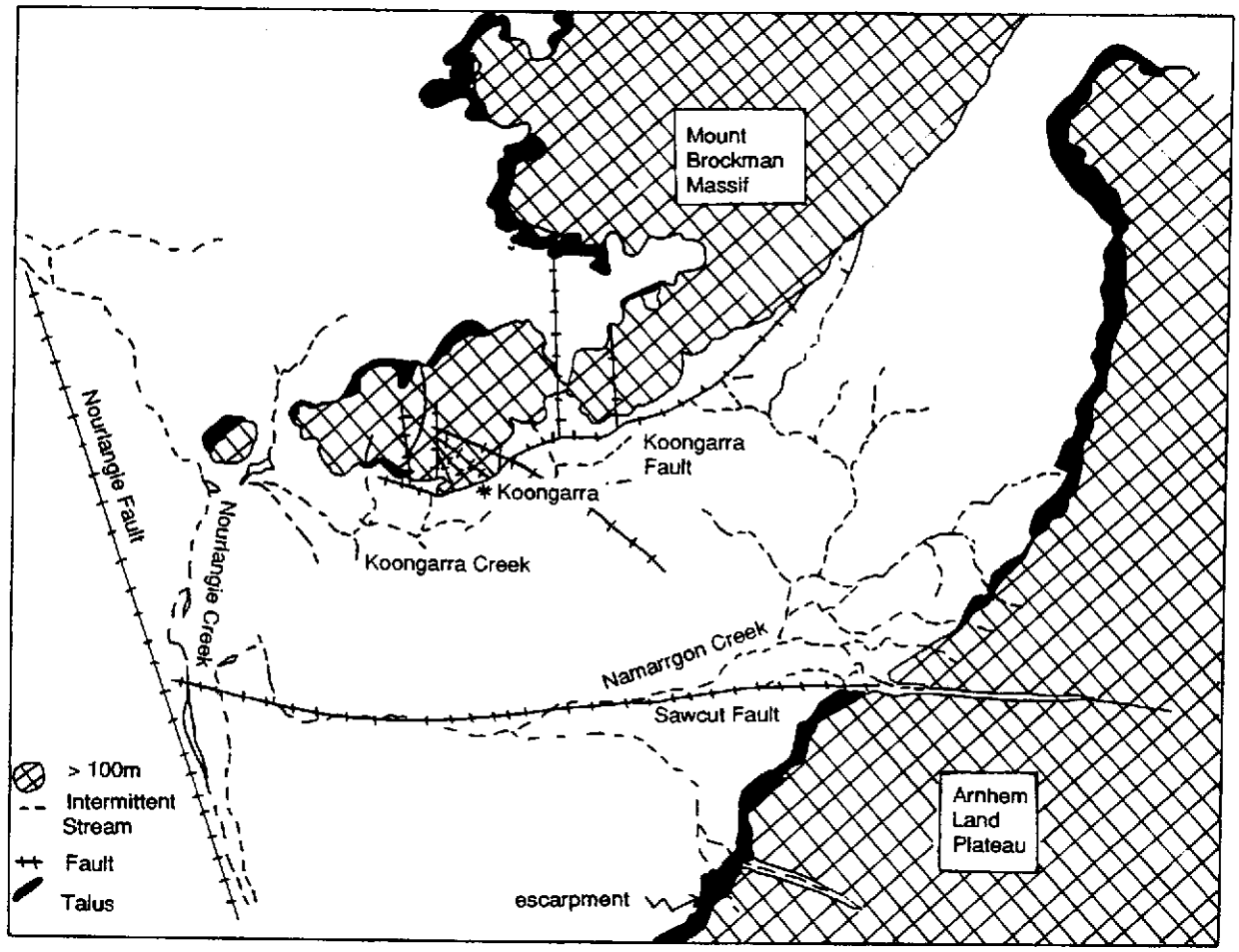

Figure 3.14 Plan view of the Koongarra Valley today for comparison, showing the positions of the escarpments and fault, and the drainage pattern.

produced and shaped the development of the secondary ore zone at Koongarra, the focus of this natural analogue study. Therefore, the geomorphical development is discussed in detail in Volume 3 of this series.

The Koongarra deposit today lies beneath a gently sloping ground surface below the sandstone escarpment of the Mount Brockman Massif. The area is covered in open woodland vegetation and is drained by a few short seasonal watercourses into Koongarra Creek, which flows west into Nourlangie Creek 7 km away. Figures 3.15 and 3.16 are oblique aerial photographs of the Koongarra area, while Figures 3.17–3.20 are ground photographs looking across the orebody and surrounding areas where ARAP investigations were conducted.

Apart from the Kombolgie sandstone of the Mount Brockman Massif, there is very little outcrop of the Cahill Formation in the area. Along the escarpment margins a coarse sandstone debris talus slope and eluvial sand on the flatter ground just beyond, blanket the weathered Cahill schists as far as Koongarra Creek. The main stream channels and flood plains largely consist of alluvial quartz sand, but in many swampy areas humic material formed by organic decay is present. Sandy loams cover most of the interfluves, where some locally extensive ferricrete also crops out. To the south-east beyond Koongarra Creek the ground surface is not sand covered, but is littered with quartz rubble weathered from the Cahill schists beneath. (For a fuller description of the geomorphology and surficial geology of the Koongarra area, see Volume 3 of this series.)

Of primary interest, however, is the immediate area containing the Koongarra orebodies, from the Kombolgie sandstone escarpment to Koongarra Creek. Figure 3.21 shows the topographic contours across that area, and Figure 3.22 is a schematic cross-section through the No. 1 orebody which defines and illustrates the different components of the profile down to the fresh schists. Covering the area, as already described, is the sandstone debris talus and eluvial sand that has been broken and washed down from the Kombolgie sandstone escarpment; Figure 3.23 is an isopach map showing the thickness of this surficial sand cover.

Beneath the sand cover is the zone of weathered schist (see Figure 3.22 again). There are, of course, subdivisions within the profile down through this weathered zone as reflected in the appearance, physical properties and mineralogical constituents of the weathered schists, and these will be dealt with in detail in Volumes 4, 5, 8 and 9 of this series.

Between the weathered schist zone and the unweathered (fresh) schists below is what has been called the transitional zone (see Figure 3.22 again). In this region there is marked change in colour of the rock, from the reddish and yellowish browns of the weathered schist to a greenish light grey, which is still distinct from the dark greys of the fresh schists. Fractures in this zone, as well as the schistosity surfaces, are still often coated with yellowish-brown iron oxides, so this zone reflects the onset of the weathering process on the fresh schists, but the process in not yet complete. Again, these colour changes reflect physical properties and

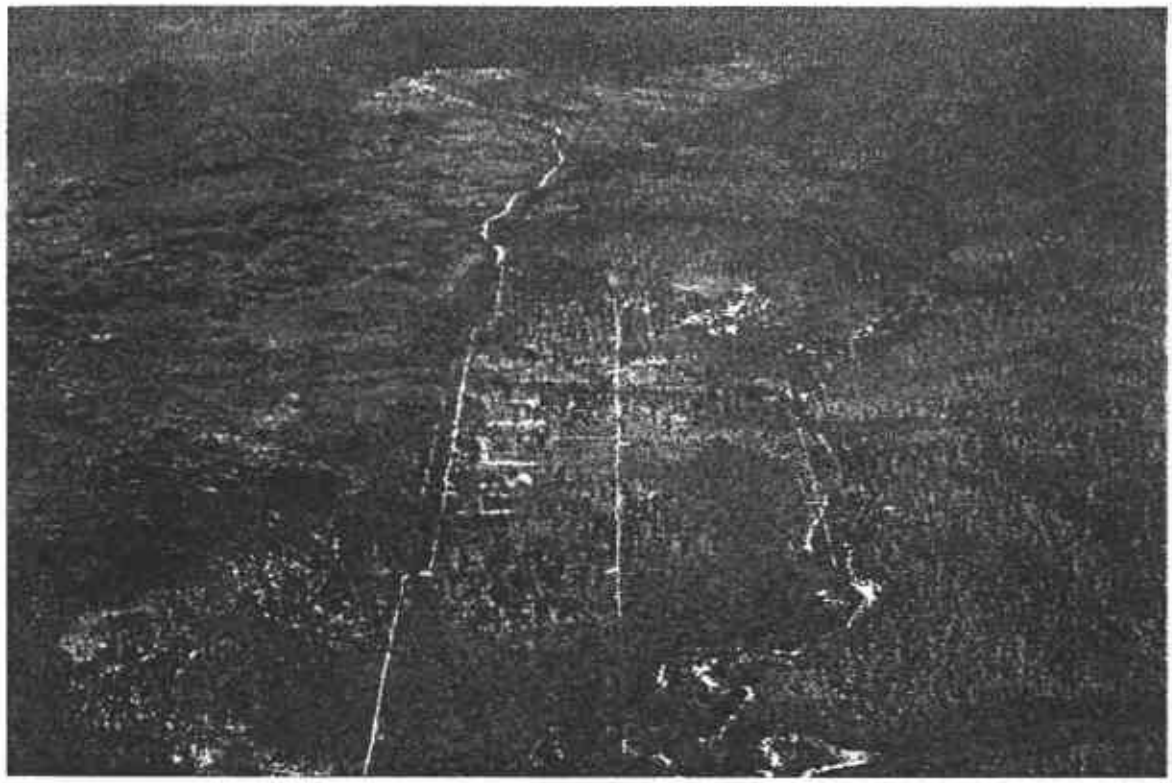

Figure 3.15 Oblique aerial photograph of the Koongarra area looking north-east (true) along the mine grid. The tracks running cross-wise in the centre view are the grid-lines along which cross-sections through the orebodies were drilled. To the left (true north-west) are the Kombolgie sandstone cliffs of Mt Brockman and to the right (true south-east) is Koongarra Creek.

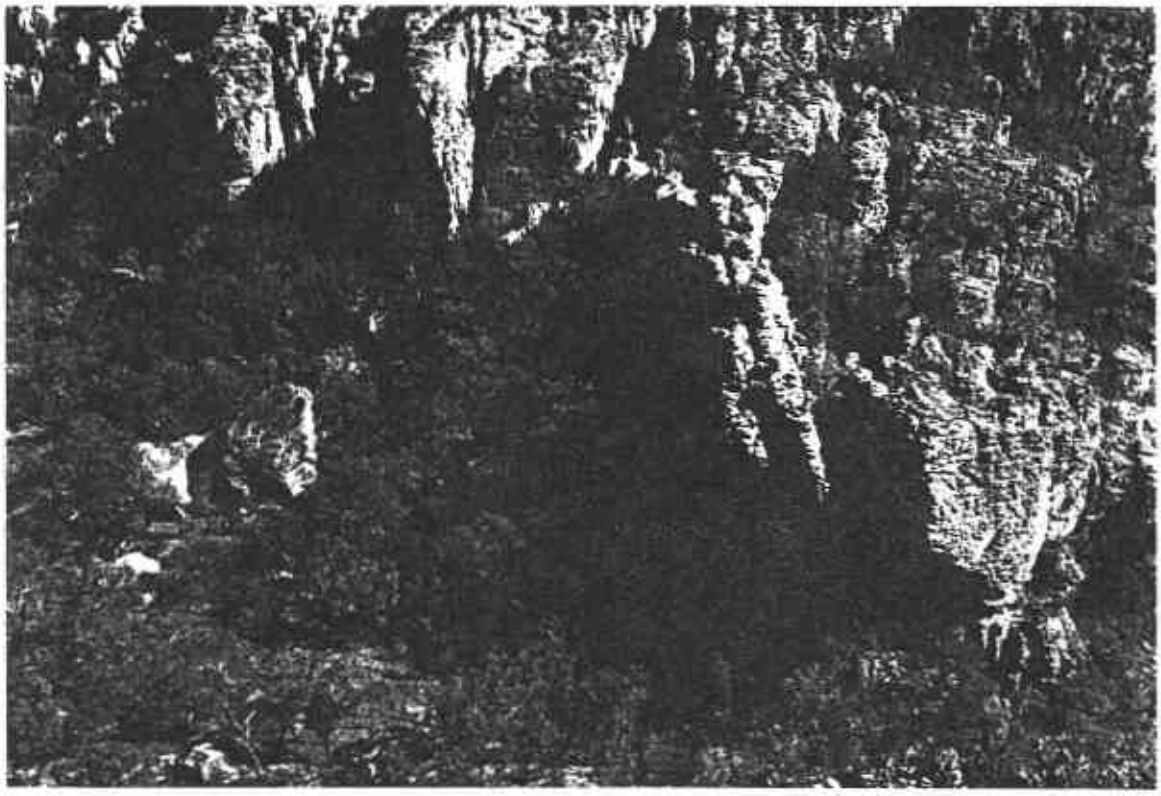

Figure 3.16 Oblique aerial view of the Kombolgie sandstone cliffs of Mt Brockman just to the north-west of the Koongarra No. 1 orebody.

Figure 3.17 View of the Koongarra No. 1 orebody area (across the centre of the photograph) as seen from Mt Brockman. In the distance is the line of Kombolgie sandstone cliffs that mark the edge of the Arnhem Land Plateau.

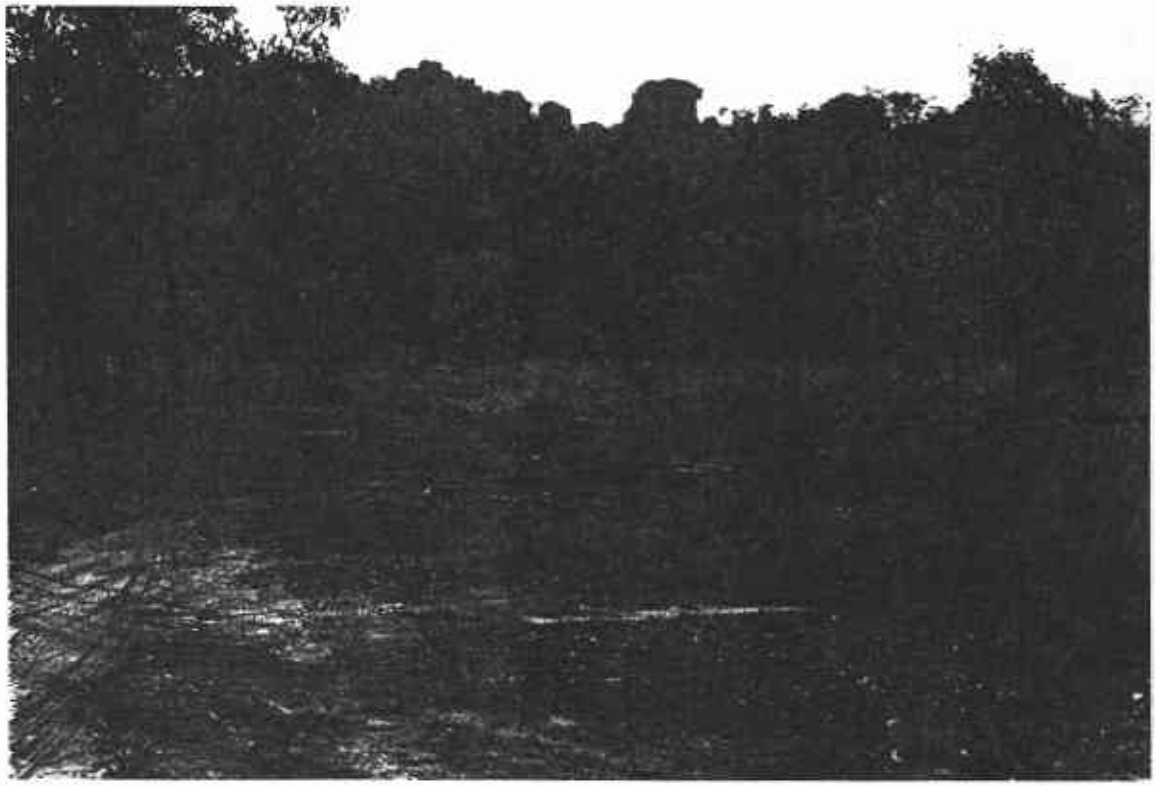

Figure 3.18 Ground level photograph looking across the Koongarra No. 1 orebody area along grid-line 6109 mN towards Mt Brockman.

Figure 3.19 Negotiating the sandy, terrain is not easy. Open boreholes (bottom right and centre right) can be seen here along grid-line 5865 mN. During torrential downpours in the "wet" season access is difficult as the water can run off faster than it infiltrates the sands.

Figure 3.20 Various methods of obtaining water samples were used. Here a double packer (black sections at each end) pump system is being prepared for lowering down PH 15 on grid-line 6048 mN. Work was mostly done during the "dry" season—the dry brown "spear" grass attests to the intense seasonal aridity and high temperatures (around 35°C).

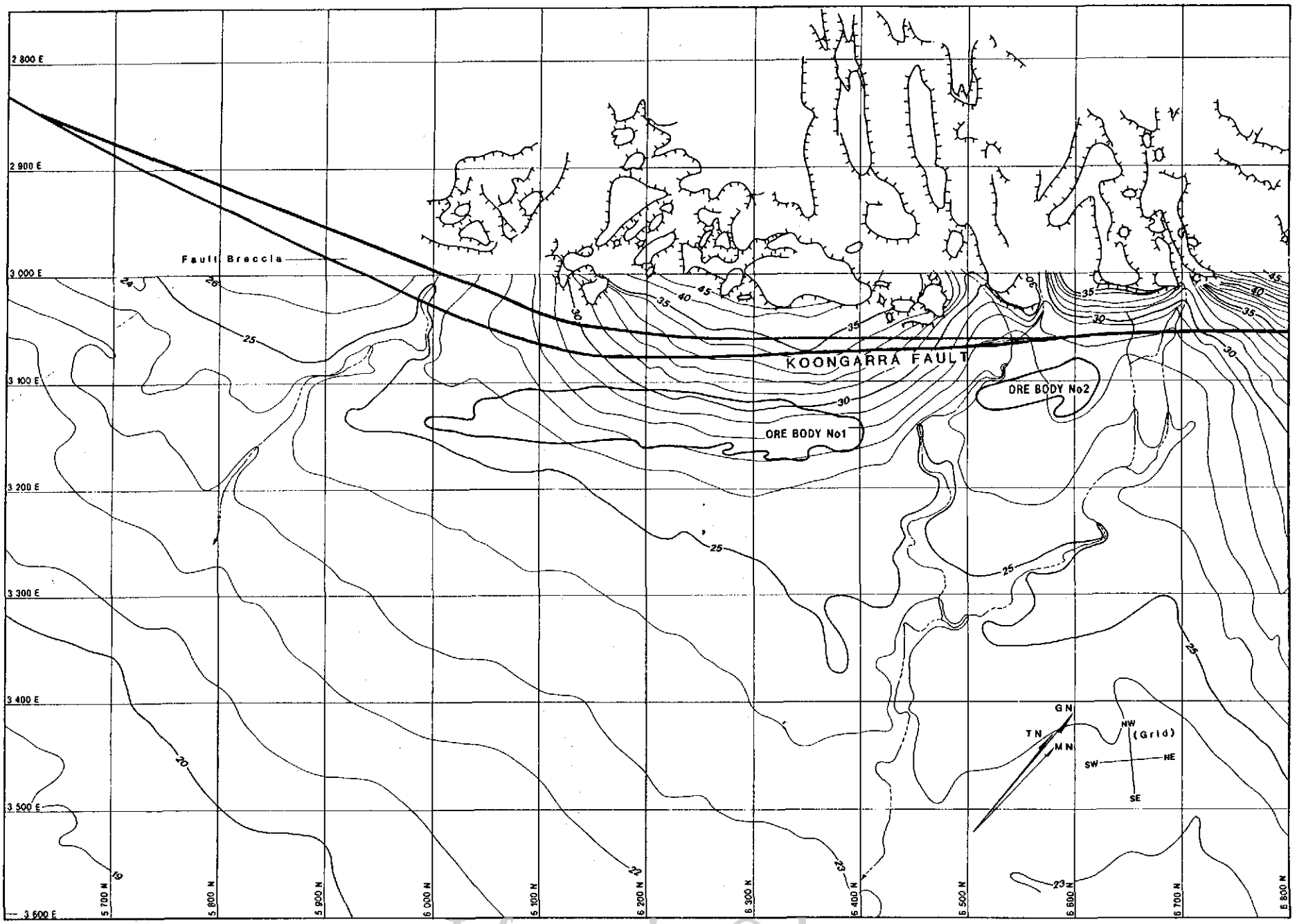

Figure 3.21 Site plan of the Koongarra area showing the Kombolgie sandstone escarpment and the topographic contours of the ground surface above the orebodies.

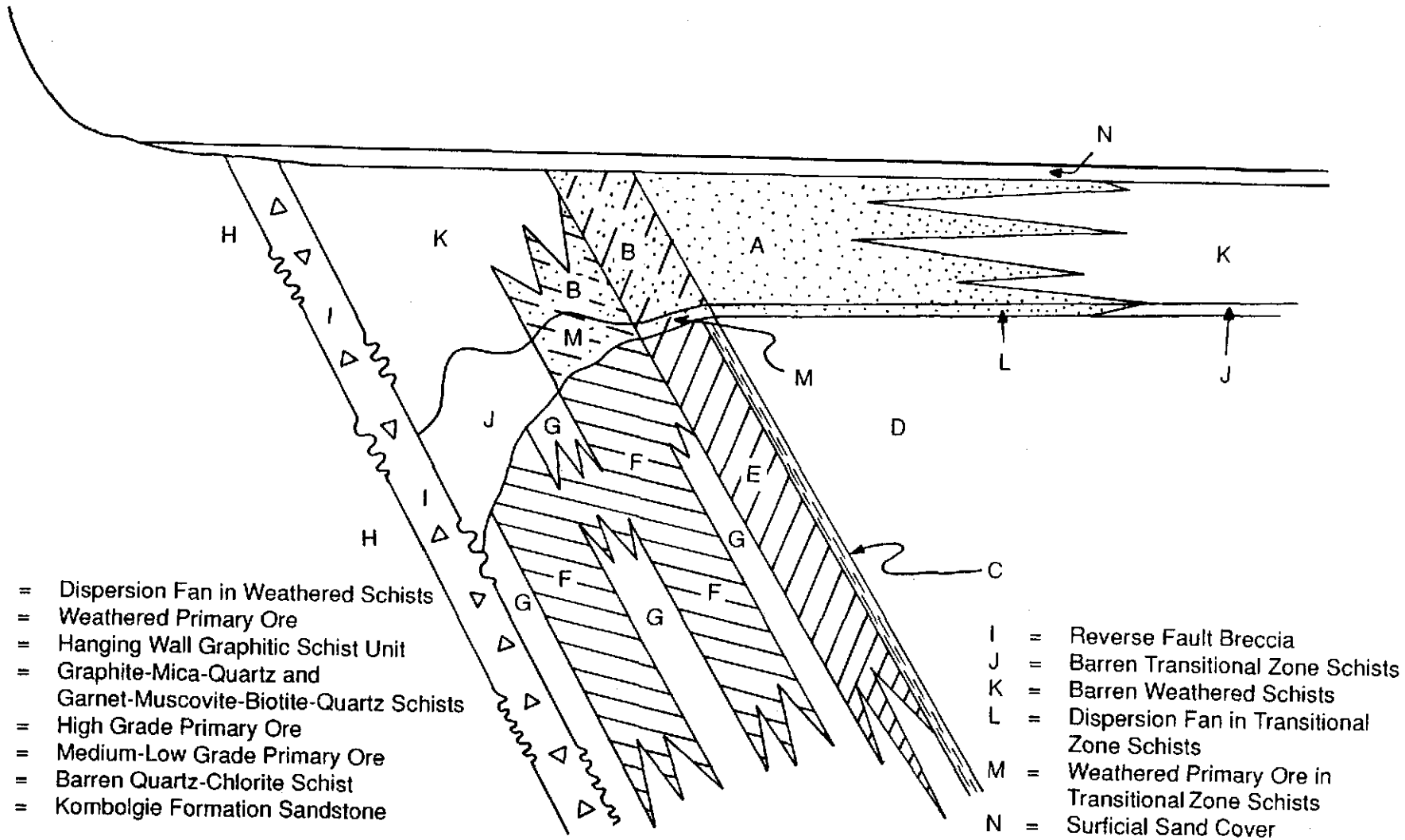

Figure 3.22 Schematic cross-section through the Koongarra No. 1 orebody showing the rock units of the mine sequence, the weathered and transitional zones, and definitions of the ore zones.

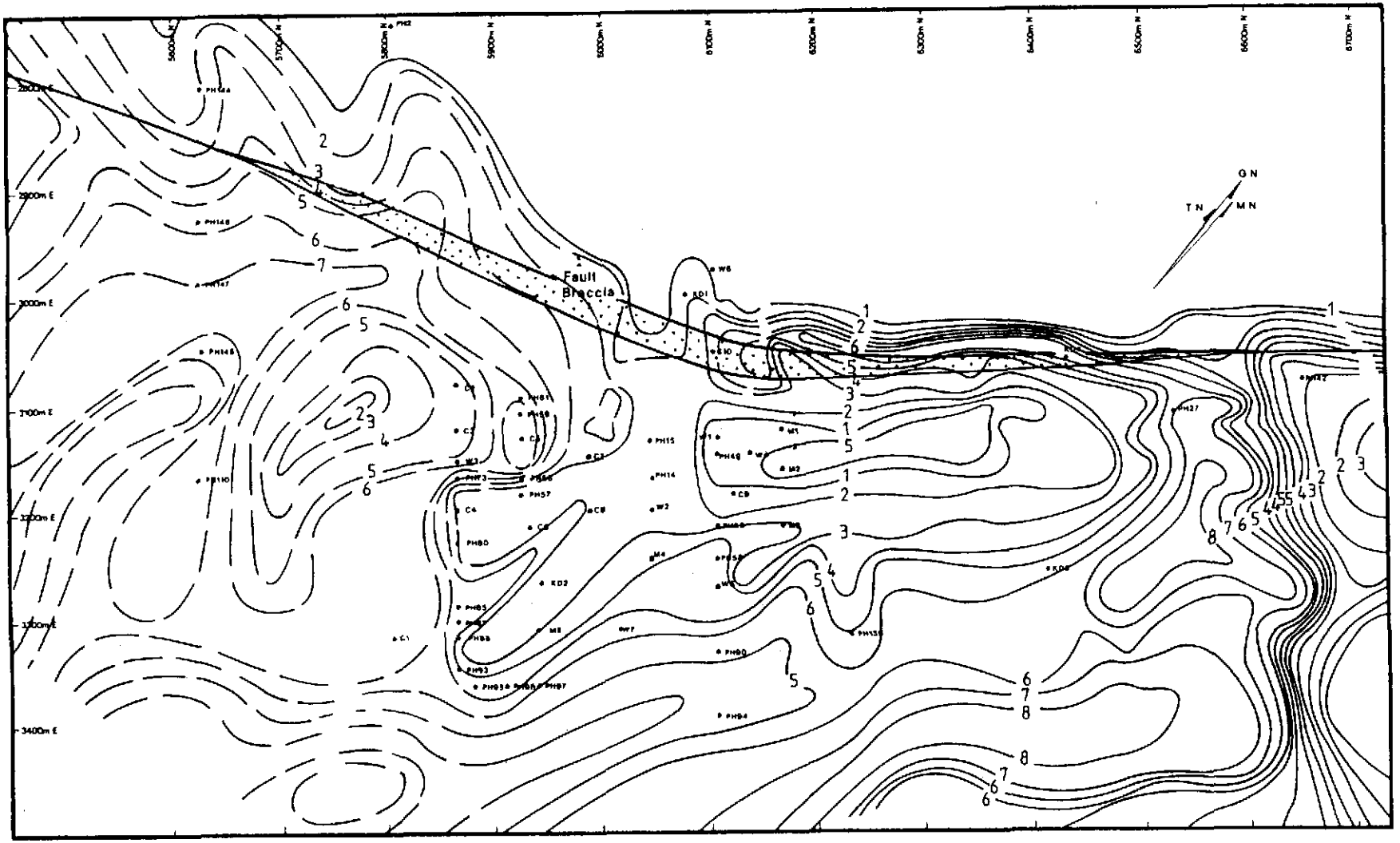

Figure 3.23 Koongarra site plan showing isopachs for the thickness of the surficial sands

mineralogical changes that will be described in Volumes 4,5, 8 and 9 of this series. Figure 3.24 is an isopach map showing the total thickness of the zones of surficial sands and weathered schists, that is, the depth (thickness) from the surface of the unweathered (fresh) schists.

Figure 3.22 also depicts schematically the different ore zones or types within the Koongarra No. 1 orebody. These boundaries between what constitutes ore and non-ore (barren schist) are of course not arbitrary, but are based on what are considered to be economically exploitable concentrations of uranium, the boundaries representing a mining "cutoff grade". For Noranda the cutoff grade was 0.018% or 180 ppm U_3O_8, while for Denison it is currently 0.02% or 200 ppm U_3O_8.

In the unweathered (fresh) schists are both high-grade and medium-low grade ores and, as has already been depicted on Figure 2.4, these are uraninite dominated ore and uranyl silicates dominated ore, respectively. However, all these ore types here constitute what will be called the primary ore, in the primary ore zone within the unweathered schists. It should be noted that the use of the word "primary" in this context does not necessarily imply timing and/or genesis, although of course, the primary ore at Koongarra, being in the unweathered schists, was in place before weathering occurred.

Immediately above, and up-dip of, this primary ore in both the transitional zone and the weathered schist is ore that was obviously once primary but now is weathered. Consequently it is here designated as weathered primary ore, which consists of uranyl phosphates. Adjacent to it and downslope of it, again within the weathered schist and transitional zone, is ore that represents uranium which has been mobilised from the weathered primary ore and dispersed downslope to form what has been designated as the dispersion fan. Its depicted boundaries are an economic cutoff grade although uranium is still to be found dispersed in the weathered schist further downslope (see Volume 8 of this series). Until now, uranyl phosphates have only been identified in the dispersed ore adjacent to the weathered primary ore (see Figure 2.4 again). The weathered primary ore and the dispersion fan together are here called the secondary ore.

It is important that those geological variations across the site that are important in the characterising and study of the natural analogue are emphasized. The site is not uniform throughout, there being spatial variations and heterogeneities in the geology in the region of the natural analogue — the weathered primary ore and dispersion fan. For example, in Figure 3.20 the weathered schist which contains the natural analogue is schematically depicted as a uniform zone, but this can be misleading. The weathered primary ore is in weathered quartz-chlorite schist and weathered graphite-quartz-chlorite schist, whereas the dispersion fan is in weathered graphite-mica-quartz schist and garnet-muscovite-biotite-quartz schist. There is also the schistosity which dips at 55° to the south-east, and there are fractures at different angles. Hence, these geological variations and heterogeneities impinge on the natural analogue and need to be taken into account in the modelling of radionuclide transport.

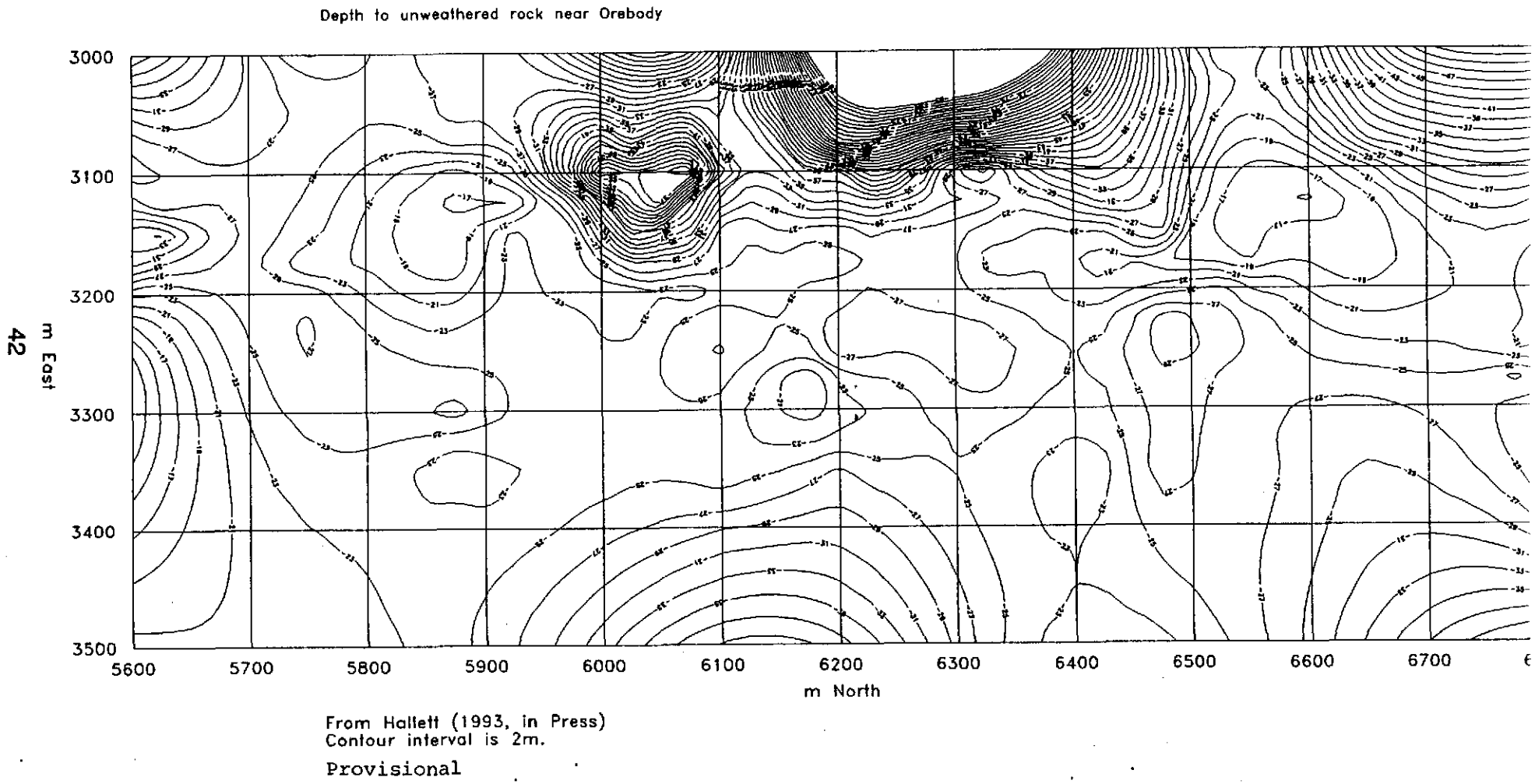

Figure 3.24 Koongarra site plan showing isopachs for the total thickness of the surficial sands and weathered schists.

In summary, the following geological factors contribute to variations and heterogeneities across the natural analogue site:

(a) the different host schist units with different mineral constituents and percentage compositions;

(b) mineralogical and geochemical variations within each of the host schist units (for example, the graphite-mica-quartz schist with its variable graphite content and accompanying sulfide minerals);

(c) the presence of the hydrothermal alteration halo centred on the primary ore (including the weathered primary ore) which decreases outwards in its effects, mineralogy and geochemistry;

(d) the general 55° dip to the south-east of the host schist units and their schistosity; and

(e) the presence of fractures and breccia zones which cross-cut the schistosity at different angles, and occasionally parallel the schistosity.

4 SAMPLING FOR THE NATURAL ANALOGUE STUDY

4.1 Reference Grid Used for Drilling and Sampling

The reference grid over the Koongarra mineralisation as surveyed in by Noranda is orientated at 46° east of true north, with its origin an arbitrary datum located approximately at latitude 12° 52' 02" south, longitude 132° 47' 50" east. This orientation was chosen to coincide with the orientation of the mineralisation. All the drilling, therefore, was along cross-sections through the mineralisation, perpendicular to the strike of both the host schists and the mineralisation, that are northings on the grid. Unfortunately, Noranda chose to use imperial measurements, so these cross-sections are 100 feet (30.5 metres) apart. Denison later converted all cross-sections to metric, but also shifted the origin datum 3000 m grid south so that the northings and eastings for any given grid point are now dissimilar.

The advantage of such a grid system is that any point can be located anywhere in the area by simply referring to its coordinates. Thus in the original Noranda system, for example, the first four diamond drill holes were drilled along the cross-section 10200 feet N, which cuts through the area of highest ground surface radioactivity. The positions of the drill hole collars along the 10200 feet N grid line were then each assigned an easting — 10401 feet E, 10425 feet E, 10518 feet E and 10583 feet E respectively. The Denison metric system, used for the natural analogue study, involves conversion of the northings and eastings from feet to metres, but 3000 m is added to the northings, so the cross-section becomes 3109 m + 3000 m = 6109 mN, while the eastings become 3170 mE, 3178 mE, 3206 mE and 3226 mE respectively. It should thus be self-evident that the northings being in the 6000s and the eastings in the 3000s avoids potential confusion, particularly if they are inadvertently misquoted.

Figure 3.24 Koongarra site plan showing isopachs for the total thickness of the surficial sands and weathered schists.

Elevations are referenced in metres above the Australian Height Datum (AHD).

4.2 Pre-ARAP Drilling and Uranium Analyses

Because the schistosity and metamorphic layering of the rocks that host the uranium mineralisation at Koongarra dip at approximately 55° to the south-east, the cored holes were all drilled at an inclination of approximately 50° to the north-west so as to intersect the mineralisation perpendicular to the schistosity and thus sample the true thickness. This also means that the drill holes were all along the desired cross-sections on grid northings. On average there were at least five of these inclined cored holes drilled on each cross-section, the latter being 30.5 metres apart. Beyond the limits of economic mineralisation to the north-east and south-west, only vertical percussion exploration holes were drilled, still on cross-sections 30.5 metres apart. Figure 4.1 is a site plan of the Koongarra deposits showing the Denison metric mine grid and the locations of drill holes. The prefix 'DDH' indicates diamond drill hole, while 'PH' indicates a percussion hole.

Samples from a large number of these drill holes have been used in the course of this natural analogue study, so it is important to have some background on the way Noranda handled these drill cores and percussion drilling rock chips. The cores were placed in metal trays by the drillers, the trays being 3 feet (almost 1 metre) long with 5 or 7 rows per tray depending on the drill core thickness. Small coloured wooden blocks were placed in the trays at regular intervals and the hole depths recorded on them. In the core splitting shed on site, the cores were first washed and cleaned before a geologist inspected them and recorded the geological details/description, along with scintillometer radiometric counts for each section in the trays. On this basis, cores were selected for assay. Each assayed section of core was normally 5 feet (1.53 metres) long but occasionally less in very distinctive high grade ore zones.

Each section of core was then split using a screw type core splitter. One half of the split core was sent for assay, the remaining half being returned to the trays for record purposes. All the trays of drill core were then stored in racks in core sheds on the site. At the assay laboratories each section of half core was crushed and rolled before being split into a 150 g assay sample and a pulp residue. The assay sample was pulverised and only 3–4 g of it was used for uranium assay. The pulp residue and the pulverised assay residue were both returned to Noranda for storage in boxes above the corresponding racks of core trays in the sheds at Koongarra.

Percussion drilling, on the other hand, does not produce core. Instead, rock chips and pulverised rock powder are blown or washed out of the hole, where they are collected as the drill-bit continues to advance downwards. These rock chips and rock powders were collected over each 1.53 metre interval during drilling, with a Noranda field assistant maintaining a radiometric (scintillometer) and sample number record. From each of these 1.53 metre intervals of accumulated rock chips and powder, a geological record sample, a 1.36 kg assay sample and a bulk residue sample were collected.

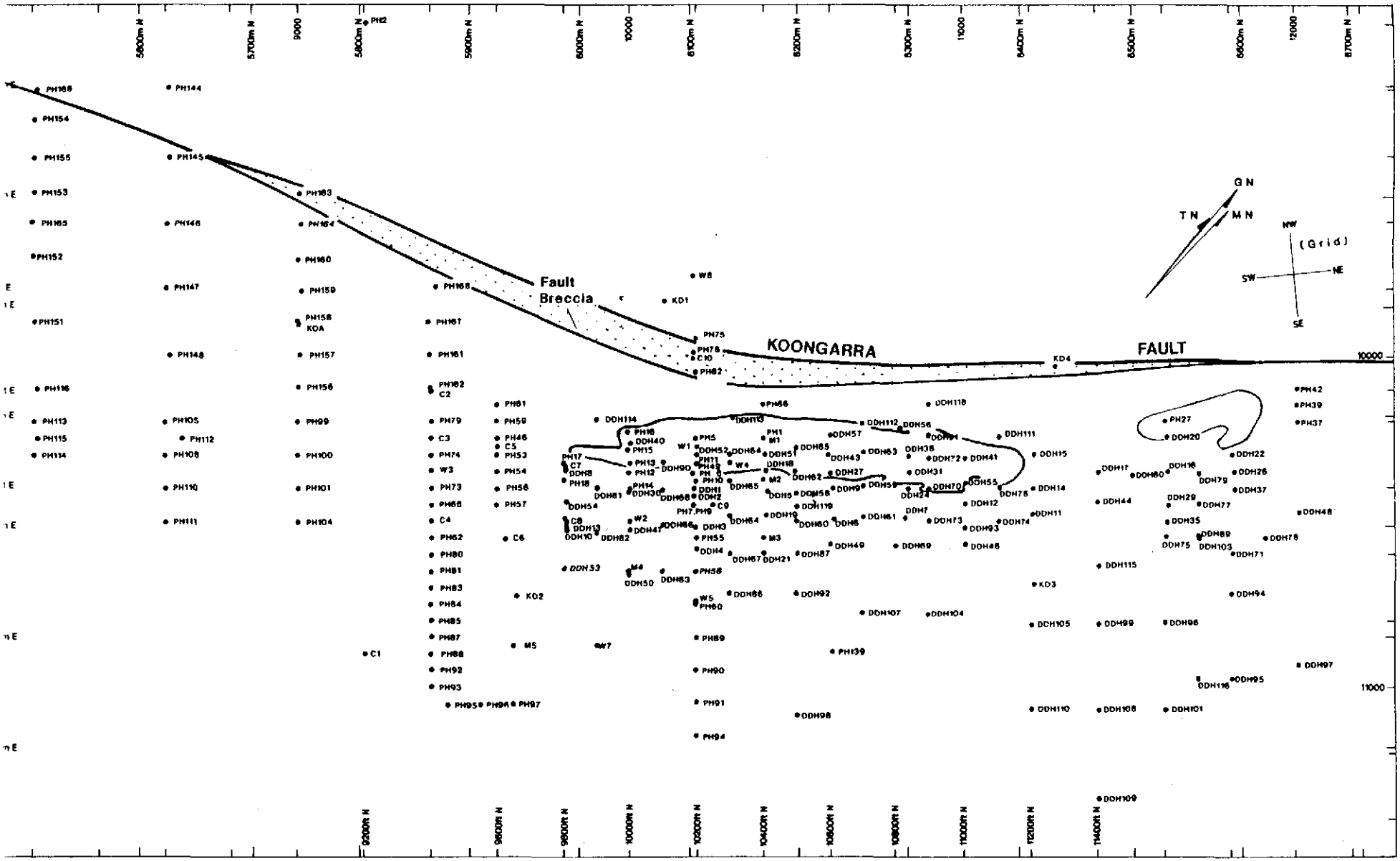

Figure 4.1 Koongarra site plan showing the mine grid and all drill hole locations.

The geological record and bulk residue samples were stored in boxes above the core tray racks in the Koongarra sheds, while the assay samples were despatched to the assay laboratories. There the same procedure as for the drill core was followed — crushing and rolling, separation into a 150 g assay sample and a pulp residue, pulverising of the assay sample, with 3–4 g being assayed for uranium. Again the pulp residue and the pulverised assay residue were both returned to Koongarra for storage.

All assay data were recorded on the same record sheets as the geological details and radiometric measurements for each drill hole. It is these record sheets that are usually referred to as drill logs, and the data on these, being the major description of what is actually in the ground, forming the basis for the natural analogue study and the sampling associated with it.

4.3 ARAP Sampling and Drilling

The availability of well catalogued, stored and retrievable drilling samples, and access to them and the drill core, has been critical for the natural analogue study, and the support of Denison Australia Pty Ltd is gratefully acknowledged by the ARAP. A large number of the drill holes plotted on Figure 4.1 have been sampled during this study, particularly those holes that cover the south-western half of the No. 1 orebody and its environs, where there are more open vertical boreholes (PHs) available for sampling the groundwater. Both pulp residues from percussion and diamond drill holes, and core samples were used. Figures 4.2–4.12 are all the relevant cross-sections along which drill holes were sampled. The geology and outlines of economic mineralisation are also shown with the drill holes. All the drill logs for the holes are available from Denison Australia Pty Ltd.

As the natural analogue study progressed it was found that

(a) detailed coverage of the south-western half of the No. 1 orebody and its environs was not as complete as needed for hydrogeological characterisation of the site, and monitoring and modelling of the groundwater chemistry and flow;

(b) since the holes were drilled in the period 1970–73 there was concern that the samples and drill core, having sat in the sheds at Koongarra for so long, were now oxidised and degraded; and

(c) coverage of the weathered zone dispersion fan, the principal modelling objective of the analogue study, was in places quite sparse, particularly near to the surface where there were either large core losses or the core was very degraded.

Consequently, late in 1988 twenty-two new holes were drilled for the natural analogue study by drilling crews from the Northern Territory's Power and Water Authority. The financial support of the Northern Territory Government for this work is gratefully acknowledged by the ARAP.

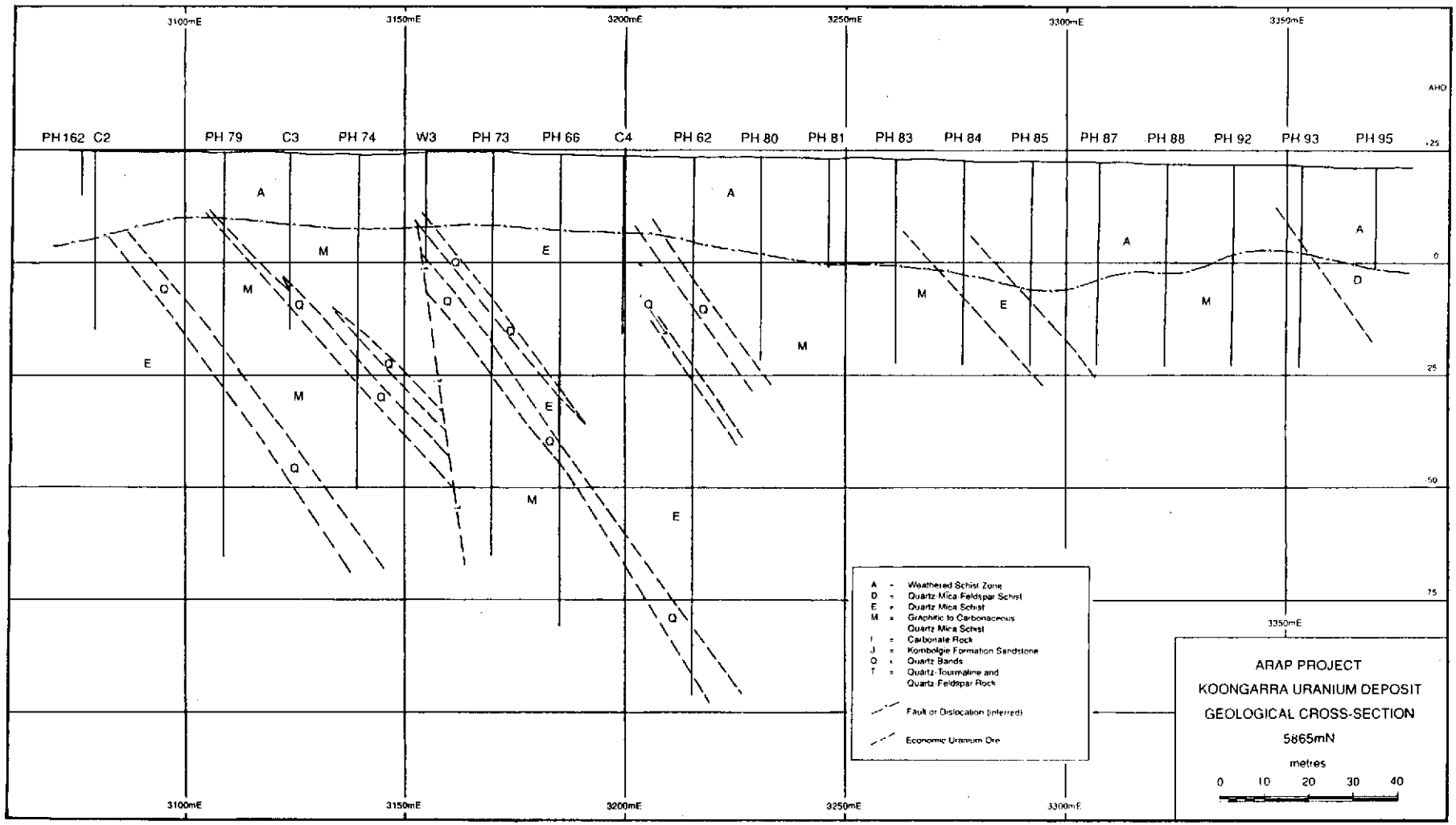

Figure 4.2 Koongarra cross-section 9400 ft (5865 m)N showing geology, drill holes and outlines of economic mineralisation grades.

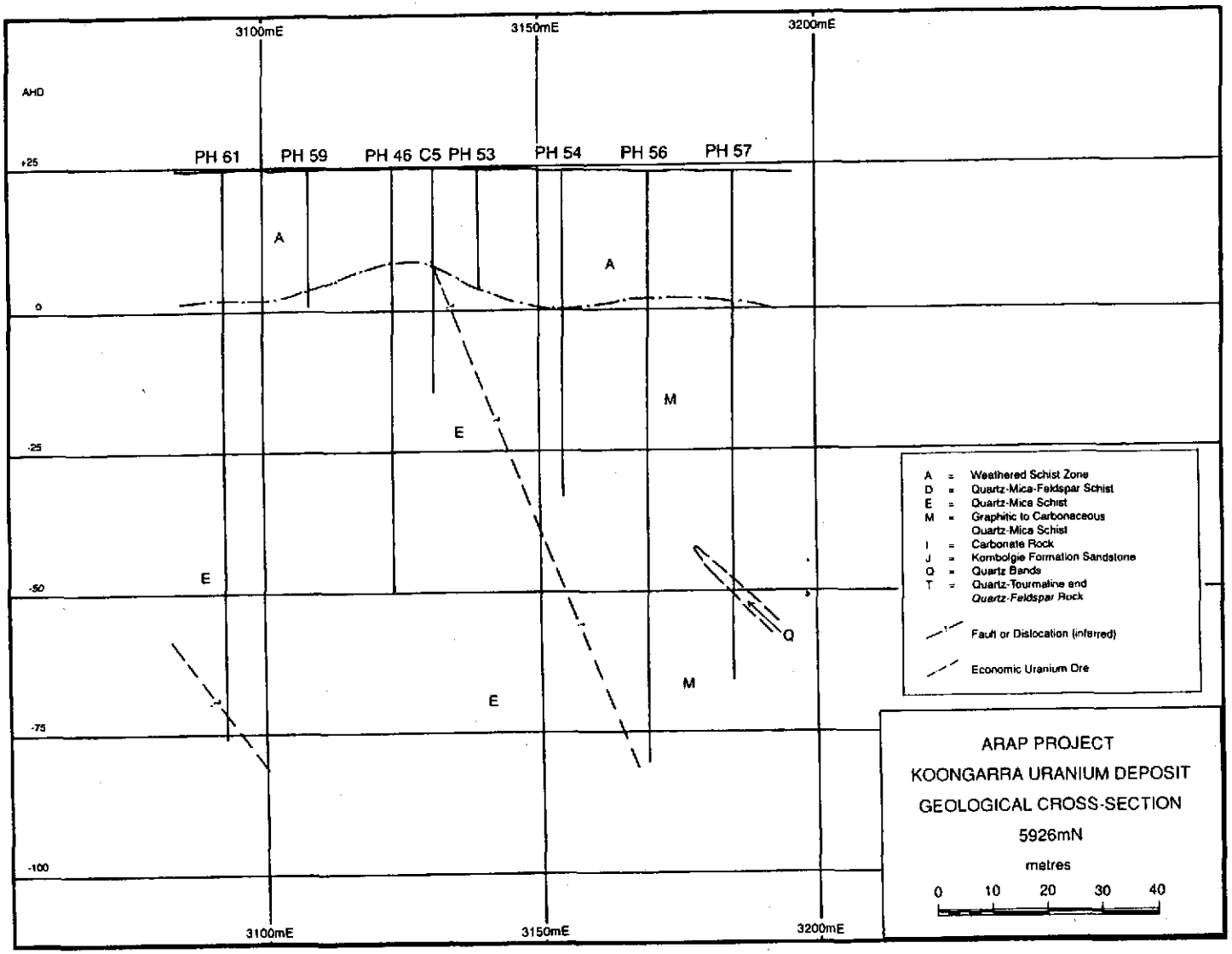

Figure 4.3 Koongarra cross-section 9600 ft (5926 m)N showing geology, drill holes and outlines of economic mineralisation grades.

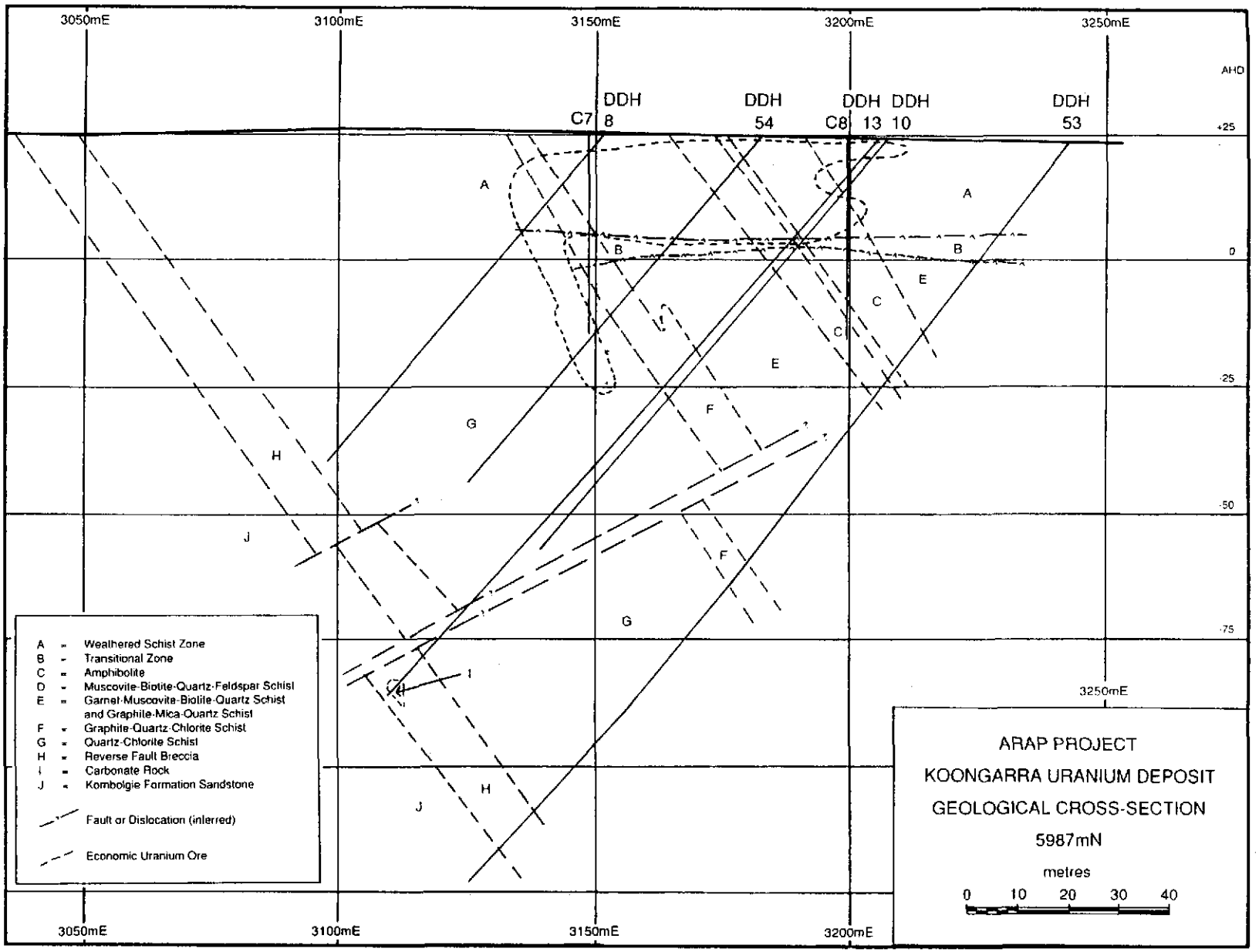

Figure 4.4 Koongarra cross-section 9800 ft (5987 m)N showing geology, drill holes and outlines of economic mineralisation grades.

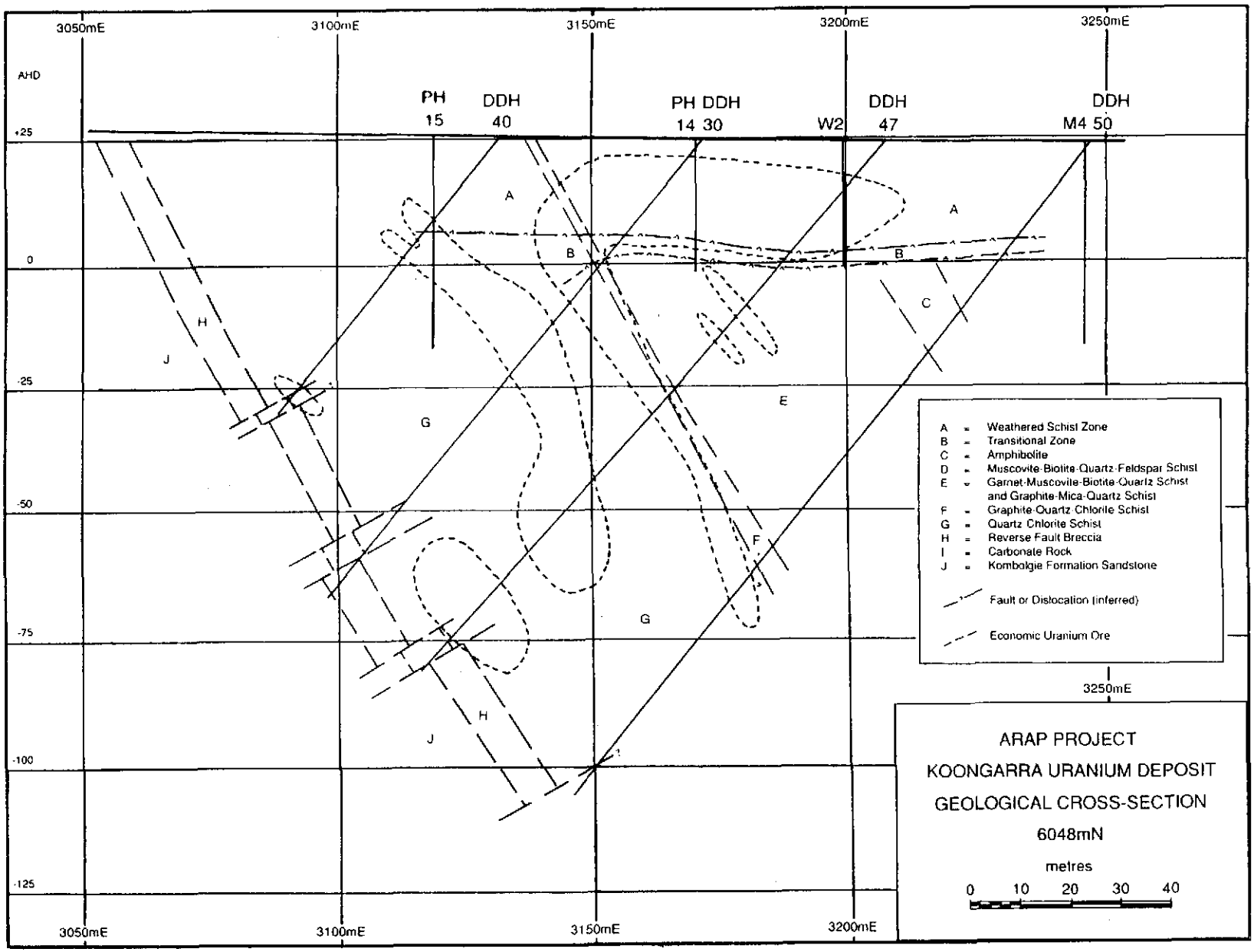

Figure 4.5 Koongarra cross-section 10000 ft (6048 m)N showing geology, drill holes and outlines of economic mineralisation grades.

Figure 4.5 Koongarra cross-section 10000 ft (6048 m)N showing geology, drill holes and outlines of economic mineralisation grades.

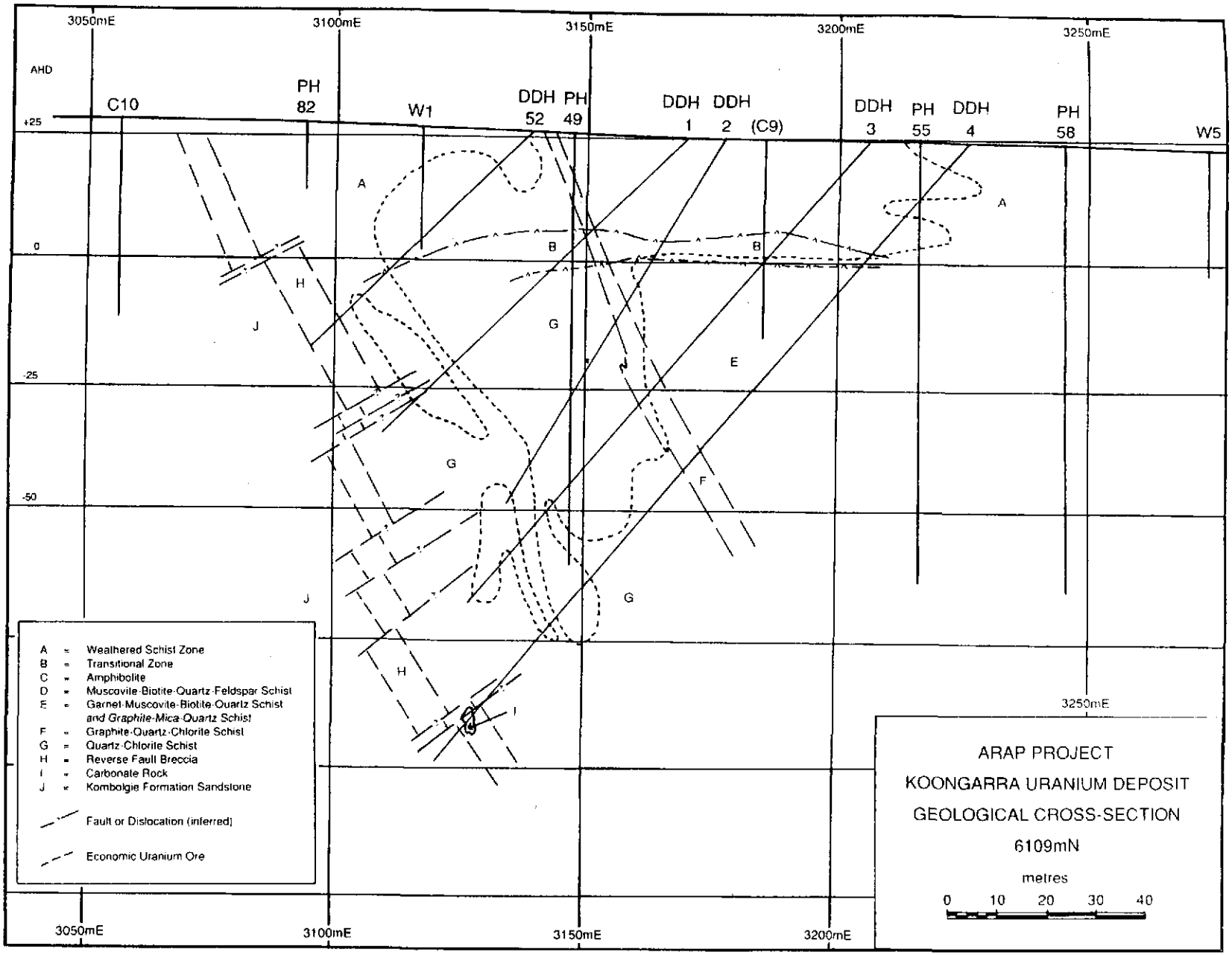

Figure 4.6 Koongarra cross-section 10200 ft (6109 m)N showing geology, drill holes and outlines of economic mineralisation grades.

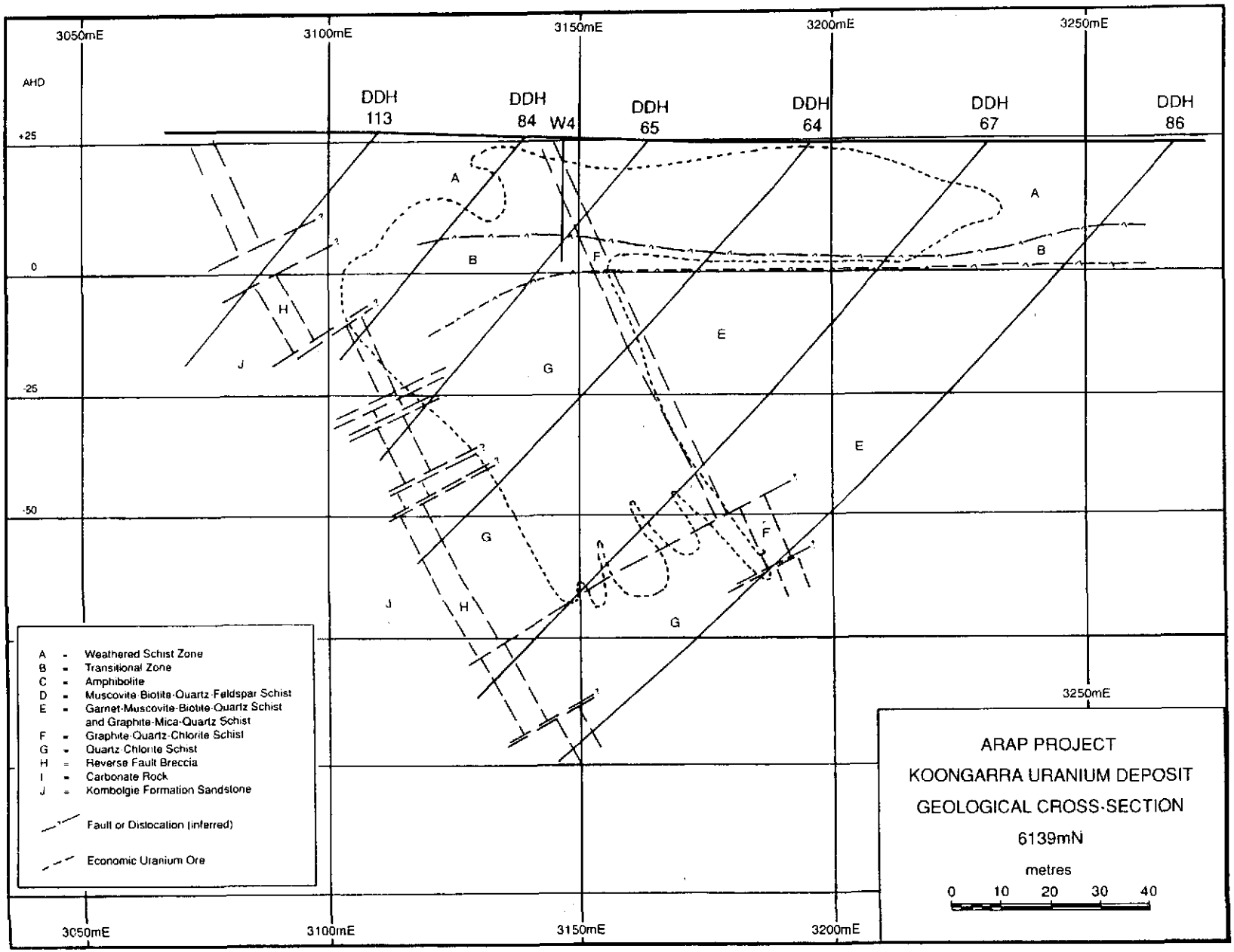

Figure 4.7 Koongarra cross-section 10300 ft (6139 mN showing geology, drill holes and outlines of economic mineralisation grades.

3050mE

Figure 4.7 Koongarra cross-section 10300 ft (6139 m)N showing geology, drill holes and outlines of economic mineralisation grades.

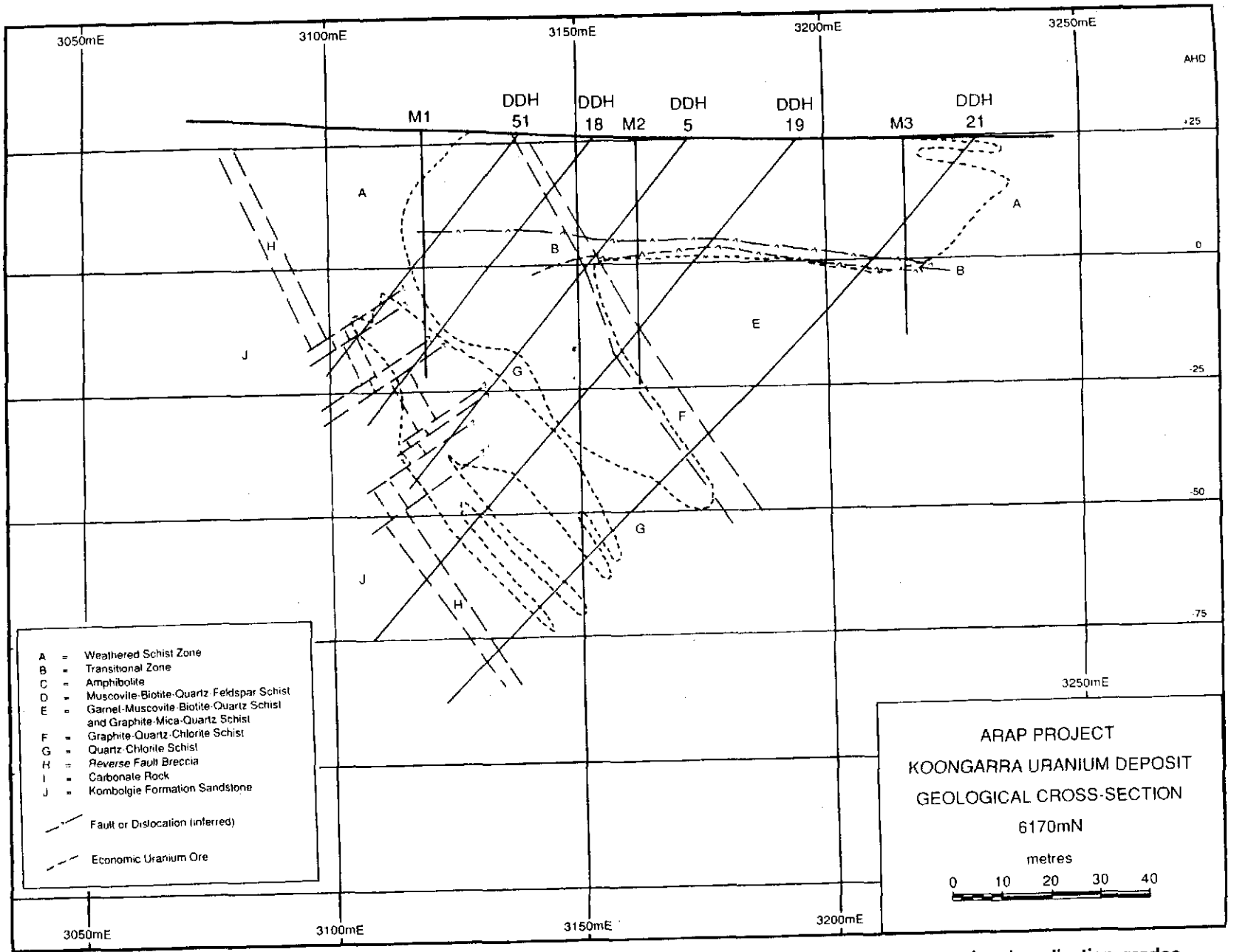

Figure 4.8 Koongarra cross-section 10400 ft (6170 m)N showing geology, drill holes and outlines of economic mineralisation grades.

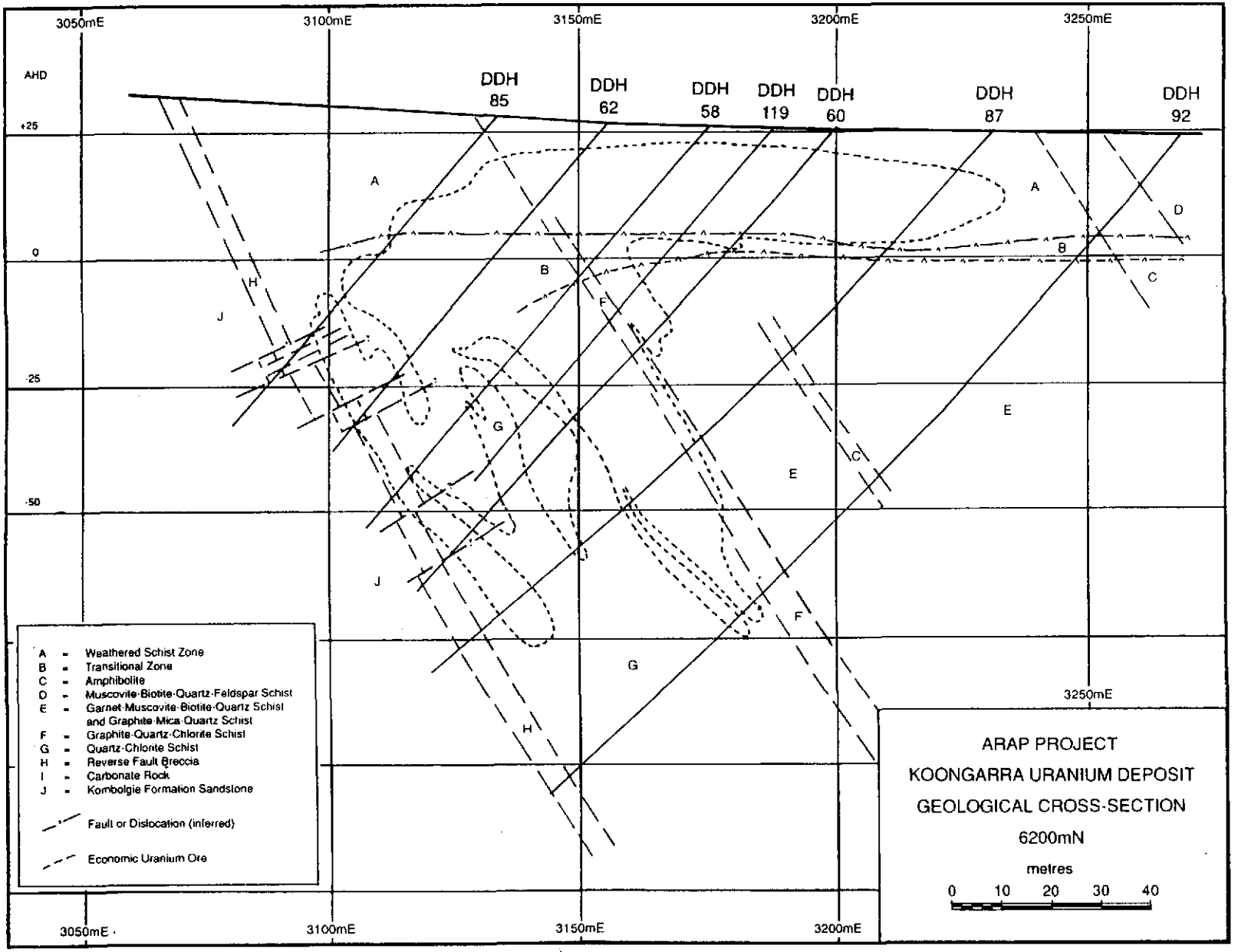

Figure 4.9 Koongarra cross-section 10500 ft (6200 m)N showing geology, drill holes and outlines of economic mineralisation grades.

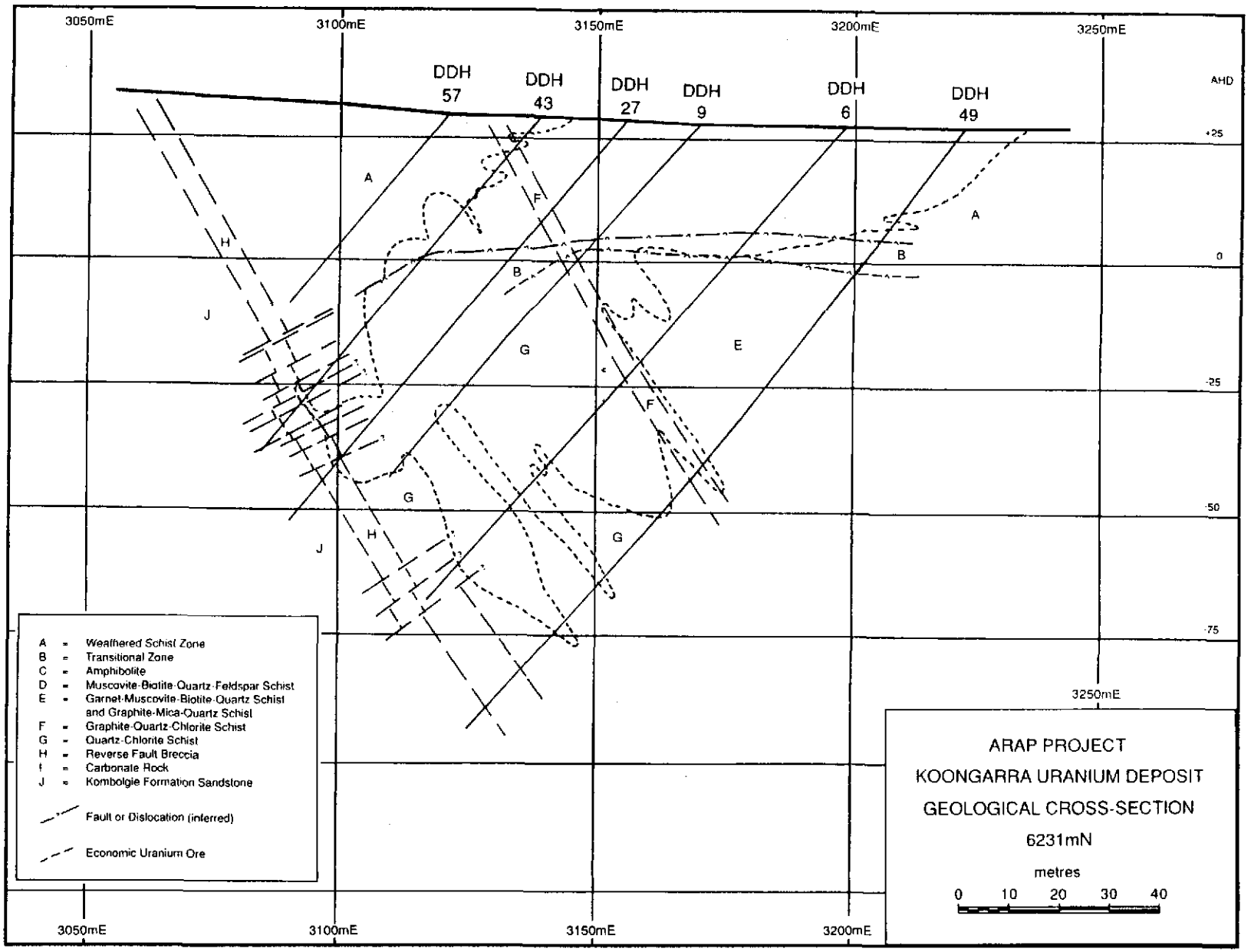

Figure 4.10 Koongarra cross-section 10600 ft (6231 m)N showing geology, drill holes and outlines of economic mineralisation grades.

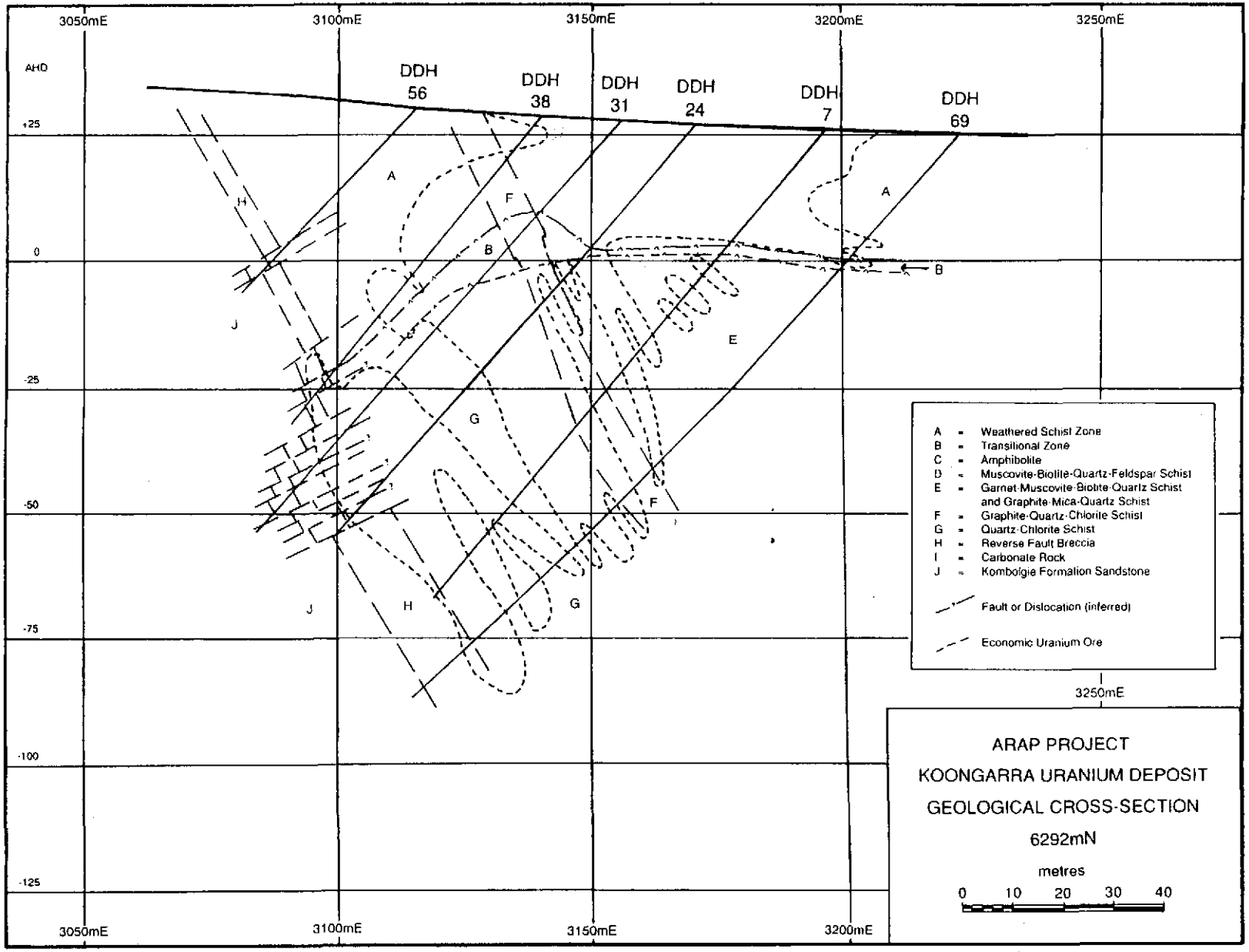

Figure 4.11 Koongarra cross-section 10800 ft (6292 m)N showing geology, drill holes and outlines of economic mineralisation grades.

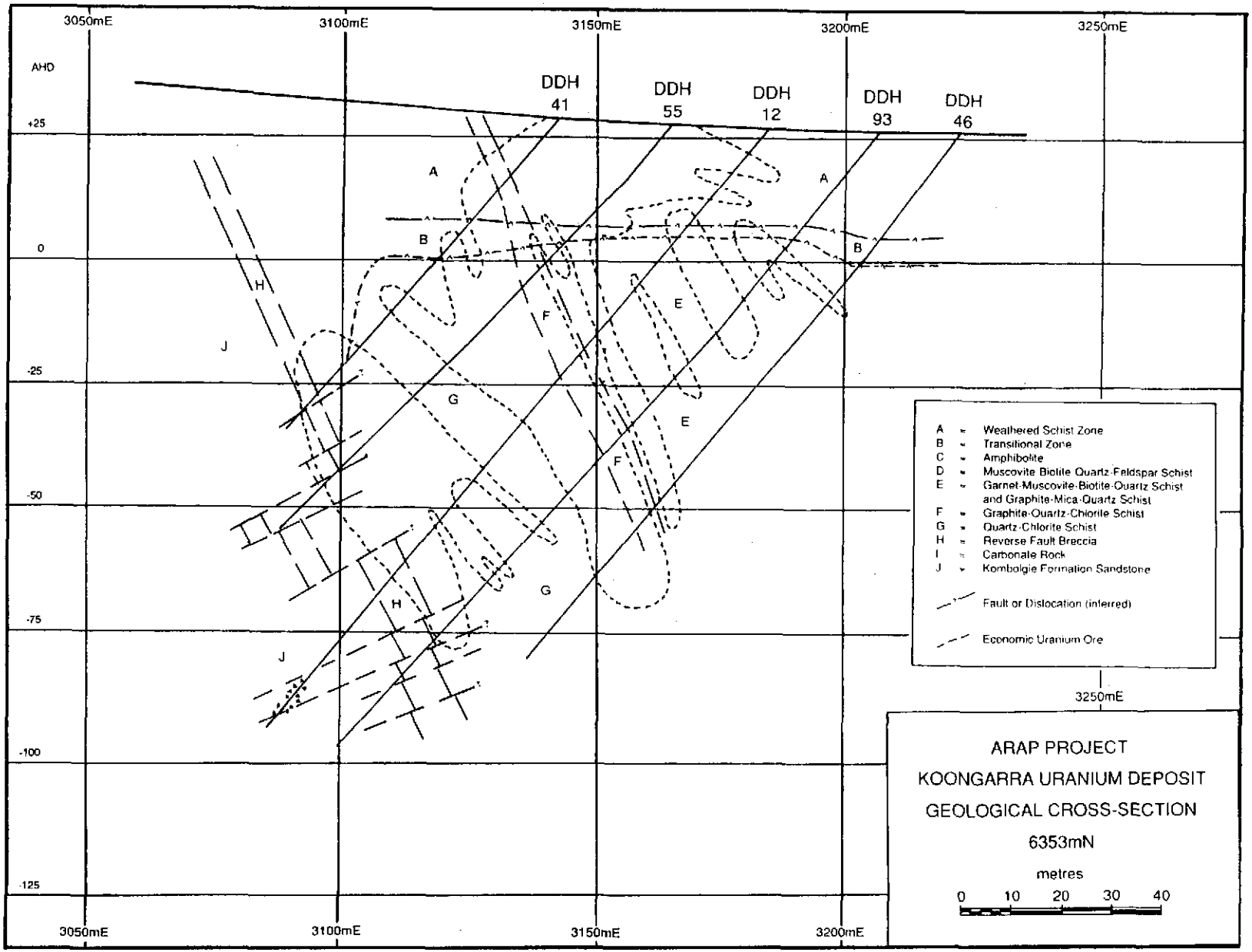

Figure 4.12 Koongarra cross-section 11000 ft (6353 m)N showing geology, drill holes and outlines of economic mineralisation grades.

The Koongarra site plan (Figure 4.1) shows the locations and designations of the ARAP-drilled holes, while Appendix 7 contains the geological details of these holes as drill logs. There were three series of holes drilled:-

(a) M1–M5 were to be monitoring holes from which strategic samples through the weathered zone would be obtained;

(b) W1–W7 were designated as water sampling holes and constructed accordingly; and

(c) C1–C10 were to be cleared holes for pump tests, standing water levels monitoring and general purposes.

Two different drill rigs were used, thus providing different types of samples. The cable tool rig, the slower of the two machines, works on the principle of pulverising the rock by the up and down pounding movement of a drill bit on a long cable.

When drill core is required, a drive tube is pounded into the rock. The process is thus tedious, and so is really only suited to penetrable weathered rock, from which it obtains a far better core than does a diamond drill. The weathered zone was in this manner sampled at a rate of 0.2–0.3 m of core in every metre drilled in as many of the M- and W-series holes as possible.

Because of the inability of the cable tool rig to penetrate and effectively sample fresh rock, the deeper sections of some holes were completed using the second rig, a rotary air blast or percussion rig. This works on the principle of using compressed air to drive a hammer head with button bits or a blade. Penetration is much faster than the cable tool rig, and the compressed air released down the hole through the drill bit forces the pulverised rock and rock chips continuously back up the hole to the surface. Thus the method of sampling was to collect this continuous 'stream' of chips and pulverised rock over 2 m intervals.

The W-series water sampling holes were drilled through the weathered zone to 25 m and back-filled with cement so as to encase slotted PVC tubes as water sampling ports at 13–15 m and 23–25 m. This enabled tight depth control on water sampling, compared to bailing or pumping from a specified depth in an open hole or between packers.

Figures 4.2–4.8 are the cross-sections through the No. 1 orebody along which some of these new M-, W- and C-series holes were drilled and show the positions of these holes with respect to the economic mineralisation.

Additionally, late in the field program a number of shallow holes were drilled with an auger rig for the monitoring of standing water levels and for shallow groundwater chemistry samples.

4.4 Groundwater Measurements and Sampling

One of the most important parameters needed for the natural analogue study is a hydrological/hydrogeological model for groundwater flow through and around the weathered zone. Additionally, since the groundwater presumably transports radionuclides and various cations and anions, it is necessary to be able to determine the groundwater chemistry at different points in and around the natural analogue.

The only way to accomplish these objectives directly is via drill hole access to the groundwater system for measurements and sampling. While the diamond drill holes drilled by Noranda had collapsed because of the angle they had been drilled, many of the vertical percussion holes were still open and wide enough for pumping and sampling equipment to be lowered into the groundwater system. Unfortunately, very few of these available open percussion holes intersected the weathered primary ore and the dispersion fan, the majority of them being scattered beyond the perimeter of the economic ore, particularly to the south-west of the No.1 orebody. These include not only the exploration holes, but holes that were drilled in 1978 for data collection for mine planning and environmental purposes. Table 4.1 lists location, depth and casing details for all these open vertical holes used for groundwater measurements and sampling during the natural analogue study, while Figure 4.1 is the Koongarra site plan showing only the locations of these holes.

Groundwater measurements included standing water levels and various pump tests, all of which are reported in Volume 5 of this series. Most groundwater samples were collected for analyses using pumps with or without other attachments. Full details and results are reported in Volumes 7 and 15 of this series.

TABLE 4.1

OPEN VERTICAL DRILL HOLES THAT WERE USED FOR GROUNDWATER MEASUREMENTS AND SAMPLING

Section	Hole	N (m)	E (m)	Elevation (m) (AHD)	Present Depth Below Top of Casing (m)	Length of Casing (m)	Collar Height (m)
5499 mN	PH 113	5499	3109	19.79	16	15	.067
	PH 115	5502	3124	19.66	18	17	.158
5621 mN	PH 146	5623	2927	25.21	89	17	.188
	PH 147	5622	2985	23.68	21	20	.13
	PH 148	5626	3047	22.16	17	13	.186
	PH 110	5621	3160	21.72	60	30	.367

Section	Hole	N (m)	E (m)	Elevation (m) (AHD)	Present Depth Below Top of Casing (m)	Length of Casing (m)	Collar Height (m)
5743 mN	PH 158	5743	3016	24.90	25	24	.356
5804 mN	C 1	5804	3322	-	40	22	-
5865 mN	PH 162	5864	3078	24.90	10	7	.1
	C 2	5865	3081	-	40	19	-
	C 3	5865	3124	-	40	17	-
	W 3	5865	3153	-	25	25	-
	PH 73	5865	3170	24.29	85	14	.323
	C 4	5865	3199	-	40	23	-
	PH 80	5865	3231	23.14	24	17	.192
	PH 83	5865	3267	22.68	35	24	.230
	PH 84	5865	3277	22.50	38	23	.130
	PH 85	5865	3293	22.46	40	19	.105
	PH 87	5865	3307	22.47	37	22	.165
	PH 88	5865	3322	22.16	41	21	.15
	PH 92	5865	3337	22.15	45	21	.155
	PH 93	5865	3353	22.03	38	21	.190
5880 mN	PH 95	5880	3370	22.05	19	18	.186
5911 mN	PH 96	5911	3370	22.16	44	16	.079
5926 mN	PH 61	5926	3094	24.59	95	33	.18
	PH 59	5926	3108	24.76	20	15	0
	C 5	5926	3132	-	40	18	-
	PH 54	5926	3155	24.52	57	23	.218
	PH 56	5928	3170	24.38	69	22	.152
	C 6	5933	3216	-	40	23	-
5941 mN	KD 2	5945	3268	23.45	120	120	.375
	M 5	5941	3315	-	40	27	-
	PH 97	5941	3370	22.45	16	ND	.160

Section	Hole	N (m)	E (m)	Elevation (m) (AHD)	Present Depth Below Top of Casing (m)	Length of Casing (m)	Collar Height (m)
5987 mN	C 7	5988	3149	-	40	21	-
	C 8	5989	3200	-	40	22	-
6018 mN	W 7	6018	3315	-	25	25	-
6048 mN	PH 15	6046	3119	25.33	42	24	.157
	PH 14	6048	3171	25.21	26	20	.123
	W 2	6048	3200	-	25	25	-
	M 4	6046	3246	-	40	26	-
6079 mN	KD 1	6081	2998	26.95	120	70	.189
6109 mN	W 6	6107	2975	-	25	-	-
	PH 75	6108	3032	28.38	14	ND	.183
	C 10	6109	3056	-	40	27	-
	PH 82	6109	3094	28.18	14	ND	.290
	W 1	6109	3117	-	25	25	-
	PH 49	6109	3147	26.02	87	16	.892
	PH 55	6109	3216	24.38	89	20	.132
	PH 58	6109	3246	24.24	90	23	.067
	W 5	6109	3274	-	25	25	-
	PH 94	6109	3399	23.17	76	24	.435
6124 mN	C 9	6124	3185	-	40	26	-
				casing sealed through 22-26 m			
6139 mN	W 4	6139	3147	-	25	25	-
6170 mN	M 1	6170	3124	-	50	22	-
	M 2	6170	3162	-	50	36	-
				sealed at 36 m			
	M 3	6170	3216	-	40	15	-
6231 mN	PH 139	6233	3322	23.99	118	23	.497
6414 mN	KD 3	6416	3258	25.57	120	25	.415

Section	Hole	N (m)	E (m)	Elevation (m) (AHD)	Present Depth Below Top of Casing (m)	Length of Casing (m)	Collar Height (m)
6536 mN	PH 27	6537	3109	25.51	36	32	.312
6658 mN	PH 37	6658	3109	26.53	53	12	.43
6780 mN	PH 109	6779	3139	29.32	20	19	.47

5 SUMMARY

The secondary ore of the Koongarra No. 1 uranium orebody provides a natural analogue suitable for validation of models for radionuclide transport. Although the primary uranium mineralisation occurs as uraninite veins and veinlets in fractures and brecciated zones that crosscut the steeply dipping (55°) host schists, weathering and dispersion of uranium within the zone of weathered schists has formed this secondary ore. The interaction of the weathering processes with the mineralogy and geochemistry of the unweathered host schists, and of the primary hydrothermal alteration halo with and around the primary uranium mineralisation, has also been critical in the development of the secondary ore. This secondary ore natural analogue being at a shallow depth, plus the availability of open boreholes and drill core/borehole samples, has facilitated groundwater and rock investigations. Results of these and other ARAP investigations are reported in subsequent volumes in this series.

6 REFERENCES

Airey, P.L. (1986) Radionuclide migration around uranium ore bodies in the Alligator Rivers region in the Northern Territory of Australia — Analogue of radioactive waste repositories — A review. Chemical Geology 55, 255–268.

Airey, P.L., Roman, D., Golian, C., Short, S., Nightingale, T., Lowson, R.T. and Calf, G.E. (1982) Radionuclide migration around uranium ore bodies — Analogues of radioactive waste repositories. U.S. Nuclear Regulatory Commission Contract NRC-04-81-172, Annual Report 1981–82, AAEC Report C29.

Airey, P.L., Roman, D., Golian, C., Short, S., Nightingale, T., Lowson, R.T. and Calf, G.E. (1984) Radionuclide migration around uranium ore bodies — Analogues of radioactive waste repositories. U.S. Nuclear Regulatory Commission Contract NRC-04-81-172, Annual Report 1982–83, AAEC Report C40 (NUREG/CR-391, Vol. 1).

Airey, P.L., Roman D., Golian, C., Short S., Nightingale, T., Payne, T., Lowson, R.T. and Duerden, P. (1985) Radionuclide migration around uranium ore bodies — Analogues of radioactive waste repositories. U.S. Nuclear Regulatory Commission

Contract NRC-04-81-172, Annual Report 1983-84, AAEC Report C45.

Airey, P.L. and Ivanovich, M. (1986) Geochemical analogues of high-level radioactive waste repositories. Chemical Geology 55, 203–213.

Airey, P.L., Golian C. and Lever, D.A. (1986) An approach to the mathematical modelling of the uranium series redistribution within ore bodies. Australian Atomic Energy Commission, Topical Report AAEC/C49 (NUREG/CR-5060).

Airey, P.L., Duerden, P., Roman, D., Golian, C., Nightingale, T., Payne, T., Davey, B.G. and Gray, D. (1986a) Radionuclide migration around uranium ore bodies — Analogues of radioactive waste repositories. U.S. Nuclear Regulatory Commission Contract NRC-04-81-172, Annual Report 1984–85, AAEC Report C55 (NUREG/CR-5040).

Airey, P.L., Duerden, P., Roman D., Golian, C., Nightingale, T., Payne, T., Davey, B.G., Gray, D., Snelling, A.A. and Lever, D.A. (1986b) Koongarra ore body: a natural analogue of radionuclide migration in the far field of HLW repositories. In: Commission of European Communities, Natural Analogue Working Group, Brussels, 5-7 November, 1985, Final Meeting Report, B. Come and N.A. Chapman (eds), Report EUR 10315 EN-FR.

Airey, P.L., Duerden, P., Roman, D., Golian, C., Nightingale, T., Payne, T., Davey, B.G., Gray, D., Snelling, A.A. and Lever, D.A. (1987) The prediction of the long-term migration of radionuclides in the far field of high level waste repositories: results from the Alligator Rivers natural analogue study. In: The Geological Disposal of High Level Radioactive Wastes, D.G. Brookins (ed), Theophrastus Publications, S.A. , Athens, Greece, pp. 507–524.

Australian Groundwater Consultants and McMahon Burgess and Yeates (1978) Report on investigation of groundwater and the design of the water management and tailings retention systems for the Koongarra Project. In: Koongarra Draft Environmental Impact Statement, Appendix 11, Noranda Australia Limited, Melbourne.

Birchard, G.F. and Alexander, D.H. (1983) Natural analogues — A way to increase confidence in predictions of long-term performance of radioactive waste disposal. In: Scientific Basis for Nuclear Waste Management, Volume 6, D.G. Brookins (ed), North Holland, New York, pp. 323–329.

Carr, G.R., Wilmshurst, J.R. and Ryall, W.R. (1986) Evaluation of mercury pathfinder techniques: base metal and uranium deposits. Journal of Geochemical Exploration 26, 1–117.

Carson, D.J.T. (1978) Content of deleterious elements in the ore and waste zones of the Koongarra deposit, Australia. In: Koongarra Project Draft Environment Impact Statement, Appendix 6, Noranda Australia Limited, Melbourne.

Chapman, N.A., McKinley, I.G. and Smellie, J.A.T. (1984) The potential of natural analogues in assessing systems for deep disposal of high-level radioactive waste. Swiss Federal Institute for Reactor Research (EIR), Report No. 545.

Dickson, B.L., Gulson, B.L. and Snelling, A.A. (1985) Evaluation of lead isotopic methods for uranium exploration, Koongarra area, Northern Territory, Australia. Journal of Geochemical Exploration 24, 81–102.

Dickson, B.L., Gulson, B.L. and Snelling, A.A. (1987) Further assessment of stable lead isotope measurements for uranium exploration, Pine Creek Geosyncline, Northern Territory, Australia. Journal of Geochemical Exploration 27, 63–75.

Dickson, B.L. and Snelling, A.A. (1980) Movements of uranium and daughter isotopes in the Koongarra uranium deposit. In: Uranium in the Pine Creek Geosyncline, J. Ferguson and A.B. Goleby (eds), International Atomic Energy Agency, Vienna, pp. 499–507.

Donnelly, T.H. and Ferguson, J. (1980) A stable isotope study of three deposits in the Alligator Rivers Uranium Field, N.T. In: Uranium in the Pine Creek Geosyncline, J. Ferguson and A.B. Goleby (eds), International Atomic Energy Agency, Vienna, pp. 397–406.

Duerden, P., Roman, D., Golian, C., Nightingale, T., Payne, T., Davey, B.G. and Edghill, R. (1988) Radionuclide migration around uranium ore bodies — Analogues of radioactive waste repositories. U.S. Nuclear Regulatory Commission Contract NRC-04-81-172, Annual Report 1986–87, ANSTO Report C72.

Ewers, G.R. and Ferguson, J. (1980) Mineralogy of the Jabiluka, Ranger, Koongarra and Nabarlek uranium deposits. In: Uranium in the Pine Creek Geosyncline, J. Ferguson and A.B. Goleby (eds), International Atomic Energy Agency, Vienna, pp. 363–374..

Ferguson, J., Ewers, G.R. and Donnelly, T.H. (1980) Model for the development of economic uranium mineralisation in the Alligator Rivers Uranium Field. In: Uranium in the Pine Creek Geosyncline, J. Ferguson and A.B. Goleby (eds), International Atomic Energy Agency, Vienna, pp. 563–574.

Foy, M.F. and Pedersen, C.P. (1975) Koongarra uranium deposit. In: Economic Geology of Australia and Papua New Guinea, Vol. 1 Metals, C.L. Knight (ed.), The Australasian Institute of Mining and Metallurgy, Melbourne, pp. 317–321.

Foy, M.F. and Gingerich, J.E. (1977) A stream sediment orientation programme for uranium in the Alligator Rivers Province, Northern Territory, Australia. Journal of Geochemical Exploration 8, 357–364.

Gasparrini, C. (1978) Mineralogical and chemical study of 35 samples from a uranium deposit in Australia. In: Koongarra Project Draft Environmental Impact Statement, Appendix 7, Noranda Australia Limited, Melbourne.

Giblin, A.M. and Snelling, A.A. (1983) Application of hydrogeochemistry to uranium exploration in the Pine Creek Geosyncline, Northern Territory, Australia. Journal of Geochemical Exploration 19, 33–55.

Gole, M.J., Butt, C.R.M. and Snelling, A.A. (1986) A groundwater helium survey of the Koongarra uranium deposits, Pine Creek Geosyncline, Northern Territory. Uranium 2, 343–360.

Hegge, M.R., Mosher, D.V. Eupene, G.S. and Anthony, P.J. (1980) Geologic setting of the East Alligator uranium deposits, and prospects. In: Uranium in the Pine Creek Geosyncline, J. Ferguson and A.B. Goleby (eds), International Atomic Energy Agency, Vienna, pp. 259–272.

Hills, J.H. and Richards, J.R. (1976) Pitchblende and galena ages in the Alligator Rivers region, Northern Territory, Australia. Mineralium Deposita 11, 133–154.

Ivanovich, M., Duerden, P., Payne, T., Nightingale, T., Longworth, G., Wilkins, M.A., Hasler, S.E., Edghill, R.B., Cockayne, D.J. and Davey, B.G. (1988) Natural analogue study of the distribution of uranium series radionuclides between the colloid and solute phases in the hydrogeological system of the Koongarra uranium deposit, Australia. U.K. Atomic Energy Authority, Harwell, Report AERE-R 12975.

Johnston, D.J. (1984) Structural evolution of the Pine Creek Inlier and mineralisation therein, Northern Territory, Australia. Ph.D. thesis (unpublished), Monash University.

Maas, R. (1987) The application of Sm-Nd and Rb-Sr isotope systematics to ore deposits. Ph.D. thesis (unpublished), Australian National University.

Maas, R. (1989) Nd-Sm isotope constraints on the age and origin of unconformity-type uranium deposits in the Alligator Rivers Uranium Field, Northern Territory, Australia. Economic Geology 84, 64–90.

Needham, R.S. (1982) Cahill NT 1:100,000, Geological Map and Commentary. Bureau of Mineral Resources, Canberra, Australia.

Needham, R.S. (1984) Alligator River, N.T.: 1:250,000 geological series, Bureau of Mineral Resources, Geology and Geophysics, Australia, Explanatory Notes SD 53-1.

Needham, R.S. (1988) Geology of the Alligator Rivers Uranium Field, Northern Territory. Bureau of Mineral Resources, Australia, Bulletin 224.

Needham, R.S. and Stuart-Smith, P.G. (1976) The Cahill Formation — host to uranium deposits in the Alligator Rivers Uranium Field, Australia. BMR Journal of Australian Geology and Geophysics 1, 321–333.

Needham, R.S. and Stuart-Smith, P.G. (1980) Geology of the Alligator Rivers

Uranium Field. In: Uranium in the Pine Creek Geosyncline, J. Ferguson and A.B. Goleby (eds), International Atomic Energy Agency, Vienna, pp. 233–257.

Noranda Australia Limited (1978) Koongarra Project Draft Environmental Impact Statement, 3 Volumes, Noranda Australia Limited, Melbourne.

Page, R.W., Compston, W. and Needham, R.S. (1980) Geochronology and evolution of the late Archaean basement and Proterozoic rocks of the Alligator Rivers Uranium Field, Northern Territory, Australia. In: Uranium in the Pine Creek Geosyncline, J. Ferguson and A.B. Goleby (eds), International Atomic Energy Agency, Vienna, pp. 39–68.

Pedersen, C.P. (1978) The geology of the Koongarra deposits, including investigations of contained elements. In: Koongarra Project Draft Environmental Impact Statement, Appendix 5, Noranda Australia Limited, Melbourne.

Snelling, A.A. (1980a) A geochemical study of the Koongarra uranium deposit, Northern Territory, Australia. Ph.D. thesis (unpublished), The University of Sydney.

Snelling, A.A. (1980b) Uraninite and its alteration products, Koongarra uranium deposit. In: Uranium in the Pine Creek Geosyncline, J. Ferguson and A.B. Goleby (eds), International Atomic Energy Agency, Vienna, pp. 487–498.

Snelling, A.A. (1984) A soil geochemistry orientation survey for uranium at Koongarra, Northern Territory. Journal of Geochemical Exploration 22, 83–99.

Snelling, A.A. (1990) Koongarra uranium deposits. In: The Geology of the Mineral Deposits of Australia and Papua New Guinea, F.E. Hughes (ed), The Australasian Institute of Mining and Metallurgy, Melbourne, pp. 807–812.

Snelling, A.A. and Dickson, B.L. (1979) Uranium/daughter disequilibrium in the Koongarra uranium deposit, Australia. Mineralium Deposita 14, 109–118.

Tucker, D.C. (1975) Wall rock alteration at the Koongarra uranium deposit, N.T.. M.Sc. thesis (unpublished), James Cook University of North Queensland.

Wilde, A.R. (1988) On the origin of unconformity-related uranium deposits. Ph.D. thesis (unpublished), Monash University.

Wilde, A.R., Wall, V.J. and Bloom, M.S. (1985) Wall-rock alteration associated with unconformity-related uranium deposits, Northern Territory, Australia: implications for uranium transport and depositional mechanisms. In: Extended Abstracts, Conference on Concentration Mechanisms of Uranium in Geological Environments, Nancy, France, pp. 231–239.

Wilde, A.R., Mernagh, T.P., Bloom, M.S. and Hoffman, C.F. (1989) Fluid inclusion evidence on the origin of some Australian unconformity-related uranium deposits. Economic Geology 84, 1627–1642.

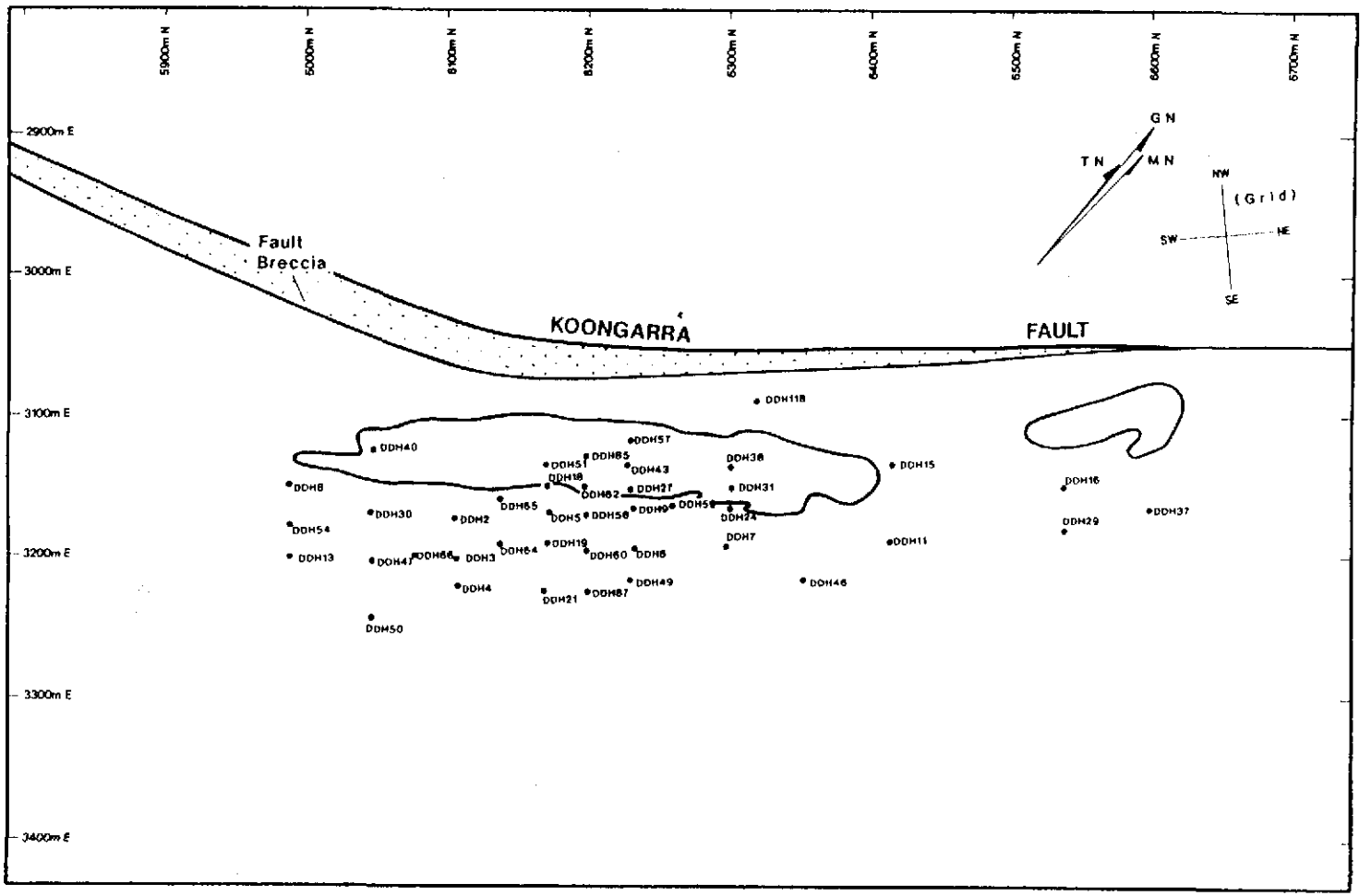

Figure A.1 Koongarra site plan showing the locations of the drill-holes to which the samples referred to in Appendices 1–6 belong.

APPENDIX 1
ANALYSES OF KOONGARRA CHLORITES (Snelling, 1980a)
(a) Above the Graphitic Hanging Wall Zone

DDH 2/26.5 m

	1	2	3	4	5	6	7	8	9	10	11	12
%SiO_2	22.46	26.35	24.54	26.90	28.40	28.74	28.98	29.31	29.71	29.22	30.26	36.27
%Al_2O_3	21.99	19.24	21.72	18.65	19.18	18.02	20.69	21.11	24.18	21.65	26.17	31.25
%ΣFe (FeO)	37.68	26.50	29.30	25.62	19.41	22.23	17.40	15.35	12.71	12.50	9.29	5.87
%MnO	0.97	0.15	0.58	0.16	0.13	0.10	0.17	0.08	0.10	0.09	0	0
%MgO	5.40	17.35	13.40	18.41	21.31	20.61	21.55	22.79	22.13	24.03	24.13	11.87
%CaO	-	-	-	-	-	-	-	-	-	-	-	-
%Na_2O	-	-	-	-	-	-	-	-	-	-	-	-
%K_2O	0.005	0.002	0.01	0.01	0.20	0.15	0.34	0.11	0.04	0.12	0.05	4.27
%TiO_2	0.03	0.09	-	-	-	-	-	0.00	0.01	0.00	-	-
Total	88.54	89.68	89.55	89.75	88.67	89.85	89.13	88.75	88.88	87.61	89.90	89.53
Si	5.07	5.47	5.19	5.55	5.75	5.81	5.73	5.76	5.70	5.69	5.63	6.63
Al	5.85	4.72	5.41	4.52	4.52	4.28	4.83	4.87	5.45	5.01	5.74	6.74
Fe	7.08	4.60	5.18	4.44	3.27	3.75	2.88	2.52	2.07	2.04	1.45	0.90
Mn	0.19	0.03	0.10	0.03	0.03	0.02	0.03	0.01	0.02	0.01	0	0
Mg	1.81	5.34	4.22	5.67	6.41	6.17	6.35	6.64	6.33	7.04	6.69	3.24
Ca	-	-	-	-	-	-	-	-	-	-	-	-
Na	-	-	-	-	-	-	-	-	-	-	-	-
K	-	-	0.003	-	0.05	0.04	0.09	0.03	0.01	0.03	0.01	1.00
Ti	0.005	0.01	-	-	-	-	-	-	0.002	-	-	-
Total	20.00	20.17	20.10	20.21	20.03	20.07	19.91	19.83	19.58	19.82	19.52	18.51
Mg/(Mg+Fe)	0.204	0.537	0.449	0.561	0.662	0.622	0.688	0.725	0.754	0.775	0.822	0.783
Al/Si	1.154	0.863	1.042	0.814	0.786	0.737	0.843	0.845	0.956	0.880	1.020	1.017

DDH 4/39.0 m

	1	2	3	4	5	6	7	8
%SiO_2	28.55	29.04	33.62	28.30	36.47	35.43	32.89	29.77
%Al_2O_3	17.67	19.53	23.12	21.74	21.10	21.52	24.51	18.84
%ΣFe (FeO)	28.38	21.51	8.19	15.60	28.26	7.41	10.06	18.63
%MnO	0.22	0.15	-	0.10	0.12	-	-	-
%MgO	11.77	14.88	18.27	19.30	6.22	21.89	16.28	16.91
%CaO	0.11	0.10	0.30	0.20	-	-	-	-
%Na_2O	0.05	0	-	0.01	-	-	-	-
%K_2O	0.92	1.90	1.56	0.21	0.13	2.02	1.59	2.09
%TiO_2	0.38	0.66	0.02	0.06	0.09	0	0	1.54
Total	88.05	87.77	85.08	85.52	92.39	88.26	85.33	87.79
Si	6.1	6.03	6.56	5.75	7.12	6.66	6.45	6.07
Al	4.45	4.72	5.31	5.22	4.86	4.77	5.66	4.53
Fe	5.07	3.73	1.29	2.69	4.61	1.16	1.65	3.18
Mn	0.04	0.03	-	0.02	0.02	-	-	-
Mg	3.74	4.60	5.27	5.88	1.81	6.13	4.76	5.14
Ca	0.02	0.02	0.12	0.04	-	-	-	-
Na	0.02	-	-	-	-	-	-	-
K	0.25	0.50	0.47	0.05	0.03	0.48	0.40	0.54
Ti	0.06	0.12	-	-	0.01	-	-	0.24
Total	19.75	19.75	19.02	19.65	18.47	19.20	18.92	19.70
Mg/(Mg+Fe)	0.425	0.552	0.803	0.686	0.282	0.841	0.743	0.618
Al/Si	0.730	0.783	0.809	0.908	0.682	0.716	0.878	0.746

DDH 4/53.0 m

	1	2	3	4	5	6	7	8	9
%SiO_2	31.20	31.70	34.95	29.39	33.08	37.47	36.97	35.95	32.64
%Al_2O_3	20.76	21.18	23.53	25.93	27.74	26.26	25.33	27.57	22.27
%ΣFe (FeO)	13.38	12.04	8.85	13.72	9.74	2.78	7.67	6.38	10.16
%MnO	0.01	0.01	0.01	-	-	0.02	0.02	0.02	0
%MgO	24.07	23.49	19.54	18.64	17.36	22.19	17.44	17.66	20.97
%CaO	0.05	-	-	-	-	-	-	-	-
%Na_2O	0.01	-	-	-	-	-	-	-	-
%K_2O	0.11	0.35	1.52	0.11	0.02	0.13	1.99	1.45	1.22
%TiO_2	0.01	-	0	0.01	0	0.01	0.02	0.05	0
Total	89.60	88.77	88.40	87.80	87.94	88.86	89.44	89.08	87.26
Si	5.97	6.07	6.57	5.72	6.21	6.69	6.79	6.57	6.30
Al	4.69	4.78	5.21	5.95	6.13	5.53	5.48	5.94	5.06
Fe	2.14	1.94	1.39	2.23	1.53	0.42	1.18	0.98	1.64
Mn	0.002	-	0.002	-	-	0.003	0.003	0.003	-
Mg	6.87	6.71	5.48	5.40	4.85	5.90	4.78	4.81	6.03
Ca	0.01	-	-	-	-	-	-	-	-
Na	0.002	-	-	-	-	-	-	-	-
K	0.02	0.09	0.18	0.02	0.004	0.01	0.46	0.33	0.30
Ti	0.001	-	-	0.002	-	0.001	0.001	0.007	-
Total	19.71	19.59	18.83	19.32	18.72	18.55	18.69	18.64	19.33
Mg/(Mg+Fe)	0.762	0.776	0.798	0.707	0.761	0.934	0.802	0.831	0.786
Al/Si	0.786	0.787	0.793	1.04	0.988	0.827	0.807	0.904	0.803

DDH 4/53.0 m

	10	11	12	13	14	15	16	17
%SiO_2	37.86	32.03	39.20	32.02	34.42	42.47	42.74	43.68
%Al_2O_3	30.29	24.10	27.09	30.34	25.67	27.13	28.52	32.34
%ΣFe (FeO)	4.01	12.95	5.74	4.55	7.67	9.21	4.47	1.56
%MnO	-	-	0	0	0.07	-	-	-
%MgO	14.94	16.29	13.04	18.90	21.21	9.25	9.82	9.98
%CaO	-	-	-	-	-	-	-	-
%Na_2O	-	-	-	-	-	-	-	-
%K_2O	1.16	2.28	3.65	0.13	0.5	4.29	5.23	3.36
%TiO_2	0.47	0.14	0.03	-	-	0.14	0	0.02
Total	88.73	87.79	88.75	85.93	89.55	92.49	90.78	90.94
Si	6.78	6.25	7.18	5.99	6.32	7.56	7.60	7.51
Al	6.39	5.54	5.84	6.69	5.55	5.69	5.97	6.55
Fe	0.60	2.11	0.88	0.71	1.18	1.37	0.66	0.23
Mn	-	-	-	-	0.01	-	-	-
Mg	3.99	4.74	3.57	5.27	5.80	2.45	2.60	2.56
Ca	-	-	-	-	-	-	-	-
Na	-	-	-	-	-	-	-	-
K	0.26	0.57	0.86	0.03	0.12	0.97	1.18	0.74
Ti	0.07	0.02	0.005	-	-	0.02	-	0.003
Total	18.09	19.24	18.33	18.69	18.98	18.06	18.01	17.59
Mg/(Mg+Fe)	0.869	0.691	0.802	0.881	0.831	0.642	0.798	0.918
Al/Si	0.942	0.887	0.813	1.116	0.879	0.753	0.786	0.872

DDH 4/54.9 m

	1	2	3	4	5	6	7	8	9	10	11	12
%SiO_2	32.58	28.51	31.93	30.80	32.40	31.38	32.64	30.92	29.72	30.37	30.90	32.29
%Al_2O_3	24.09	24.73	23.31	24.85	24.96	25.10	25.07	24.30	24.33	21.29	22.06	24.72
%ΣFe (FeO)	13.26	19.75	15.54	16.71	14.60	12.83	18.71	22.36	23.85	26.48	20.39	12.29
%MnO	0.09	0.28	0.13	0.15	0.09	0.01	-	-	-	-	-	-
%MgO	19.00	12.55	18.08	17.10	18.60	19.60	17.25	15.98	14.59	13.85	17.16	21.03
%CaO	-	-	-	-	-	-	-	-	-	-	-	-
%Na_2O	-	-	-	-	-	-	-	-	-	-	-	-
%K_2O	0.69	0.21	0.63	0.64	0.93	0.54	0.54	0.14	0.06	0.09	0.27	0.42
%TiO_2	0.62	1.21	1.73	0.93	0.99	0.38	0.74	0.42	0.06	0.56	0.66	0.69
Total	90.33	87.24	91.35	91.18	92.57	89.84	94.95	94.12	92.61	92.64	91.44	91.44
Si	6.16	5.78	6.00	5.90	6.03	5.91	5.99	5.83	5.77	5.98	5.98	5.96
Al	5.40	5.91	5.21	5.58	5.44	5.60	5.42	5.44	5.60	4.97	5.04	5.43
Fe	2.05	3.35	2.49	2.64	2.23	2.04	2.86	3.51	3.85	4.38	3.25	1.90
Mn	0.01	0.05	0.02	0.02	0.01	-	-	-	-	-	-	-
Mg	5.36	3.79	5.10	4.82	5.14	5.57	4.72	4.53	4.20	4.03	5.00	5.80
Ca	-	-	-	-	-	-	-	-	-	-	-	-
Na	-	-	-	-	-	-	-	-	-	-	-	-
K	0.16	0.06	0.16	0.16	0.22	0.14	0.22	0.03	0.01	0.02	0.07	0.10
Ti	0.05	0.18	0.24	0.13	0.14	0.05	0.11	0.06	0.01	0.06	0.12	0.09
Total	19.19	19.11	19.22	19.25	19.21	19.31	19.32	19.40	19.44	19.44	19.46	19.28
Mg/(Mg+Fe)	0.723	0.531	0.672	0.646	0.697	0.732	0.623	0.563	0.522	0.479	0.606	0.753
Al/Si	0.877	1.022	0.868	0.946	0.902	0.948	0.905	0.933	0.971	0.831	0.843	0.911

DDH 6/33.9 m

	1	2	3	4	5	6	7	8	9	10	11
%SiO_2	30.67	30.62	31.07	27.59	23.38	33.65	37.74	32.64	35.36	37.05	32.12
%Al_2O_3	22.14	22.40	21.38	19.17	21.62	27.40	29.36	26.52	18.72	25.99	25.66
%ΣFe (FeO)	15.35	13.10	11.11	27.12	38.36	3.31	3.06	8.50	21.63	10.67	11.39
%MnO	0.02	0	0.02	0.33	0.92	0.01	0.01	0.08	0.18	0.06	0.03
%MgO	20.05	20.45	22.85	12.16	4.65	20.75	16.83	18.16	9.23	13.96	18.95
%CaO	-	-	-	-	-	-	-	-	-	-	-
%Na_2O	-	-	-	-	-	-	-	-	-	-	-
%K_2O	0.36	0.24	0.41	0.35	0.04	0.34	0.84	0.05	8.13	1.67	0.33
%TiO_2	-	-	-	-	-	-	-	-	-	-	-
Total	88.58	86.81	86.84	86.72	88.97	85.46	87.84	85.95	93.25	89.40	88.48
Si	5.99	6.02	6.05	5.93	5.25	6.29	6.81	6.25	7.02	6.88	6.08
Al	5.09	5.19	4.93	4.85	5.74	6.06	6.20	5.96	4.38	5.68	5.76
Fe	2.51	2.12	1.76	4.87	7.13	0.56	0.43	1.38	3.59	1.65	1.82
Mn	0.003	-	0.004	0.06	0.13	0.001	0.001	0.01	0.03	0.01	0.005
Mg	5.83	6.02	6.69	3.89	1.62	5.73	4.54	5.16	2.73	3.86	5.34
Ca	-	-	-	-	-	-	-	-	-	-	-
Na	-	-	-	-	-	-	-	-	-	-	-
K	0.09	0.06	0.05	0.1	0.01	0.08	0.22	0.01	2.06	0.40	0.08
Ti	-	-	-	-	-	-	-	-	-	-	-
Total	19.51	19.41	19.48	19.70	19.88	18.72	18.20	18.77	19.81	18.48	19.08
Mg/(Mg+Fe)	0.699	0.740	0.792	0.444	0.185	0.911	0.913	0.789	0.432	0.701	0.746
Al/Si	0.850	0.862	0.815	0.818	1.093	0.963	0.910	0.954	0.624	0.826	0.947

DDH 19/25.4 m

	1	2	3	4	5	6	7	8	9	10	11	12
%SiO_2	28.28	30.93	29.88	28.16	22.88	28.42	31.16	29.84	29.40	27.02	29.60	28.95
%Al_2O_3	20.04	19.42	19.42	20.03	17.41	19.88	19.94	20.00	20.68	19.63	19.67	20.94
%ΣFe (FeO)	21.40	21.60	23.99	20.35	15.24	22.57	20.64	22.51	18.79	18.46	23.61	24.12
%MnO	0.16	0.10	0.14	0.10	-	-	-	-	-	-	-	-
%MgO	19.05	14.00	13.47	20.48	12.98	17.43	15.99	15.78	19.68	22.29	14.29	15.54
%CaO	-	-	0.02	-	-	-	-	-	-	-	-	-
%Na_2O	-	-	0.05	-	-	-	-	-	-	-	-	-
%K_2O	1.01	2.57	3.39	1.06	1.34	2.05	3.37	2.25	1.05	0.28	3.22	1.85
%TiO_2	0.57	1.08	1.88	0.88	23.91	1.22	1.32	1.32	1.37	3.30	2.54	0.84
Total	90.51	89.70	92.24	91.06	93.76	91.57	92.42	91.70	90.98	90.98	92.93	92.24
Si	5.66	6.25	5.97	5.59	4.41	5.69	6.08	5.92	5.75	5.31	5.90	5.74
Al	4.73	4.61	4.58	4.68	3.95	4.71	4.06	4.70	4.77	4.54	4.61	4.94
Fe	3.61	3.64	4.03	3.36	2.45	3.76	3.39	3.74	3.07	3.03	3.92	4.02
Mn	0.03	0.02	0.02	0.02	-	-	-	-	-	-	-	-
Mg	5.66	4.25	4.03	6.04	3.72	5.17	4.68	4.68	5.74	6.53	4.22	4.60
Ca	-	-	0.005	-	-	-	-	-	-	-	-	-
Na	-	-	0.02	-	-	-	-	-	-	-	-	-
K	0.24	0.73	0.96	0.26	0.33	0.53	0.94	0.57	0.26	0.07	0.81	0.48
Ti	0.08	0.18	0.30	0.13	3.46	0.18	0.19	0.20	0.20	0.49	0.38	0.13
Total	20.01	19.68	19.91	20.08	18.32	20.04	19.88	19.81	19.79	19.97	19.84	19.91
Mg/(Mg+Fe)	0.611	0.539	0.500	0.643	0.603	0.579	0.580	0.556	0.652	0.683	0.518	0.534
Al/Si	0.836	0.738	0.767	0.837	0.896	0.828	0.757	0.794	0.830	0.855	0.781	0.861

DDH 19/35.2 m

	1	2	3	4	5	6	7	8	9	10	11
%SiO_2	23.08	31.08	31.36	30.44	26.09	29.24	28.70	30.28	29.76	30.18	31.07
%Al_2O_3	21.25	20.00	27.11	20.36	19.65	19.58	21.70	20.44	19.86	19.42	25.45
%ΣFe (FeO)	39.43	21.41	12.19	18.40	32.59	25.81	18.39	19.80	20.82	21.53	18.63
%MnO	0.78	0.32	0.03	0.32	0.26	0.35	0.17	0.26	0.34	0.34	0.06
%MgO	5.56	14.41	16.54	18.21	12.71	13.45	21.89	17.82	16.36	18.20	13.71
%CaO	0.05	0.06	0.12	0.07	0.02	0.04	0.03	0.04	0.08	0.09	0.08
%Na_2O	0.03	0.01	0.03	0.01	0	0.03	0	0.02	0.02	0	0
%K_2O	0.01	2.13	0.21	0.87	0.03	1.80	0.04	0.77	0.86	0.46	0.82
%TiO_2	0.05	1.35	0.04	1.53	0.09	1.11	0.01	1.67	1.83	1.87	0.07
Total	90.24	90.77	87.63	90.21	91.44	91.41	90.93	91.10	89.93	92.09	89.90
Si	5.12	6.16	6.00	5.95	5.47	5.92	5.59	5.93	5.93	5.89	6.04
Al	5.59	4.70	6.15	4.71	4.86	4.72	4.97	4.69	4.63	4.47	5.84
Fe	7.32	3.59	1.96	3.06	5.66	4.40	3.03	3.29	3.48	3.53	3.03
Mn	0.15	0.05	0.01	0.05	0.05	0.06	0.03	0.04	0.06	0.06	0.01
Mg	1.86	4.30	4.73	5.30	4.02	4.03	6.29	5.16	4.91	5.30	3.97
Ca	0.01	0.01	0.03	0.01	-	0.01	0.01	0.01	0.02	0.02	0.02
Na	0.01	-	0.02	-	-	0.01	-	0.01	0.01	-	-
K	-	0.55	0.05	0.24	0.01	0.46	0.01	0.23	0.24	0.11	0.20
Ti	0.01	0.20	0.01	0.24	0.02	0.17	-	0.23	0.3	0.28	0.01
Total	20.07	19.56	18.96	19.56	20.09	19.78	19.93	19.59	19.58	19.66	19.13
Mg/(Mg+Fe)	0.203	0.545	0.707	0.634	0.415	0.478	0.675	0.611	0.585	0.600	0.567
Al/Si	1.092	0.763	1.025	0.792	0.888	0.797	0.889	0.791	0.781	0.759	0.967

DDH 21/33.4 m

	1	2	3
%SiO_2	28.31	30.77	31.82
%Al_2O_3	20.18	19.58	22.35
%ΣFe (FeO)	28.87	27.06	25.82
%MnO	0.09	0.11	0.16
%MgO	13.60	15.24	14.61
%CaO	0.03	0.08	0.12
%Na_2O	0.01	0.07	0
%K_2O	0.04	0.21	0.41
%TiO_2	0.20	0.43	1.09
Total	91.33	93.55	96.09
Si	5.78	6.01	6.01
Al	4.84	4.56	4.97
Fe	4.92	4.48	4.08
Mn	0.02	0.02	0.02
Mg	4.18	4.48	4.03
Ca	0.01	0.02	0.02
Na	-	0.02	-
K	0.01	0.05	0.10
Ti	0.03	0.07	0.16
Total	19.79	19.71	19.40
Mg/(Mg+Fe)	0.459	0.500	0.497
Al/Si	0.837	0.759	0.828

DDH 21/42.0 m

	1	2	3	4	5	6	7
%SiO_2	24.85	26.03	25.31	33.69	27.22	26.99	29.15
%Al_2O_3	19.96	19.77	19.61	23.18	19.74	19.31	20.03
%ΣFe (FeO)	34.66	30.23	29.65	20.29	26.81	19.46	21.28
%MnO	0.37	0.19	0.15	0.13	0.18	0.25	0.20
%MgO	8.80	11.22	12.79	9.34	13.46	13.72	14.9
%CaO	0.11	0.09	0.04	0.03	0.05	0.12	0.16
%Na_2O	0	0	0	0	0	0	0.02
%K_2O	0.01	0.21	0	2.50	0.39	0.67	0.90
%TiO_2	0.06	0.32	0.15	0.69	0.64	6.34	1.12
Total	88.82	88.06	87.70	89.55	88.49	86.86	87.76
Si	5.45	5.63	5.47	6.61	5.74	5.69	5.97
Al	5.16	5.00	5.00	5.41	4.88	4.71	4.84
Fe	6.36	5.45	5.36	3.36	4.70	3.37	3.69
Mn	0.07	0.03	0.03	0.02	0.03	0.04	0.04
Mg	2.88	3.60	4.12	2.75	4.21	4.24	4.56
Ca	0.03	0.02	0.01	0.01	0.01	0.03	0.04
Na	-	-	-	-	-	-	0.01
K	-	0.06	-	0.63	0.11	0.18	0.25
Tl	0.01	0.05	0.02	0.10	0.10	0.99	0.17
Total	19.96	19.84	20.01	18.89	19.78	19.15	19.57
Mg/(Mg+Fe)	0.312	0.398	0.435	0.450	0.473	0.557	0.553
Al/Si	0.947	0.888	0.914	0.818	0.850	0.843	0.811

DDH 21/56.9 m

	1	2	3	4	5	6	7	8
%SiO_2	22.00	22.59	23.73	25.30	31.06	26.40	27.62	29.07
%Al_2O_3	21.30	21.51	22.17	22.26	23.20	19.53	20.32	21.65
%ΣFe (FeO)	39.69	36.20	33.69	28.73	21.72	23.72	22.07	19.69
%MnO	0.72	0.46	0.56	0.41	1.27	0.09	0.12	0.11
%MgO	2.99	5.38	7.69	10.99	9.17	13.90	14.93	16.03
%CaO	0.05	0	0.06	0.01	4.63	0.05	0.06	0.15
%Na_2O	-	0	0.06	0.09	0.06	0.05	0.05	0.04
%K_2O	0.08	0.11	0	0	0.05	0.19	0.12	0.40
%TiO_2	0.13	0	0.05	0.09	0.02	0.04	0.11	0.36
Total	86.96	86.25	88.01	87.88	91.18	83.97	85.40	87.50
Si	5.12	5.19	5.23	5.41	6.16	5.76	5.84	5.90
Al	5.85	5.82	5.76	5.61	5.42	5.03	5.07	5.18
Fe	7.73	6.95	6.21	5.14	3.60	4.33	3.90	3.34
Mn	0.14	0.09	0.11	0.07	0.21	0.02	0.03	0.02
Mg	1.04	1.84	2.53	3.50	2.72	4.52	4.71	4.86
Ca	0.01	-	0.01	-	0.99	0.01	0.01	0.04
Na	-	-	0.03	0.04	0.02	0.03	0.02	0.02
K	0.03	0.03	-	-	0.02	0.05	0.03	0.10
Tl	0.02	-	0.01	0.01	0.003	0.01	0.02	0.06
Total	19.94	19.92	19.89	19.78	19.14	19.76	19.63	19.52
Mg/(Mg+Fe)	0.119	0.209	0.289	0.405	0.430	0.511	0.547	0.593
Al/Si	1.143	1.121	1.101	1.037	0.880	0.873	0.868	0.878

DDH 21/56.9 m

	9	10	11	12	13	14	15
%SiO_2	31.51	29.78	33.34	32.25	33.99	36.39	39.54
%Al_2O_3	22.47	23.20	24.89	22.73	24.17	27.59	27.21
%ΣFe (FeO)	15.86	15.26	11.40	12.40	9.23	5.51	3.15
%MnO	0.10	0.05	0.05	0.02	0	0	0.03
%MgO	15.59	17.01	15.45	20.10	19.17	15.27	12.94
%CaO	0.17	0.09	0.09	0.07	0.12	0.08	0.12
%Na_2O	0.05	0.02	0.03	0.01	0.02	0.01	0.03
%K_2O	1.35	0.21	1.28	0.99	1.24	1.80	2.86
%TiO_2	0.03	0.24	0.05	0.02	0.06	0.16	0.03
Total	87.13	85.86	86.58	88.59	88.00	86.85	85.91
Si	6.28	5.98	6.47	6.19	6.43	6.77	7.32
Al	5.28	5.50	5.69	5.15	5.39	6.06	5.94
Fe	2.65	2.56	1.85	2.00	1.46	0.86	0.49
Mn	0.02	0.01	0.01	0.004	-	-	0.005
Mg	4.63	5.10	4.46	5.75	5.41	4.24	3.57
Ca	0.04	0.02	0.02	0.02	0.02	0.02	0.02
Na	0.02	0.01	0.01	0.005	0.01	-	0.01
K	0.34	0.05	0.33	0.23	0.30	0.43	0.67
Ti	0.01	0.04	0.01	0.003	0.01	0.02	0.005
Total	19.27	19.27	18.85	19.35	19.03	18.40	18.03
Mg/(Mg+Fe)	0.636	0.666	0.707	0.742	0.787	0.831	0.879
Al/Si	0.841	0.920	0.879	0.832	0.838	0.895	0.811

DDH 46/37.9 m

	1	2	3	4	5	6	7	8	9	10
%SiO_2	22.46	23.19	25.55	27.42	27.85	28.99	29.47	30.12	30.36	34.27
%Al_2O_3	20.39	20.08	18.24	16.74	15.83	16.48	15.58	16.25	18.96	27.66
%ΣFe (FeO)	42.78	38.84	35.14	32.68	29.20	24.22	25.12	21.71	13.66	8.70
%MnO	0.74	0.62	0.28	0.26	0.24	0.19	0.10	0.14	0.02	0.03
%MgO	1.91	5.29	9.18	11.15	13.68	17.89	15.06	19.78	24.05	15.98
%CaO	0.05	0.05	0.02	0.10	0.08	0.09	0.14	0.05	0.06	0.06
%Na_2O	0.01	0.05	0.04	0.01	0.06	0.15	0.14	0.02	0.003	0.06
%K_2O	0.03	0.01	0.04	0.18	0.49	0.02	1.63	0.02	0.01	0.07
%TiO_2	0.02	0.05	0.11	0.25	0.03	0.02	3.15	0.03	0	0.03
Total	88.39	88.18	88.60	88.79	87.46	88.05	90.38	88.12	87.12	86.86
Si	5.22	5.28	5.62	5.94	6.02	6.03	6.06	6.16	5.99	6.45
Al	5.57	5.39	4.76	4.27	4.06	4.02	3.78	3.94	4.43	6.11
Fe	8.35	7.40	6.48	5.88	5.31	4.27	4.32	3.69	2.25	1.36
Mn	0.14	0.12	0.05	0.05	0.04	0.03	0.02	0.02	-	0.005
Mg	0.70	1.78	3.04	3.60	4.40	5.53	4.62	6.03	7.11	4.53
Ca	0.01	0.01	0.003	0.02	0.02	0.02	0.03	0.01	0.01	0.01
Na	0.005	0.01	0.02	-	0.03	0.03	0.05	0.007	-	0.02
K	0.01	0.005	0.01	0.05	0.13	0.005	0.43	0.005	-	0.02
Ti	0.005	0.008	0.02	0.04	0.005	0.003	0.49	0.005	-	0.005
Total	20.01	20.00	20.00	19.92	20.01	19.94	19.80	19.87	19.79	18.51
Mg/(Mg+Fe)	0.077	0.194	0.319	0.384	0.453	0.564	0.517	0.620	0.760	0.769
Al/Si	1.067	1.021	0.847	0.719	0.674	0.667	0.624	0.640	0.740	0.947

DDH 47/32.7 m

	1	2	3	4	5	6	7	8
%SiO_2	29.84	29.90	30.39	30.26	30.62	31.88	28.41	30.37
%Al_2O_3	19.15	20.40	20.48	21.44	20.39	19.22	20.63	20.10
%ΣFe (FeO)	13.21	13.32	12.81	12.77	12.57	12.01	19.05	13.75
%MnO	0.01	-	-	-	-	-	-	-
%MgO	21.17	24.49	25.40	26.76	28.43	29.94	22.09	24.10
%CaO	0.10	-	-	-	-	-	-	-
%Na_2O	-	-	-	-	-	-	-	-
%K_2O	0.11	0.01	0.08	0.06	0.01	0.01	0	0.22
%TiO_2	0.43	0.07	0.20	0.44	0.08	0.003	0.01	1.63
Total	84.37	88.19	89.36	91.73	92.10	93.06	90.19	90.17
Si	6.07	5.83	5.83	5.67	5.73	5.84	5.60	5.81
Al	4.68	4.66	4.62	4.72	4.49	4.19	4.79	4.53
Fe	2.25	2.21	2.08	2.02	1.91	1.87	3.14	2.19
Mn	-	-	-	-	-	-	-	-
Mg	6.42	7.11	7.27	7.42	7.86	8.16	6.48	6.91
Ca	0.02	-	-	-	-	-	-	-
Na	-	-	-	-	-	-	-	-
K	0.03	-	0.02	0.02	0.004	0.002	-	0.05
Ti	0.07	0.01	0.03	0.06	0.01	-	-	0.23
Total	19.54	19.82	19.85	19.91	20.00	20.06	20.01	19.72
Mg/(Mg+Fe)	0.740	0.763	0.778	0.786	0.805	0.814	0.674	0.759
Al/Si	0.771	0.799	0.792	0.832	0.784	0.717	0.856	0.780

DDH 49/62.4 m

	1	2	3	4	5	6	7	Biotite
%SiO_2	30.95	31.78	28.13	27.63	28.41	28.70	22.81	32.68
%Al_2O_3	23.28	21.18	21.28	21.48	21.42	20.48	17.55	20.02
%ΣFe (FeO)	10.04	4.76	11.64	23.32	15.98	24.94	23.83	19.06
%MnO	0.01	0	0	0.23	0.25	0.02	0.03	0.07
%MgO	22.01	28.86	21.41	15.53	19.77	12.03	12.13	9.25
%CaO	0.05	0.04	0.06	0.08	0.06	0.02	0.02	0.05
%Na_2O	0.16	0.002	0.10	0.02	0.01	0.02	0	0.36
%K_2O	0.02	0.15	0.04	0	0.14	0.81	0.05	8.38
%TiO_2	0.12	0	3.37	0.09	0.04	0.55	10.01	2.63
Total	86.64	86.77	86.03	88.38	86.08	87.57	86.43	92.50
Si	5.98	6.01	5.60	5.70	5.81	6.02	4.92	6.51
Al	5.35	4.72	4.99	5.20	5.14	5.01	4.46	4.69
Fe	1.63	0.75	1.94	3.96	2.69	4.39	4.30	3.22
Mn	-	-	-	0.03	0.04	-	0.01	0.01
Mg	6.39	8.13	6.35	4.83	5.99	3.76	3.90	2.74
Ca	0.01	0.01	0.01	0.02	0.01	-	-	0.01
Na	0.04	-	0.03	0.01	-	0.01	-	0.24
K	0.01	0.04	0.01	-	0.04	0.21	0.02	2.14
Ti	0.02	-	0.51	0.01	0.01	0.08	1.62	0.42
Total	19.43	19.70	19.99	19.76	19.73	19.79	19.26	19.98
Mg/(Mg+Fe)	0.797	0.915	0.766	0.549	0.690	0.461	0.476	0.460
Al/Si	0.895	0.785	0.891	0.912	0.885	0.832	0.907	0.720

DDH 50/46.5 m

	1	2	Biotite	Biotite	Biotite	Biotite
$\%SiO_2$	26.76	29.55	32.72	31.06	32.15	31.72
$\%Al_2O_3$	18.74	16.41	15.14	14.47	14.86	14.15
%ΣFe (FeO)	23.67	30.25	26.81	26.78	29.56	26.90
%MnO	0.05	0.37	0.18	0.19	0.19	0.23
%MgO	17.04	9.09	7.76	8.92	5.55	6.93
%CaO	0.04	0.11	0.03	0.04	0.05	0.02
$\%Na_2O$	0	0.03	0	0	0	0
$\%K_2O$	0	3.23	7.97	5.93	8.20	8.77
$\%TiO_2$	0.10	0.79	0.82	1.42	0.33	0.63
Total	86.40	89.83	91.43	88.81	90.89	89.35
Si	5.68	6.32	6.92	6.71	6.95	6.94
Al	4.68	4.12	3.81	3.74	3.79	3.65
Fe	4.21	5.41	4.70	4.82	5.34	4.92
Mn	0.01	0.13	0.03	0.04	0.03	0.04
Mg	5.36	2.96	2.41	2.87	1.79	2.26
Ca	0.01	0.02	0.01	0.01	0.01	0.005
Na	-	0.01	-	-	-	-
K	-	0.77	2.03	1.56	2.26	2.45
Ti	9.02	0.13	0.13	0.26	0.05	0.10
Total	19.97	19.87	20.04	20.01	20.22	20.41
Mg/(Mg+Fe)	0.560	0.354	0.339	0.373	0.251	0.526
Al/Si	0.824	0.652	0.551	0.557	0.545	0.315

(b) From the Graphitic Hanging Wall Zone

DDH 7/56.5 m

	1	2	3	4	5	6	7	8
%SiO_2	25.24	26.08	27.72	26.85	27.99	28.55	28.76	28.98
%Al_2O_3	18.94	18.18	17.13	19.79	16.57	17.57	17.48	18.08
%ΣFe (FeO)	33.00	31.91	26.46	25.26	24.27	22.51	21.51	20.02
%MnO	0.23	0.26	0.17	0.17	0.15	0.14	0.12	0.12
%MgO	10.59	10.53	14.69	16.92	15.83	18.09	19.01	20.62
%CaO	0.05	0.07	0.03	0.05	0.08	0.04	0.05	0.05
%Na_2O	0	0.03	0	0	0	0	0	0.02
%K_2O	0.05	0.08	0.19	0	0.15	0.15	0.14	0.12
%TiO_2	0.07	0.08	0.52	0.20	0.53	0.52	0.76	0.35
Total	88.17	87.22	86.91	89.24	85.57	87.57	87.83	88.36
Si	5.53	5.74	5.93	5.55	6.01	5.93	5.91	5.87
Al	4.89	4.72	4.33	4.82	4.21	4.30	4.24	4.32
Fe	6.05	5.87	4.74	4.36	4.36	3.91	3.70	3.39
Mn	0.04	0.05	0.03	0.03	0.03	0.03	0.02	0.02
Mg	3.46	3.45	4.69	5.21	5.07	5.59	5.83	6.23
Ca	0.01	0.02	0.01	0.01	0.02	0.01	0.01	0.01
Na	-	0.01	-	-	-	-	-	0.01
K	0.01	0.02	0.05	-	0.04	0.04	0.04	0.03
Ti	0.01	0.01	0.09	0.03	0.09	0.08	0.12	0.05
Total	20.00	19.89	19.87	20.01	19.83	19.89	19.87	19.93
Mg/(Mg+Fe)	0.364	0.370	0.497	0.544	0.538	0.588	0.612	0.648
Al/Si	0.884	0.822	0.730	0.868	0.700	0.725	0.717	0.736

DDH 7/56.5m

	9	10	11	12	13	14	15
%SiO_2	29.03	29.25	29.30	29.73	29.82	29.65	29.23
%Al_2O_3	17.69	18.31	18.78	19.89	20.05	20.25	21.64
%ΣFe (FeO)	18.16	16.32	15.08	13.61	12.33	11.09	8.61
%MnO	0.11	0.10	0.08	0.08	0.06	0.06	0.02
%MgO	21.47	22.23	22.72	24.01	24.25	24.76	26.38
%CaO	0.05	0.05	0.04	0.05	0.05	0.04	0.03
%Na_2O	0.01	0.02	0	0.01	0.01	0.01	0
%K_2O	0.07	0.07	0.09	0.04	0.03	0.03	0.01
%TiO_2	0.43	0.29	0.32	0.38	0.11	0.20	0.06
Total	87.02	86.57	86.41	87.80	86.71	86.09	85.98
Si	5.94	5.92	5.91	5.84	5.89	5.87	5.71
Al	4.26	4.37	4.46	4.61	4.66	4.72	4.98
Fe	3.11	2.77	2.54	2.23	2.03	1.83	1.41
Mn	0.02	0.02	0.02	0.01	0.01	0.01	-
Mg	6.46	6.71	6.83	7.03	7.14	7.29	7.69
Ca	0.01	0.01	0.01	0.01	0.01	0.01	0.01
Na	-	0.01	-	-	-	-	-
K	0.02	0.02	0.02	0.01	0.01	0.01	-
Ti	0.07	0.05	0.05	0.05	0.02	0.03	0.01
Total	19.89	19.88	19.84	19.79	19.77	19.77	19.81
Mg/(Mg+Fe)	0.675	0.708	0.729	0.759	0.779	0.799	0.845
Al/Si	0.717	0.738	0.755	0.789	0.791	0.804	0.872

(c) Below the Graphitic Hanging Wall Zone

DDH 3/72.3 m

	1	2	3	4	5	6	7	8	9	10
$\%SiO_2$	34.40	28.42	31.79	27.33	25.04	27.77	29.54	30.49	30.11	33.39
$\%Al_2O_3$	28.41	20.25	19.49	18.69	20.68	19.20	19.07	19.03	18.67	20.05
%ΣFe (FeO)	5.43	20.92	17.87	25.80	27.83	27.22	22.06	19.36	20.82	15.91
%MnO	0	1.13	0.47	1.14	1.54	1.27	0.76	0.55	0.65	0.41
%MgO	14.8	17.94	15.51	14.36	11.95	11.28	14.49	15.44	15.51	15.51
%CaO	0.05	0	0.07	0.04	0.03	0.04	0.06	0.09	0.07	0.09
$\%Na_2O$	0.02	0	0	0	0.01	0	0	0.02	0.02	0.01
$\%K_2O$	0.16	0.19	1.17	0.11	0.05	0.48	0.56	0.98	0.71	1.76
$\%TiO_2$	0	0.03	1.14	0.15	0.10	0.19	0.66	0.97	0.54	1.91
Total	83.27	88.89	87.51	87.62	87.23	87.45	87.20	86.93	87.10	89.04
Si	6.57	5.77	6.40	5.79	5.42	5.91	6.13	6.25	6.22	6.53
Al	6.46	4.84	4.63	4.68	5.26	4.88	4.65	4.59	4.53	4.62
Fe	0.92	3.55	3.02	4.57	5.07	4.88	3.83	3.33	3.63	2.62
Mn	-	0.19	0.08	0.21	0.29	0.26	0.14	0.10	0.12	0.06
Mg	4.27	5.42	4.65	4.54	3.86	3.60	4.49	4.74	4.75	4.53
Ca	0.01	-	0.02	0.01	0.01	0.01	0.01	0.02	0.02	0.02
Na	-	-	-	-	-	-	-	0.01	0.01	-
K	0.05	0.05	0.30	0.03	0.01	0.13	0.15	0.26	0.19	0.44
Ti	-	0.01	0.13	0.02	0.02	0.03	0.10	0.15	0.09	0.29
Total	18.28	19.83	19.28	19.85	19.94	19.65	19.50	19.45	19.56	19.11
Mg/(Mg+Fe)	0.823	0.604	0.606	0.499	0.432	0.425	0.540	0.587	0.567	0.633
Al/Si	0.983	0.840	0.723	0.808	0.970	0.826	0.759	0.734	0.728	0.708

DDH 3/72.3 m

	11	12	13	14	15	16	17	18	19	20
$\%SiO_2$	32.46	36.92	36.30	37.55	31.80	33.64	26.07	34.48	29.59	38.30
$\%Al_2O_3$	20.15	22.21	26.83	28.10	20.01	28.73	19.34	26.36	20.92	23.24
%ΣFe (FeO)	15.26	14.40	7.26	5.48	13.72	9.46	27.16	8.10	12.56	11.68
%MnO	0.32	0.35	0.12	0.03	0.20	0.09	1.39	0.08	0.09	0.34
%MgO	17.57	10.32	15.53	13.31	20.58	14.50	13.26	14.75	22.11	10.09
%CaO	0.06	0.21	0.08	0.07	0.06	-	0.04	0.04	-	-
$\%Na_2O$	0.03	0.01	0	0.03	0.05	0	0.02	0.03	0	0.01
$\%K_2O$	1.42	3.22	1.21	2.01	1.02	0.92	0.03	1.49	0.03	4.51
$\%TiO_2$	1.35	0.70	0	0.06	1.25	0	0.07	0.02	0	0.79
Total	88.62	88.33	87.33	86.64	80.68	87.34	87.38	85.35	85.30	88.97
Si	6.36	7.17	6.76	6.96	6.19	6.35	5.61	6.63	5.93	7.30
Al	4.67	5.08	5.88	6.16	4.59	6.40	4.92	5.99	4.94	5.22
Fe	2.50	2.34	1.12	0.89	2.23	1.49	4.87	1.27	2.10	1.86
Mn	0.05	0.06	0.02	-	0.03	0.01	0.25	0.01	0.02	0.06
Mg	5.14	2.99	4.36	3.68	5.96	4.08	4.24	4.27	6.60	2.87
Ca	0.01	0.04	0.02	0.02	0.01	-	0.01	0.01	-	-
Na	0.01	-	-	0.01	0.02	-	0.01	0.01	-	-
K	0.39	0.80	0.29	0.53	0.25	0.22	0.01	0.37	0.01	1.10
Ti	0.31	0.10	-	0.01	0.18	-	0.01	-	-	0.11
Total	19.44	18.58	18.45	18.26	19.47	18.56	19.93	18.56	19.60	18.52
Mg/(Mg+Fe)	0.673	0.561	0.796	0.805	0.728	0.732	0.465	0.771	0.758	0.606
Al/Si	0.734	0.709	0.870	0.885	0.741	1.007	0.877	0.903	0.833	0.715

DDH 4/72.8 m

	1	2	3	4	5	6	7	8	9
%SiO_2	34.82	30.15	29.40	30.09	34.21	35.82	31.82	32.97	32.75
%Al_2O_3	29.17	22.43	21.78	23.24	29.11	31.57	26.30	28.41	29.24
%ΣFe (FeO)	5.10	11.02	12.63	11.43	6.31	1.31	7.21	7.92	9.97
%MnO	0.05	0.02	0.01	0.04	0.01	0.02	0.05	0	-
%MgO	16.95	22.46	21.72	20.98	16.19	17.17	19.80	17.18	14.18
%CaO	-	-	-	-	-	-	-	-	-
%Na_2O	-	-	-	-	-	-	-	-	-
%K_2O	0.52	0.03	0	0.04	0.56	0.15	0.09	0.20	0.26
%TiO_2	0.01	0	0	0.05	0	-	-	0.01	0
Total	86.62	86.11	85.54	85.87	86.39	86.04	85.27	86.69	86.40
Si	6.44	5.91	5.86	5.93	6.39	6.48	6.13	6.20	6.25
Al	6.37	5.20	5.10	5.37	6.43	6.75	5.94	6.32	6.57
Fe	0.78	1.77	2.15	1.90	1.01	0.22	1.16	1.24	1.59
Mn	0.01	-	-	0.01	-	-	0.01	-	-
Mg	4.67	6.61	6.46	6.16	4.49	4.68	5.67	4.85	4.03
Ca	-	-	-	-	-	-	-	-	-
Na	-	-	-	-	-	-	-	-	-
K	0.13	0.01	-	0.01	0.13	0.03	0.02	0.05	0.06
Ti	-	-	-	0.01	-	-	-	-	-
Total	18.40	19.50	19.57	19.39	18.46	18.16	18.93	18.66	18.50
Mg/(Mg+Fe)	0.857	0.789	0.750	0.764	0.816	0.955	0.830	0.796	0.717
Al/Si	0.989	0.880	0.870	0.906	1.006	1.042	0.969	1.019	1.052

DDH 4/77.4 m

	1	2	3	4
%SiO_2	24.40	31.98	29.39	36.51
%Al_2O_3	21.36	23.00	21.16	28.67
%ΣFe (FeO)	28.71	13.43	19.48	3.61
%MnO	0.69	0.20	0.43	0.05
%MgO	11.25	15.64	13.70	14.60
%CaO	-	-	-	-
%Na_2O	-	-	-	-
%K_2O	0.13	1.72	1.84	1.92
%TiO_2	0.06	0.05	0.13	0.01
Total	86.60	86.02	86.13	85.37
Si	5.32	6.33	6.12	6.86
Al	5.52	5.42	5.16	6.30
Fe	5.26	2.27	3.37	0.56
Mn	0.13	0.04	0.12	0.01
Mg	3.68	4.66	4.24	4.05
Ca	-	-	-	-
Na	-	-	-	-
K	0.02	0.48	0.50	0.45
Ti	0.01	0.01	0.02	-
Total	19.94	19.21	19.53	18.23
Mg/(Mg+Fe)	0.412	0.672	0.557	0.879
Al/Si	1.038	0.856	0.843	0.918

DDH 4/79.4 m

	1	2	3	4	5	6
%SiO_2	25.90	28.80	27.57	32.81	38.36	31.75
%Al_2O_3	20.90	23.52	24.82	23.08	25.90	22.61
%ΣFe (FeO)	26.68	12.97	19.88	12.10	5.73	16.20
%MnO	0.96	0.03	0.66	0.13	0.05	0.42
%MgO	12.28	19.44	13.98	15.66	13.51	12.65
%CaO	0.01	-	-	0.02	-	-
%Na_2O	0.17	0.08	-	-	-	-
%K_2O	0.19	0.31	0.19	2.13	3.72	2.58
%TiO_2	0.04	0.05	-	0.25	0.09	0.35
Total	87.13	85.20	87.10	86.38	87.36	86.76
Si	5.60	5.82	5.63	6.47	7.19	6.37
Al	5.30	5.58	5.97	5.38	5.69	5.37
Fe	4.82	2.18	3.39	2.02	0.90	2.77
Mn	0.15	0.01	0.13	0.03	0.01	0.12
Mg	3.91	5.82	4.25	4.63	3.71	3.85
Ca	-	-	-	-	-	-
Na	0.06	0.03	-	-	-	-
K	0.05	0.07	0.05	0.47	0.90	0.72
Ti	0.01	0.01	-	0.03	0.01	0.05
Total	19.90	19.52	19.42	19.03	18.41	19.25
Mg/(Mg+Fe)	0.448	0.728	0.556	0.696	0.805	0.582
Al/Si	0.946	0.959	1.061	0.832	0.791	0.843

DDH 4/82.8 m

	1	2	3	4	5	6	7	8	9
%SiO_2	22.95	23.90	24.21	23.74	24.57	24.78	24.38	25.11	25.12
%Al_2O_3	19.76	19.25	18.67	18.84	19.09	19.26	18.80	19.90	19.98
%ΣFe (FeO)	34.78	31.97	33.31	32.50	32.04	30.53	28.84	27.88	27.90
%MnO	1.47	0.90	0.75	0.84	0.85	0.87	1.05	0.87	0.84
%MgO	6.38	7.72	8.90	8.95	10.11	10.71	10.83	11.23	12.29
%CaO	-	-	-	-	0.04	0.07	0.07	0.04	0.08
%Na_2O	-	-	-	-	0	0.02	0	-	0
%K_2O	0	0	0.02	0.01	0	0.01	0	0	0.01
%TiO_2	-	-	-	-	0.11	0.09	0.07	-	0.35
Total	86.07	83.74	85.86	84.88	86.81	86.34	84.04	85.03	86.57
Si	5.33	5.54	5.51	5.46	5.48	5.50	5.54	5.58	5.49
Al	5.40	5.26	5.00	5.09	5.02	5.05	5.04	5.21	5.15
Fe	6.75	6.20	6.33	6.24	5.98	5.67	5.48	5.17	5.10
Mn	0.29	0.18	0.15	0.17	0.16	0.16	0.20	0.16	0.15
Mg	2.21	2.66	3.02	3.06	3.36	3.55	3.67	3.71	4.00
Ca	-	-	-	-	0.01	0.01	0.02	0.01	0.02
Na	-	-	-	-	-	0.01	-	-	-
K	-	-	-	-	-	-	-	-	-
Ti	-	-	-	-	0.02	0.02	0.01	-	0.06
Total	19.98	19.84	20.01	20.02	20.03	19.97	19.96	19.84	19.97
Mg/(Mg+Fe)	0.247	0.300	0.323	0.329	0.360	0.385	0.401	0.418	0.440
Al/Si	1.013	0.949	0.907	0.932	0.916	0.918	0.910	0.934	0.938

DDH 4/82.8 m

	10	11	12	13	14	15	16	17
%SiO_2	28.79	30.68	26.81	24.81	28.29	25.64	30.49	27.39
%Al_2O_3	21.95	24.65	23.07	19.31	21.89	18.49	26.13	21.32
%ΣFe (FeO)	11.53	7.41	13.12	25.09	11.00	21.06	10.83	21.66
%MnO	0.03	0.01	0.19	0.91	0.01	0.34	0	0.98
%MgO	20.76	19.26	19.96	13.30	22.91	18.80	16.67	14.87
%CaO	-	-	0.07	0.06	-	-	-	0.04
%Na_2O	-	-	-	-	-	-	-	0
%K_2O	0.18	0.03	0.02	-	0	0	0	0.14
%TiO_2	-	-	-	-	-	-	-	0.09
Total	83.24	82.04	83.24	82.98	84.09	84.33	84.12	86.49
Si	5.88	6.14	5.55	5.48	5.71	5.53	6.05	5.73
Al	5.29	5.82	5.63	5.12	5.21	4.70	6.11	5.26
Fe	1.97	1.24	2.27	4.72	1.86	3.79	1.80	3.79
Mn	0.01	0.01	0.03	0.17	-	0.06	-	0.17
Mg	6.32	5.74	6.16	4.46	6.90	6.04	4.93	4.63
Ca	-	-	0.02	0.01	-	-	-	0.01
Na	-	-	-	-	-	-	-	-
K	0.05	0.01	0.01	-	-	-	-	0.04
Ti	-	-	-	-	-	-	-	0.01
Total	19.52	18.96	19.67	19.96	19.68	20.12	18.89	19.64
Mg/(Mg+Fe)	0.762	0.822	0.731	0.486	0.788	0.614	0.733	0.550
Al/Si	0.900	0.948	1.014	0.934	0.912	0.850	1.01	0.918

DDH 4/86.5 m

	1	2	3	4	5	6	7	8	9
$\%SiO_2$	31.64	32.06	36.66	36.58	35.11	32.49	41.84	41.37	45.32
$\%Al_2O_3$	23.66	23.61	26.11	27.28	24.78	22.46	29.09	29.31	28.30
%ΣFe (FeO)	10.60	8.92	9.40	8.18	7.55	7.45	7.47	7.58	8.62
%MnO	0.02	0.01	0.06	0	-	-	0	0	0
%MgO	21.87	21.12	18.92	18.38	18.63	16.81	15.51	15.86	12.02
%CaO	-	-	-	-	-	-	-	-	-
$\%Na_2O$	-	-	-	-	-	-	-	-	-
$\%K_2O$	0.53	0.73	1.64	1.56	1.50	2.35	3.19	2.64	3.73
$\%TiO_2$	0.09	0.17	0.37	0.13	0.77	8.00	0.16	2.40	0.09
Total	88.41	86.62	93.16	92.11	88.34	89.55	97.26	99.17	98.08
Si	6.00	6.21	6.52	6.54	6.53	6.09	7.01	6.82	7.54
Al	5.34	5.34	5.49	5.72	5.43	4.96	5.78	5.70	5.55
Fe	1.72	1.39	1.39	1.18	1.23	1.17	1.05	1.05	1.20
Mn	-	-	0.01	-	-	-	-	-	-
Mg	6.18	6.04	5.02	4.93	5.13	4.69	3.88	3.90	2.98
Ca	-	-	-	-	-	-	-	-	-
Na	-	-	-	-	-	-	-	-	-
K	0.14	0.19	0.43	0.43	0.45	0.56	0.69	0.56	0.79
Ti	0.01	0.02	0.05	0.02	0.11	1.13	0.02	0.30	0.01
Total	19.39	19.19	18.91	18.82	18.88	18.59	18.43	18.31	18.07
Mg/(Mg+Fe)	0.782	0.813	0.783	0.807	0.807	0.801	0.787	0.788	0.713
Al/Si	0.890	0.860	0.842	0.875	0.832	0.815	0.825	0.835	0.736

DDH 4/96.1 m

	1	2	3	4	5	6	7	8	9	10	11
$\%SiO_2$	27.57	27.32	29.69	30.67	31.10	30.85	31.55	24.24	26.66	30.64	37.61
$\%Al_2O_3$	18.81	18.84	19.46	18.61	19.86	20.40	18.84	20.37	20.57	20.51	21.89
%ΣFe (FeO)	21.67	20.95	16.82	14.22	14.13	12.47	11.39	31.81	19.64	10.24	11.77
%MnO	0.18	0.18	0.16	0.18	0.06	0.10	0.08	0.43	0.16	0.02	0.05
%MgO	16.70	18.72	20.10	21.69	20.47	23.50	24.03	9.68	18.46	24.14	11.40
%CaO	0.06	0.05	0.08	0.12	0.04	0.07	0.09	0.04	0.03	0.09	0.11
$\%Na_2O$	0.03	0.07	0.03	0.04	0.06	0.03	0.02	0.05	0.04	0	0.06
$\%K_2O$	0.54	0.20	0.38	0.29	1.00	0.30	0.20	0.02	0	0.14	3.49
$\%TiO_2$	0.57	0	0.61	0	1.52	0.15	0	0.09	0	0	0.64
Total	86.13	86.33	87.33	85.82	88.24	87.87	86.20	86.73	85.56	85.78	87.02
Si	5.79	5.73	5.99	6.18	6.14	6.02	6.23	5.38	5.58	6.03	7.31
Al	4.71	4.65	4.63	4.42	4.62	4.68	4.36	5.33	5.07	4.74	5.01
Fe	3.82	3.67	2.84	2.40	2.33	2.04	1.89	5.91	3.44	1.70	1.91
Mn	0.03	0.03	0.03	0.03	0.01	0.02	0.01	0.08	0.03	-	0.01
Mg	5.25	5.84	6.05	6.53	6.02	6.83	7.08	3.20	5.75	7.11	3.30
Ca	0.01	0.01	0.02	0.03	0.01	0.02	0.02	0.01	0.01	0.02	0.02
Na	0.01	0.03	0.01	0.01	0.02	0.01	0.01	0.02	0.01	-	0.02
K	0.16	0.05	0.1	0.07	0.25	0.07	0.05	0.01	-	0.03	0.87
Ti	0.09	-	0.09	-	0.23	0.02	-	0.02	-	-	0.10
Total	19.87	20.01	19.76	19.67	19.63	19.71	19.65	19.96	19.89	19.63	18.55
Mg/(Mg+Fe)	0.579	0.614	0.681	0.731	0.721	0.770	0.789	0.351	0.626	0.807	0.603
Al/Si	0.813	0.812	0.773	0.715	0.752	0.777	0.700	0.991	0.909	0.786	0.685

DDH 4/96.1 m

	12	13	14	15	16	17	18	19	20	21	22
$\%SiO_2$	39.85	26.66	27.01	26.08	25.35	29.25	33.95	29.71	30.11	31.26	26.21
$\%Al_2O_3$	24.56	17.89	18.63	18.67	19.41	21.18	20.44	18.66	18.42	21.73	18.08
%ΣFe (FeO)	7.15	26.15	24.39	22.95	22.35	8.55	12.75	18.49	15.50	15.16	27.59
%MnO	0.13	0.20	0.19	0.19	0.19	0.17	0.07	0.13	0.14	0.14	0.17
%MgO	14.47	14.59	15.20	16.34	17.39	24.24	18.48	19.18	19.76	15.03	12.92
%CaO	0.15	0.07	0.02	0.04	0.04	-	0.07	0.08	0.09	0.08	-
$\%Na_2O$	0.01	0.05	0.06	0.05	0.02	-	0.05	0.04	0.03	0.07	-
$\%K_2O$	2.67	0.05	0.05	0.11	0	0	1.82	0.07	0.38	0.47	0
$\%TiO_2$	0	0.13	0.21	0.10	0.11	-	0.60	0.01	0.02	0.65	-
Total	88.99	85.79	85.76	84.53	84.86	83.40	88.23	86.37	84.45	84.59	84.97
Si	7.31	5.79	5.81	5.66	5.47	5.88	6.58	6.09	6.22	6.40	5.97
Al	5.31	4.58	4.71	4.77	4.93	5.02	4.67	4.50	4.48	5.24	4.70
Fe	1.10	4.76	4.38	4.16	4.03	1.44	2.06	3.17	2.68	2.59	5.09
Mn	0.02	0.04	0.03	0.04	0.03	0.03	0.01	0.02	0.03	0.03	0.03
Mg	3.96	4.73	4.87	5.28	5.58	7.26	5.33	5.85	6.09	4.58	4.25
Ca	0.03	0.02	0.01	0.01	0.01	-	0.01	0.02	0.02	0.02	-
Na	-	0.02	0.02	0.02	0.01	-	0.02	0.02	0.01	0.03	-
K	0.63	0.01	0.02	0.03	-	-	0.45	0.02	0.10	0.13	-
Ti	-	0.02	0.04	0.02	0.01	-	0.09	-	-	0.10	-
Total	18.36	19.97	19.89	19.99	20.07	19.63	19.22	19.69	19.63	19.12	19.86
Mg/(Mg+Fe)	0.783	0.498	0.526	0.559	0.581	0.834	0.721	0.649	0.694	0.638	0.455
Al/Si	0.726	0.791	0.811	0.843	0.901	0.854	0.710	0.739	0.720	0.819	0.812

DDH 4/96.1 m

	23	24	25	26	27	28	29	30	31	32	33
$\%SiO_2$	30.55	24.50	31.01	25.20	32.50	34.87	30.93	31.73	36.45	32.36	32.70
$\%Al_2O_3$	20.59	22.25	24.46	22.17	26.30	26.53	27.46	27.51	28.89	21.33	22.17
%ΣFe (FeO)	11.85	28.08	25.37	25.10	11.36	6.19	9.28	6.11	5.26	10.45	12.10
%MnO	0.08	0.47	0.73	0.43	0.21	0.17	0.12	0.12	0.19	0.01	0
%MgO	21.22	10.91	5.69	12.92	13.99	16.17	15.19	18.37	13.74	22.14	25.82
%CaO	-	-	-	-	-	-	-	-	-	-	-
$\%Na_2O$	-	-	-	-	-	-	-	-	-	-	-
$\%K_2O$	0.24	0	0.37	0	0.19	0.14	0.01	0	0.29	0.78	0.52
$\%TiO_2$	-	-	-	-	-	-	-	-	-	-	-
Total	84.53	86.22	87.64	85.82	84.55	84.07	82.99	83.84	84.82	87.07	93.31
Si	6.14	5.34	6.40	5.42	6.40	6.68	6.15	6.14	6.84	6.27	5.97
Al	4.89	5.72	5.94	5.62	6.11	6.00	6.43	6.28	6.39	4.86	4.77
Fe	1.99	5.12	4.37	4.51	1.87	0.99	1.54	0.99	0.83	1.69	1.85
Mn	0.02	0.09	0.13	0.08	0.04	0.03	0.02	0.02	0.03	-	-
Mg	6.37	3.54	1.75	4.14	4.11	4.62	4.50	5.30	3.84	6.39	7.02
Ca	-	-	-	-	-	-	-	-	-	-	-
Na	-	-	-	-	-	-	-	-	-	-	-
K	0.06	0	0.10	-	0.05	0.04	-	-	0.07	0.20	0.12
Ti	-	-	-	-	-	-	-	-	-	-	-
Total	19.47	19.81	18.69	19.77	18.58	18.36	18.64	18.73	18.00	19.41	19.73
Mg/(Mg+Fe)	0.762	0.409	0.286	0.479	0.687	0.824	0.745	0.843	0.822	0.791	0.791
Al/Si	0.796	1.071	0.928	1.037	0.955	0.898	1.046	1.023	0.934	0.775	0.799

DDH 4/96.1 m

	34	35	36	37	38	39	40	41	42	43	44
%SiO_2	34.67	30.24	32.55	32.15	31.11	35.03	31.11	29.86	29.89	34.87	39.20
%Al_2O_3	21.56	21.42	22.41	23.63	23.10	20.67	22.98	21.99	17.44	22.56	19.05
%ΣFe (FeO)	9.75	13.43	10.93	12.28	13.17	7.68	11.58	14.01	16.87	8.21	6.87
%MnO	0.15	0.02	0.02	0.04	0.02	0	0.08	0.25	0.44	0.23	0
%MgO	18.65	25.92	26.16	29.76	27.50	19.83	23.25	22.83	18.27	16.98	14.17
%CaO	-	-	-	-	-	-	-	-	-	-	-
%Na_2O	-	-	-	-	-	-	-	-	-	-	-
%K_2O	0.77	0.56	0.45	0.05	0.26	2.56	0.07	0.86	0.21	0.29	6.90
%TiO_2	-	-	-	-	-	-	-	-	-	-	-
Total	85.55	91.59	92.52	97.90	95.16	85.77	89.08	89.80	83.12	83.14	86.19
Si	6.74	5.70	5.95	5.60	5.61	6.80	5.92	5.77	6.32	6.87	7.66
Al	4.94	4.76	4.83	4.85	4.91	4.73	5.15	5.00	4.35	5.24	4.39
Fe	1.59	2.12	1.67	1.79	1.99	1.25	1.84	2.26	2.98	1.35	1.12
Mn	0.03	-	-	0.01	-	-	0.01	0.04	0.08	0.04	-
Mg	5.40	7.28	7.13	7.72	7.40	5.74	6.59	6.56	5.76	4.98	4.13
Ca	-	-	-	-	-	-	-	-	-	-	-
Na	-	-	-	-	-	-	-	-	-	-	-
K	0.19	0.14	0.11	0.01	0.06	0.64	0.02	0.21	0.06	0.07	1.72
Ti	-	-	-	-	-	-	-	-	-	-	-
Total	18.89	20.00	19.69	19.98	19.97	19.16	19.53	19.84	19.55	18.55	19.02
Mg/(Mg+Fe)	0.773	0.774	0.810	0.812	0.788	0.821	0.782	0.744	0.659	0.787	0.787
Al/Si	0.733	0.835	0.812	0.866	0.875	0.696	0.870	0.867	0.688	0.763	0.573

DDH 4/103.9 m

	1	2	3	4	5	6	7	8	9	10	11	12	13
%SiO_2	25.96	25.33	26.25	25.30	24.56	26.65	31.20	34.66	30.09	42.46	42.53	36.12	40.62
%Al_2O_3	18.58	19.93	19.83	20.07	18.97	19.76	20.89	23.25	22.40	24.55	25.95	23.27	24.86
%ΣFe (FeO)	28.48	27.96	27.25	27.81	25.41	25.81	20.76	11.20	17.09	6.57	9.33	17.89	12.05
%MnO	0.40	0.31	0.30	0.22	0.31	0.28	0.25	0.07	0.11	0.02	0.05	0.24	0.09
%MgO	11.74	12.51	13.29	12.85	11.92	13.96	12.71	15.92	15.69	10.31	6.39	9.54	8.11
%CaO	0.04	0.04	0.03	0.03	0	0.03	0.10	0.08	0.04	0.12	0.03	0	0.06
%Na_2O	0	0	0	0	0	0	0.01	0	0	0.01	0.04	0	0.05
%K_2O	0.08	0.08	0.19	0.05	0.15	0.18	1.37	1.92	0.61	4.76	5.61	3.18	4.86
TiO_2	0.11	0.21	0.26	0.30	4.74	0.64	0.03	0.01	0.14	0.01	0.19	0.32	0.36
Total	85.39	86.37	87.40	86.63	86.06	87.31	87.32	87.11	86.17	88.81	90.12	90.56	91.06
Si	5.74	5.52	5.61	5.48	5.33	5.66	6.38	6.70	6.10	7.80	7.83	6.96	7.52
Al	4.84	5.12	5.00	5.13	4.85	4.95	5.04	5.29	5.35	5.32	5.63	5.29	5.43
Fe	5.26	5.10	4.88	5.04	4.61	4.58	3.56	1.81	2.90	1.01	1.44	2.88	1.86
Mn	0.08	0.06	0.05	0.04	0.06	0.05	0.05	0.01	0.02	-	0.01	0.04	0.02
Mg	3.87	4.06	4.24	4.15	3.85	4.42	3.88	4.59	4.74	2.83	1.75	2.74	2.24
Ca	0.01	0.01	0.01	0.01	-	0.01	0.03	0.02	0.01	0.03	0.01	-	0.01
Na	-	-	-	-	-	-	-	-	-	-	0.01	-	0.02
K	0.02	0.02	0.05	0.02	0.04	0.05	0.36	0.47	0.16	1.11	1.33	0.78	1.15
Ti	0.02	0.04	0.04	0.05	0.78	0.10	0.01	-	0.02	-	0.03	0.05	0.06
Total	19.84	19.93	19.88	19.92	19.52	19.82	19.31	18.89	19.30	18.10	18.04	18.74	18.31
Mg/(Mg+Fe)	0.424	0.443	0.465	0.452	0.455	0.491	0.522	0.717	0.620	0.737	0.548	0.488	0.546
Al/Si	0.843	0.928	0.891	0.936	0.910	0.875	0.790	0.790	0.877	0.682	0.719	0.760	0.723

DDH 18/37.1 m

	1	2	3	4	5	6	7	8
%SiO_2	24.59	32.07	31.16	29.45	29.89	30.23	29.88	30.85
%Al_2O_3	21.95	24.04	22.23	21.35	20.32	21.02	22.13	23.92
%ΣFe (FeO)	24.29	11.50	11.95	12.17	13.57	12.42	13.67	10.08
%MnO	-	0.14	0.10	-	0.06	0.04	0.01	-
%MgO	15.66	20.34	22.14	23.57	26.57	24.85	22.66	23.15
%CaO	-	-	-	-	0.05	-	-	-
%Na_2O	-	-	-	-	0.13	-	-	-
%K_2O	0.01	0.08	0.04	0.05	0.03	0.03	0.09	0.03
%TiO_2	0.05	0.05	0.05	0.20	0.04	0.50	0.13	0
Total	86.55	88.22	87.67	86.79	90.66	89.09	88.57	88.03
Si	5.23	6.13	6.03	5.80	5.67	5.81	5.79	5.91
Al	5.50	5.42	5.03	4.97	4.58	4.76	5.07	5.35
Fe	4.32	1.83	1.97	2.01	2.18	1.96	2.22	1.61
Mn	-	0.02	0.02	-	0.01	0.01	-	-
Mg	4.96	5.73	6.38	6.87	7.56	7.13	6.55	6.54
Ca	-	-	-	-	0.01	-	-	-
Na	-	-	-	-	0.05	-	-	-
K	-	0.02	0.01	0.01	0.01	0.01	0.02	0.01
Ti	0.01	0.01	0.01	0.03	0.01	0.06	0.02	-
Total	20.02	19.16	19.45	19.69	20.08	19.74	19.67	19.42
Mg/(Mg+Fe)	0.535	0.758	0.764	0.774	0.776	0.784	0.747	0.802
Al/Si	1.052	0.884	0.834	0.857	0.808	0.819	0.876	0.905

DDH 24/62.7 m

	1	2	3	4	5	6	7	8	9	10	11	12
%SiO_2	24.69	24.25	28.74	30.94	27.58	29.24	27.87	30.01	32.54	27.20	29.62	30.79
%Al_2O_3	21.37	21.31	23.99	18.60	22.05	25.61	23.73	20.85	20.73	16.82	20.17	20.79
%ΣFe (FeO)	28.73	27.31	21.39	18.88	15.81	14.38	14.50	11.98	10.33	9.15	12.35	10.91
%MnO	1.09	1.02	0.70	0.04	0.31	0.24	0.15	0.03	0.04	0.03	0.02	0.02
%MgO	9.96	11.90	13.42	17.04	18.46	17.30	21.36	20.79	18.49	17.05	23.56	21.84
%CaO	0.04	0.03	0.04	0.05	0.03	0.02	0.04	0.07	0.04	0.08	0.08	0.07
%Na_2O	0	0.01	0	0	0	0	0	0.26	0.23	0	0.04	0.07
%K_2O	0.02	0.03	0.33	1.16	0.02	0.13	0.03	0.25	1.14	1.04	0.14	0.45
%TiO_2	0.08	0.10	0.01	0.07	0.01	0	0.01	0	0.83	15.46	0.02	0.02
Total	85.98	85.96	88.62	86.80	84.27	86.92	87.69	84.24	83.86	86.83	86.00	84.96
Si	5.44	5.31	5.80	6.33	5.71	5.77	5.50	6.07	6.53	5.40	5.90	6.14
Al	5.55	5.50	5.71	4.48	5.38	5.96	5.52	4.97	4.91	3.93	4.74	4.88
Fe	5.29	4.98	3.62	3.23	2.74	2.37	2.39	2.03	1.74	1.52	2.06	1.82
Mn	0.20	0.18	0.12	0.01	0.05	0.04	0.02	0.01	0.01	-	0.004	0.004
Mg	3.27	3.93	4.04	5.20	5.69	5.09	6.28	6.27	5.54	5.04	6.99	6.49
Ca	0.01	0.01	0.01	0.01	0.01	-	0.01	0.02	0.01	0.02	0.02	0.02
Na	-	-	-	-	-	-	-	0.10	0.10	-	0.02	0.03
K	0.01	0.01	0.07	0.30	0.01	0.03	0.01	0.06	0.29	0.26	0.05	0.11
Ti	0.01	0.02	-	0.01	-	-	-	-	0.05	2.30	-	0.003
Total	19.78	19.94	19.37	19.57	19.59	19.26	19.73	19.53	19.18	18.47	19.88	19.50
Mg/(Mg+Fe)	0.382	0.441	0.527	0.617	0.675	0.682	0.724	0.755	0.761	0.768	0.772	0.781
Al/Si	1.020	1.036	0.984	0.708	0.942	1.033	1.004	0.819	0.752	0.728	0.803	0.795

DDH 24/62.7 m

	13	14	15	16	17	18	19	20	21	22	23
%SiO_2	35.71	30.08	38.44	33.51	31.41	43.02	31.02	40.32	38.15	35.02	41.69
%Al_2O_3	23.47	20.12	24.04	22.44	19.00	26.45	18.08	21.61	20.75	15.40	22.28
%ΣFe (FeO)	7.99	11.89	6.11	8.99	10.11	4.11	9.59	4.79	5.90	6.55	7.65
%MnO	0.02	0	0.02	0.03	0.02	0	0.01	0.02	0.01	0.04	0.04
%MgO	16.30	25.12	13.40	19.78	23.63	9.58	24.39	14.05	18.68	22.56	12.11
%CaO	0.40	0.05	0.04	0.06	0.04	0.02	0.04	0.06	0.06	0.05	0.04
%Na_2O	0.02	0.15	0.06	0.27	0.29	0.07	0.05	0.46	0.16	1.60	0.08
%K_2O	2.51	0.20	3.77	1.31	0.44	5.67	0.38	3.06	1.70	1.93	1.73
%TiO_2	0.52	0.01	1.42	0.09	0.04	0.05	0.02	0.02	0.02	0.03	0.09
Total	86.94	87.62	87.30	86.48	84.98	88.97	83.58	84.39	85.43	83.18	85.71
Si	6.81	5.87	7.27	6.47	6.25	7.81	6.26	7.72	7.27	7.04	7.85
Al	5.28	4.63	5.36	5.11	4.45	5.66	4.3	4.88	4.66	3.65	4.95
Fe	1.27	1.94	0.97	1.45	1.69	0.62	1.63	0.77	0.94	1.10	1.21
Mn	0.003	-	-	0.01	-	-	-	-	-	0.01	0.01
Mg	4.63	7.31	3.78	5.70	7.00	2.59	7.34	4.01	5.30	6.76	3.40
Ca	0.08	0.01	0.01	0.01	0.01	0.004	0.01	0.01	0.01	0.01	0.01
Na	0.007	0.05	0.02	0.10	0.12	0.02	0.02	0.16	0.05	0.62	0.02
K	0.62	0.05	0.91	0.32	0.12	1.31	0.05	0.74	0.41	0.50	0.41
Ti	0.08	-	0.21	0.01	0.01	0.005	-	-	-	0.01	0.01
Total	18.78	19.86	18.53	19.18	19.65	18.02	19.61	18.29	18.64	19.70	17.87
Mg/(Mg+Fe)	0.785	0.790	0.796	0.797	0.806	0.807	0.818	0.839	0.849	0.860	0.738
Al/Si	0.775	0.789	0.737	0.790	0.712	0.725	0.687	0.632	0.641	0.518	0.631

DDH 24/65.4 m

	1	2	3	4	5	6	7	8
%SiO_2	25.11	32.42	30.11	27.19	33.88	27.50	33.24	27.51
%Al_2O_3	23.56	25.86	24.34	23.83	24.77	23.10	25.26	25.53
%ΣFe (FeO)	28.95	10.09	10.70	21.10	10.41	23.41	8.44	16.67
%MnO	0.78	0.07	0.01	0.51	0.03	0.56	0.02	0.19
%MgO	14.42	22.85	25.68	17.64	19.97	16.96	19.44	20.47
%CaO	0.03	0.08	-	-	-	-	-	-
%Na_2O	-	-	-	-	0.33	-	-	-
%K_2O	0.03	0.74	0.26	0.06	0.96	0.07	1.33	0.04
%TiO_2	-	-	-	-	-	-	-	-
Total	92.88	91.61	91.10	90.33	89.85	91.60	87.73	90.41
Si	5.11	5.95	5.57	5.38	6.23	5.46	6.31	5.32
Al	5.60	5.59	5.35	5.58	5.46	5.38	5.61	5.82
Fe	4.87	1.54	1.67	3.47	1.57	3.91	1.36	2.69
Mn	0.12	0.02	-	0.12	-	0.12	-	0.03
Mg	4.38	6.06	7.13	5.26	5.61	4.98	5.45	5.90
Ca	0.01	0.02	-	-	-	-	-	-
Na	-	-	-	-	0.11	-	-	-
K	0.01	0.11	0.06	0.01	0.22	0.07	0.32	0.01
Ti	-	-	-	-	-	-	-	-
Total	20.10	19.29	19.78	19.82	19.21	19.92	19.05	19.77
Mg/(Mg+Fe)	0.474	0.797	0.810	0.603	0.781	0.560	0.800	0.686
Al/Si	1.096	0.939	0.961	1.037	0.876	0.985	0.889	1.093

DDH 24/65.6 m

	9	10	11	12	13	14	15	16
%SiO_2	35.89	32.62	33.60	34.00	38.95	40.21	33.18	34.83
%Al_2O_3	27.28	26.94	27.55	29.25	29.18	32.25	25.35	29.54
%ΣFe (FeO)	6.42	7.70	8.19	7.34	5.94	3.75	8.62	5.35
%MnO	0	0	0.01	0.01	0	0.01	0	0
%MgO	16.17	17.85	20.55	20.24	17.47	15.84	17.40	19.22
%CaO	0.10	0.10	-	-	-	-	0.08	0.08
%Na_2O	-	-	-	-	-	-	0.62	-
%K_2O	1.98	0.52	1.2	0.70	3.24	2.23	0.65	0.67
%TiO_2	0.03	-	-	-	-	-	-	-
Total	87.87	85.73	91.10	91.54	94.78	94.28	85.90	89.69
Si	6.66	6.26	6.12	6.09	6.71	6.80	6.37	6.27
Al	5.97	6.05	5.90	6.17	5.92	6.43	5.79	6.27
Fe	1.01	1.26	1.20	1.10	0.86	0.53	1.39	0.76
Mn	-	-	-	-	-	-	-	-
Mg	4.47	5.05	5.57	5.40	4.48	3.99	4.98	5.19
Ca	0.02	0.02	-	-	-	-	0.02	0.02
Na	-	-	-	-	-	-	0.23	-
K	0.47	0.23	0.28	0.16	0.71	0.48	0.16	0.15
Ti	-	-	-	-	-	-	-	-
Total	18.60	18.87	19.07	18.92	18.68	18.23	18.94	18.66
Mg/(Mg+Fe)	0.816	0.8	0.823	0.831	0.839	0.883	0.782	0.872
Al/Si	0.896	0.966	0.964	1.013	0.882	0.946	0.909	1.000

DDH 49/83.1 m

	1	2	3	4	5	6
%SiO_2	30.97	29.67	31.20	33.02	35.09	41.67
%Al_2O_3	22.90	23.60	20.51	24.08	27.01	26.69
%ΣFe (FeO)	14.69	11.17	11.34	8.31	4.70	4.97
%MnO	-	0.10	-	0.01	-	-
%MgO	19.93	21.87	24.01	21.61	16.47	11.98
%CaO	-	-	-	-	-	-
%Na_2O	-	-	-	-	-	-
%K_2O	0.54	0.22	0.32	0.53	2.57	6.16
%TiO_2	0.14	0.09	0.06	0.06	0.10	0.38
Total	89.17	86.73	87.44	87.62	85.95	91.85
Si	5.98	5.80	6.06	6.22	6.63	7.40
Al	5.21	5.43	4.66	5.35	6.01	5.61
Fe	2.37	1.82	1.86	1.36	0.74	0.75
Mn	-	0.02	-	-	-	-
Mg	5.73	6.36	6.99	6.11	4.64	3.19
Ca	-	-	-	-	-	-
Na	-	-	-	-	-	-
K	0.13	0.06	0.07	0.14	0.62	1.49
Ti	0.02	0.01	0.01	0.01	0.01	0.05
Total	19.46	19.50	19.65	19.10	18.66	18.49
Mg/(Mg+Fe)	0.707	0.777	0.790	0.818	0.862	0.810
Al/Si	0.871	0.937	0.769	0.860	0.907	0.758

(d) Associated with Ore

DDH 2/33.3 m

	1	2	3	4	5	6	7	8	9	10
%SiO_2	34.25	30.56	33.97	36.11	34.27	36.56	43.24	36.40	35.81	36.81
%Al_2O_3	14.28	23.96	26.87	24.83	25.14	22.02	19.67	20.85	24.73	23.32
%ΣFe (FeO)	35.66	15.59	10.92	12.69	11.73	19.87	16.82	18.03	13.69	12.15
%MnO	0.08	0.15	0.09	0.09	0.14	0.07	0.09	0.11	0.16	0.12
%MgO	5.95	19.38	17.73	15.28	16.28	7.90	8.57	12.51	12.87	14.20
%CaO	-	-	-	-	-	-	-	-	-	-
%Na_2O	-	-	-	-	-	-	-	-	-	-
%K_2O	2.83	0.03	0.19	0.42	0.11	2.38	2.86	0.80	1.21	0.51
%TiO_2	-	-	-	-	-	-	-	-	-	0.04
Total	93.06	89.66	89.76	89.42	87.68	88.80	91.26	88.70	88.47	86.75
Si	7.14	5.88	6.29	6.73	6.52	7.21	8.09	7.09	6.83	6.98
Al	3.51	5.43	5.86	5.46	5.63	5.12	4.35	4.77	5.56	5.31
Fe	6.22	2.51	1.69	2.02	1.86	3.28	2.59	2.93	2.18	1.96
Mn	0.01	0.02	0.01	0.01	0.02	0.01	0.01	0.02	0.03	0.02
Mg	1.85	5.55	4.89	4.26	4.61	2.32	2.36	3.63	3.65	4.04
Ca	-	-	-	-	-	-	-	-	-	-
Na	-	-	-	-	-	-	-	-	-	-
K	0.75	0.01	0.05	0.10	0.03	0.60	0.67	0.19	0.29	0.12
Ti	-	-	-	-	-	-	-	-	-	0.01
Total	19.48	19.40	18.79	18.58	18.67	18.54	18.07	18.63	18.54	18.44
Mg/(Mg+Fe)	0.229	0.689	0.743	0.678	0.713	0.414	0.477	0.553	0.626	0.673
Al/Si	0.492	0.923	0.932	0.811	0.863	0.710	0.538	0.673	0.814	0.761

DDH 58/31.0 m

	1	2	3	4	5	6	7	8	9
%SiO_2	32.58	33.27	33.06	35.04	34.50	35.89	35.90	35.37	34.90
%Al_2O_3	23.86	24.07	23.71	22.17	22.72	21.93	24.22	24.97	24.24
%ΣFe (FeO)	13.23	14.60	15.48	13.61	11.24	15.39	13.59	11.87	13.69
%MnO	0.08	0.08	0.16	0.10	0.11	0.13	0.15	0.06	0.20
%MgO	20.74	19.20	17.78	13.47	15.57	13.54	15.38	16.48	14.59
%CaO	-	-	-	-	-	-	-	-	-
%Na_2O	-	-	-	-	-	-	-	-	-
%K_2O	0.05	0.04	0.02	0.10	0.03	0.09	0.09	0.08	0.12
%TiO_2	-	-	-	0	0.03	0.05	0.16	0	0.07
Total	90.54	91.26	90.21	84.49	84.20	87.02	89.49	88.83	87.81
Si	6.08	6.21	6.27	6.97	6.81	6.99	6.73	6.62	6.69
Al	5.25	5.30	5.30	5.19	5.28	5.03	5.36	5.52	5.47
Fe	2.06	2.28	2.46	2.26	1.85	2.50	2.13	1.86	2.19
Mn	0.01	0.01	0.03	0.02	0.02	0.02	0.03	0.01	0.04
Mg	5.77	5.34	5.02	3.99	0.58	3.93	4.29	4.60	4.17
Ca	-	-	-	-	-	-	-	-	-
Na	-	-	-	-	-	-	-	-	-
K	0.01	0.01	0.01	0.03	0.01	0.02	0.02	0.02	0.03
Ti	-	-	-	-	-	0.01	0.02	-	0.01
Total	19.18	19.15	19.09	18.46	18.55	18.5	18.58	18.63	18.60
Mg/(Mg+Fe)	0.737	0.701	0.671	0.638	0.712	0.611	0.668	0.712	0.656
Al/Si	0.863	0.853	0.845	0.745	0.775	0.72	0.796	0.834	0.818

DDH 58/31.0 m

	10	11	12	13	14	15	16	17	18
%SiO_2	36.70	39.36	35.18	32.62	36.44	37.33	37.55	33.41	33.94
%Al_2O_3	24.62	22.03	25.01	23.87	27.48	25.65	24.47	26.20	27.53
%ΣFe (FeO)	12.46	10.71	10.65	14.48	10.58	12.82	11.25	12.65	10.41
%MnO	*0.20*	*0.17*	*0.13*	*0.11*	*0.08*	*0.06*	*0.03*	*0.07*	*0.16*
%MgO	15.50	12.16	18.12	17.01	13.74	13.54	11.87	15.46	16.25
%CaO	-	-	-	-	-	-	-	-	-
%Na_2O	-	-	-	-	-	-	-	-	-
%K_2O	0.11	0.79	0.05	-	-	-	-	-	-
%TiO_2	0.14	0	0	-	-	-	-	-	-
Total	89.73	85.22	89.14	88.09	88.32	89.40	86.17	87.79	88.29
Si	6.81	7.58	6.54	6.30	6.76	6.92	7.23	6.37	6.35
Al	5.39	5.00	5.48	5.43	6.01	5.61	5.55	5.89	6.07
Fe	1.93	1.73	1.65	2.34	1.64	1.98	1.82	2.02	1.63
Mn	0.03	0.03	0.02	0.02	0.01	0.01	0.01	0.01	0.02
Mg	4.28	3.49	5.02	4.90	3.80	3.75	3.34	4.39	4.53
Ca	-	-	-	-	-	-	-	-	-
Na	-	-	-	-	-	-	-	-	-
K	0.02	0.19	0.01	-	-	-	-	-	-
Ti	0.02	-	-	-	-	-	-	-	-
Total	18.48	18.02	18.72	18.99	18.22	18.27	18.01	18.68	18.60
Mg/(Mg+Fe)	0.689	0.669	0.753	0.677	0.699	0.654	0.647	0.685	0.735
Al/Si	0.791	0.660	0.838	0.862	0.889	0.811	0.768	0.925	0.956

DDH 58/31.2 m

	1	2	3	4	5	6	7	8	9	10
%SiO_2	35.42	29.69	34.13	30.93	36.18	36.27	36.33	35.19	31.32	34.75
%Al_2O_3	24.93	24.34	23.96	23.91	25.17	25.81	24.57	27.03	24.73	28.04
%ΣFe (FeO)	10.25	16.42	11.64	15.49	7.58	9.57	11.06	8.88	14.60	9.21
%MnO	0.15	0.63	0.29	0.32	0.15	0.13	0.14	0.04	0.25	0
%MgO	14.50	18.02	15.77	15.68	14.64	14.59	16.80	18.34	17.54	17.15
%CaO	-	-	-	-	-	-	-	-	-	-
%Na_2O	-	-	-	-	-	-	-	-	-	-
%K_2O	0.10	0.05	0.12	0.06	0.30	0.17	0.15	0.06	0.17	0.06
%TiO_2	0.12	-	-	-	-	-	-	-	-	-
Total	85.47	89.15	85.91	86.39	84.02	86.54	89.06	89.55	88.62	89.21
Si	6.84	5.77	6.64	6.51	6.97	6.88	6.76	6.44	6.05	6.39
Al	5.64	5.60	5.51	5.61	5.72	5.76	5.38	5.83	5.63	6.07
Fe	1.62	2.68	1.86	2.58	1.22	1.48	1.72	1.36	2.36	1.42
Mn	0.02	0.12	0.05	0.05	0.02	0.02	0.02	0.01	0.04	-
Mg	4.17	5.25	4.54	4.65	4.20	4.09	4.65	5.00	5.04	4.70
Ca	-	-	-	-	-	-	-	-	-	-
Na	-	-	-	-	-	-	-	-	-	-
K	0.03	0.01	0.03	0.01	0.07	0.04	0.03	0.01	0.04	0.01
Ti	0.02	-	-	-	-	-	-	-	-	-
Total	18.34	19.43	18.63	19.05	18.21	18.27	18.57	18.65	19.16	18.58
Mg/(Mg+Fe)	0.720	0.662	0.709	0.643	0.775	0.734	0.730	0.786	0.681	0.768
Al/Si	0.825	0.971	0.830	0.912	0.821	0.837	0.796	0.905	0.931	0.950

DDH 60/46.4 m

	1	2	3	4	5	6	7
%SiO_2	30.61	32.16	33.65	34.76	34.18	34.09	34.65
%Al_2O_3	23.14	24.44	24.84	24.89	25.16	24.79	25.55
%ΣFe (FeO)	17.77	15.40	15.28	16.92	14.83	14.20	12.45
%MnO	0.15	0.08	0.05	0.09	0.10	0.08	0.05
%MgO	16.83	17.11	13.91	15.51	14.56	15.28	14.56
%CaO	-	-	-	-	-	-	-
%Na_2O	-	-	-	-	-	-	-
%K_2O	0	0	0.02	0	0.01	0.02	0.04
%TiO_2	-	-	-	-	-	-	-
Total	88.50	89.19	87.75	92.16	88.84	88.46	87.30
Si	6.03	6.17	6.50	6.45	6.51	6.48	6.62
Al	5.37	5.53	5.65	5.44	5.63	5.58	5.76
Fe	2.93	2.47	2.44	2.63	2.40	2.29	1.96
Mn	0.02	0.01	0.01	0.01	0.02	0.01	0.01
Mg	4.94	4.89	4.06	4.29	4.11	4.36	4.15
Ca	-	-	-	-	-	-	-
Na	-	-	-	-	-	-	-
K	-	-	0.01	-	-	0.01	0.01
Ti	-	-	-	-	-	-	-
Total	19.29	19.07	18.67	18.82	18.67	18.73	18.51
Mg/(Mg+Fe)	0.628	0.664	0.625	0.620	0.631	0.656	0.679
Al/Si	0.891	0.895	0.869	0.844	0.865	0.861	0.870

DDH 87/67.6 m

	1	2	3	4	5	6	7	8	9	10	11	12
%SiO_2	33.1	37.13	32.75	33.96	38.24	30.61	36.74	33.13	31.12	32.03	35.65	32.21
%Al_2O_3	23.56	14.96	24.69	23.95	23.96	23.36	23.56	24.05	22.35	22.72	23.56	21.9
%ΣFe (FeO)	12.17	10.7	10.88	12.07	10.81	14.27	10.15	11.17	16.7	11.81	11.15	13.47
%MnO	0.05	0.16	0.07	0.09	-	0.13	0.08	0.14	0.13	0.01	0.06	-
%MgO	17.43	25.32	18.54	16.41	14.94	19.98	16.36	17.14	16.52	20.07	15.37	18.28
%CaO	-	-	-	-	-	-	-	-	-	-	-	-
%Na_2O	-	-	-	-	-	-	-	-	-	-	-	-
%K_2O	0.03	0	0.02	0.11	0.06	0	0.08	0.02	0	0.07	0.35	0.05
%TiO_2	0.08	-	-	-	0.08	-	-	0.03	-	0	-	0.18
Total	86.42	88.27	86.95	86.59	88.1	88.35	86.97	85.68	86.81	86.71	86.15	86.09
Si	6.44	7.05	6.28	6.56	7.12	5.93	6.94	6.41	6.21	6.24	6.86	6.35
Al	5.38	3.34	5.61	5.42	5.26	5.35	5.23	5.52	5.25	5.21	5.35	5.09
Fe	1.99	1.71	1.73	1.97	1.68	2.33	1.59	1.86	2.78	1.87	1.79	2.22
Mn	0.01	0.03	0.01	0.02	0.02	-	0.01	0.02	-	0.02	-	0.01
Mg	5.03	7.16	5.3	4.76	4.15	5.82	4.66	5.01	4.91	5.83	4.41	5.37
Ca	-	-	-	-	-	-	-	-	-	-	-	-
Na	-	-	-	-	-	-	-	-	-	-	-	-
K	0.01	-	0.01	0.03	0.01	-	0.02	0.01	-	0.02	0.09	0.01
Ti	0.01	-	-	-	0.01	-	-	0.01	-	-	-	0.03
Total	18.87	19.29	18.94	18.76	18.24	19.45	18.45	18.84	19.17	19.17	18.51	19.08
Mg/(Mg+Fe)	0.717	0.807	0.754	0.707	0.712	0.714	0.746	0.729	0.638	0.757	0.711	0.708
Al/Si	0.835	0.474	0.893	0.826	0.739	0.902	0.754	0.861	0.845	0.835	0.78	0.802

DDH 5/51.4 m

	1	2	3
%SiO_2	24.97	32.84	37.36
%Al_2O_3	21.63	26.24	31.58
%ΣFe (FeO)	28.95	14.95	5.14
%MnO	-	-	-
%MgO	8.98	16.07	15.04
%CaO	0.07	0.15	0.16
%Na_2O	-	-	-
%K_2O	-	-	-
%TiO_2	-	-	-
%UO_2	8.34	0	0
Total	92.94	90.25	89.28
Si	5.39	6.18	6.64
Al	5.51	5.82	6.62
Fe	5.23	2.35	0.77
Mn	-	-	-
Mg	2.9	4.51	3.98
Ca	0.01	0.03	0.03
Na	-	-	-
K	-	-	-
Ti	-	-	-
U	0.81	-	-
Total	19.85	18.89	18.04
Mg/(Mg+Fe)	0.357	0.657	0.838
Al/Si	1.022	0.942	0.997

DDH 9/35.2 m

	1
%SiO_2	29.46
%Al_2O_3	27.97
%ΣFe (FeO)	7.26
%MnO	-
%MgO	16.05
%CaO	-
%Na_2O	-
%K_2O	-
%TiO_2	-
%UO_2	0.63
Total	81.37
Si	5.96
Al	6.67
Fe	1.23
Mn	-
Mg	4.84
Ca	-
Na	-
K	-
Ti	-
U	0.05
Total	18.75
Mg/(Mg+Fe)	0.797
Al/Si	1.119

DDH 18/27.5 m

	1
%SiO_2	37.27
%Al_2O_3	21.76
%ΣFe	9.54
%MnO	-
%MgO	21.54
%CaO	0
%Na_2O	-
%K_2O	-
%TiO_2	-
%UO_2	0
Total	90.11
Si	6.68
Al	4.6
Fe	1.43
Mn	-
Mg	5.75
Ca	-
Na	-
K	-
Ti	-
U	-
Total	18.46
Mg/(Mg+Fe	0.801
Al/Si	0.689

DDH 19/47.6 m

	1
%SiO_2	33.80
%Al_2O_3	26.13
%ΣFe (FeO)	10.42
%MnO	0.16
%MgO	19.58
%CaO	0.04
%Na_2O	-
%K_2O	-
%TiO_2	-
Total	90.13
Si	6.11
Al	5.56
Fe	1.57
Mn	0.03
Mg	5.27
Ca	0.01
Na	-
K	-
Ti	-
Total	18.55
Mg/(Mg+Fe)	0.770
Al/Si	0.910

DDH 5/47.2 m

	1
%SiO_2	25.91
%Al_2O_3	16.97
%ΣFe (FeO)	18.53
%MnO	0
%MgO	30.94
%CaO	0
%Na_2O	-
%K_2O	-
%TiO_2	-
Total	92.35
Si	5.06
Al	3.90
Fe	3.03
Mn	-
Mg	9.00
Ca	
Na	-
K	-
Ti	-
Total	20.99
Mg/(Mg+Fe)	0.748
Al/Si	0.771

DDH 9/49.9 m

	1
%SiO_2	29.26
%Al_2O_3	20.95
%ΣFe (FeO)	30.59
%MnO	0.26
%MgO	5.69
%CaO	0.12
%Na_2O	-
%K_2O	-
%TiO_2	-
Total	86.87
Si	6.30
Al	5.32
Fe	5.51
Mn	0.05
Mg	1.82
Ca	0.03
Na	-
K	-
Ti	-
Total	19.03
Mg/(Mg+Fe)	0.248
Al/Si	0.844

APPENDIX 2

REPRESENTATIVE ANALYSES OF KOONGARRA URANINITES (Snelling, 1980a)

DDH/m	2/33.3		2/58.2	5/34.4		5/47.2			5/51.4	6/52.9			6/53.1	
$\%UO_2$	89.17	91.29	81.06	92.20	88.91	86.45	86.64	89.81	89.70	87.77	89.59	87.67	87.14	87.22
%PbO	7.67	4.57	13.30	5.70	4.66	10.25	6.79	6.27	6.15	8.82	5.95	4.82	2.28	2.52
%CaO	1.64	2.13	3.80	0.38	0.27	1.56	1.81	2.09	2.21	2.23	2.44	5.14	7.30	5.55
$\%SiO_2$	0.39	0.50	1.25	0.24	2.34	0.46	0.78	0.63	0.66	0.58	1.17	1.65	2.02	1.34
%ΣFe(FeO)	0.45	0.46	nd	nd	0.46	0.52	2.09	0.58	0.43	0.43	0.58	nd	0.24	2.01
%MnO	-	-	0.16	-	-	0.38	0.29	0.35	0.43	-	-	-	-	-
%MgO	nd	0.12	nd	0.39	1.86	0.13	0.18	nd	nd	nd	nd	0.23	0.17	0.32
$\%P_2O_5$	0.21	0.30	0.16	0.13	0.13	0.17	1.14	0.19	0.17	0.17	nd	0.22	nd	nd
$\%V_2O_3$	-	-	0.48	-	-	-	-	-	0.21	-	-	-	-	-
Total	99.53	99.37	100.21	99.04	98.91	99.92	99.72	99.92	99.96	100.00	99.73	99.73	99.13	98.96

* nd denotes "not detected"
* - denotes "not measured"

DDH/m	6/55.8		9/27.9			9/35.2				16/61.1m		19/44.5		
%UO_2	86.24	81.84	92.39	94.86	96.78	84.19	89.50	90.40	85.18	88.31	86.61	85.40	87.79	90.52
%PbO	6.24	5.59	6.84	4.48	1.61	10.57	5.39	2.45	4.13	8.06	6.74	12.22	8.79	5.93
%CaO	3.50	5.03	0.21	0.24	0.26	0.25	0.26	0.92	0.43	2.98	4.26	1.17	1.79	1.95
%SiO_2	2.51	2.37	0.21	0.25	0.43	1.18	0.96	1.43	2.00	0.60	2.40	0.33	0.47	0.48
%ΣFe(FeO)	nd	0.39	0.31	0.26	0.21	0.49	0.32	0.56	0.34	0.36	nd	0.37	0.49	0.45
%MnO	0.45	2.17	-	-	-	nd	nd	-	-	-	-	0.27	0.32	0.35
%MgO	0.26	1.56	nd	nd	0.54	nd	0.44	0.15	0.12	nd	0.18	0.34	0.18	0.18
%P_2O_5	0.23	0.25	nd	nd	0.33	-	-	-	-	nd	0.11	0.13	0.14	0.16
%Al_2O_3	0.25	0.19	-	-	-	-	-	-	-	-	-	-	-	-
%BaO	-	-	-	-	-	-	-	2.59	5.92	-	-	-	-	-
%Ce_2O_3	-	-	-	-	-	-	0.72	-	-	-	-	-	-	-
Total	99.68	99.39	99.96	100.09	100.16	96.90	97.59	98.50	98.12	100.31	100.30	100.23	99.97	100.02

DDH/m	19/47.7			19/52.8		19/53.9			19/71.0			26/40.1	29/77.8		
%UO_2	91.78	89.69	88.25	91.77	88.54	84.81	82.63	86.86	89.03	85.12	82.41	93.53	82.18	87.51	90.53
%PbO	3.99	7.13	5.18	0.27	nd	10.49	11.12	7.09	5.19	8.34	10.29	3.76	11.55	6.92	4.65
%CaO	0.89	1.21	5.27	6.19	5.45	1.37	1.97	1.62	2.70	4.68	4.06	0.24	3.08	3.14	3.06
%SiO_2	2.84	1.55	0.97	0.64	3.74	2.38	3.96	2.66	1.20	0.83	0.99	0.66	1.48	1.38	1.14
%ΣFe(FeO)	nd	nd	nd	0.32	0.60	0.33	nd	0.43	0.43	nd	nd	0.25	0.80	1.09	0.41
%MnO	-	-	-	-	-	-	nd	nd	-	-	-	-	-	-	-
%MgO	0.28	nd	nd	0.19	0.80	0.54	nd	0.66	0.10	0.19	0.16	0.44	nd	nd	nd
%P_2O_5	0.20	0.16	0.17	0.37	0.23	nd	0.19	0.17	0.14	0.56	0.50	0.20	nd	nd	nd
Total	99.98	99.74	99.84	99.75	99.36	99.92	99.87	99.49	98.79	99.72	98.41	99.08	99.09	100.04	99.68

DDH/m	29/77.8				47/52.3			58/31.0			58/31.	58/43.0		60/46.5		
%UO_2	89.96	89.73	84.56	88.29	93.49	88.85	80.73	86.74	89.98	91.40	83.57	91.50	86.67	86.49	89.15	92.59
%PbO	3.81	2.35	9.85	6.67	3.55	3.64	7.00	9.98	6.32	4.42	12.36	4.12	5.44	10.60	7.72	4.67
%CaO	3.44	2.40	3.05	3.00	1.42	1.12	1.65	1.55	1.83	1.76	0.61	1.15	4.00	1.48	1.65	1.73
%SiO_2	1.21	5.24	2.17	1.36	0.31	1.84	6.95	0.43	0.63	0.65	0.38	1.46	1.34	0.35	0.42	0.41
%ΣFe(FeO)	0.41	nd	0.15	0.29	0.26	3.21	0.28	0.51	0.51	0.42	0.26	0.19	nd	0.38	0.41	0.40
%MnO	-	-	-	-	-	-	-	-	0.35	0.29	0.23	-	0.23	-	-	-
%MgO	nd	nd	nd	nd	0.14	0.17	0.23	0.16	0.12	nd	0.21	nd	nd	nd	nd	nd
%P_2O_5	nd	0.19	nd	nd	0.83	0.96	2.78	nd	0.13	nd	0.13	0.44	0.79	nd	nd	nd
Total	98.83	98.91	99.78	99.61	100.00	99.79	99.62	99.37	99.87	98.94	97.75	98.86	98.59	99.30	99.35	99.80

DDH/m	87/63.9			87/65.2		87/67.6			87/68.7
%UO_2	90.05	93.25	95.92	87.64	82.47	86.49	89.74	88.41	95.00
%PbO	6.92	3.54	1.65	2.86	1.74	10.48	6.63	4.33	1.90
%CaO	1.52	1.79	0.89	3.50	3.07	1.58	1.98	2.62	0.71
%SiO_2	1.10	1.04	0.33	1.97	5.59	0.27	0.56	2.01	0.64
%ΣFe(FeO)	0.43	0.39	0.42	nd	nd	0.30	0.44	0.76	0.40
%MnO	-	-	-	-	-	0.34	0.38	0.33	-
%MgO	nd	nd	nd	0.90	3.48	0.19	nd	0.65	0.54
%P_2O_5	-	-	-	1.49	0.95	0.19	0.16	0.15	nd
Total	100.02	100.01	99.21	98.36	97.30	99.84	99.89	99.26	99.19

* nd denotes "not detected"
* - denotes "not measured"

APPENDIX 3

REPRESENTATIVE ANALYSES OF KOONGARRA SULFIDE MINERALS (Snelling, 1980a)

GALENA (PbS)

DDH/m	58/31.0	60/46.5	87/63.9	87/65.2	47/53.3	29/77.8	5/26.6
%Pb	86.39	86.60	83.56	84.52	86.08	85.78	86.02
%Fe	0.25	nd	1.09	0.84	nd	0.91	0.65
%Cu	-	nd	1.82	0.73	0.14	nd	nd
%Zn	-	nd	-	0.61	nd	-	nd
%S	0.25	13.32	13.12	13.17	13.37	13.18	13.32
%Se	nd	nd	0.39	nd	nd	-	nd
Total	99.98	99.92	99.98	99.87	99.59	99.87	99.99

GALENA (PbS)-CLAUSTHALITE (PbSe)

DDH/m	21/83.8	16/56.3		87/67.6A					87/67.6B		87/67.6C	
%Pb	80.43	77.21	78.76	70.86	74.19	76.91	85.04	85.91	83.47	85.88	85.28	83.28
%Fe	0.96	0.71	1.07	nd	nd	nd	nd	nd	-	-	-	-
%Cu	2.99	nd	nd	nd	nd	nd	nd	nd	-	-	-	-
%Zn	nd	nd	nd	nd	nd	nd	nd	nd	-	-	-	-
%S	12.24	5.45	6.22	1.25	3.20	5.25	12.41	12.94	10.86	12.96	13.15	10.90
%Se	3.36	16.62	13.94	27.89	22.61	17.84	2.45	1.15	5.67	1.16	1.57	5.82
Total	99.98	99.99	99.99	100.00	100.00	100.00	100.00	100.00	100.00	100.00	100.00	100.00

CHALCOPYRITE ($CuFeS_2$)

DDH/m	2/33.3	60/48.4	60/45.4	87/63.9		87/65.2		87/67.6		7/27.2	7/56.5	47/52.3	15/36.9	9/23.8
%Cu	31.25	34.64	34.56	34.40	34.61	34.12	34.39	32.54	34.14	34.59	34.40	34.28	34.31	34.69
%Fe	29.73	30.24	30.37	30.04	29.87	30.23	30.31	28.53	30.35	30.05	30.10	30.34	30.09	29.55
%Co	nd	nd	0.10	0.26	0.12	nd	nd	2.05	0.13	0.36	nd	nd	0.10	nd
%Ni	nd	nd	nd	0.21	0.42	nd	nd	0.79	nd	nd	nd	nd	nd	0.37
%Pb	0.98	nd	nd	nd	nd	nd	nd	0.36	nd	nd	0.16	nd	nd	nd
%Zn	nd	-	-	-	-	0.77	0.64	0.31	0.26	nd	nd	nd	nd	nd
%S	34.37	34.34	34.76	35.03	34.99	34.55	34.53	35.04	34.80	34.81	34.30	34.18	34.86	34.75
%As	0.26	0.52	-	nd	nd	nd	0.23	0.22	0.36	nd	0.27	0.33	0.25	nd
%Se	nd	nd	-	nd	nd	nd	nd	0.16	nd	nd	nd	nd	nd	nd
Total	99.59	99.74	99.79	99.94	100.01	99.67	100.10	100.00	100.04	99.81	99.23	99.13	99.61	99.36

PYRITE (FeS_2)

DDH/m	58/30.0		58/31.0	87/63.9	87/67.6		4/39.0	4/62.4	19/35.2	19/40.1	47/53.3		49/39.0	49/62.4	50/46.5	9/23.8
%Fe	41.27	46.01	45.67	45.20	40.81	45.15	45.86	46.24	46.36	45.87	43.49	45.34	46.24	40.22	45.35	44.67
%Co	0.22	0.21	0.25	0.39	0.36	0.24	0.25	0.12	0.13	0.12	nd	0.33	0.24	0.16	0.53	nd
%Ni	0.43	0.18	0.12	0.22	0.40	0.15	nd	nd	nd	nd	nd	0.19	0.14	nd	0.14	0.44
%Cu	0.24	nd	nd	nd	nd	nd	nd	nd	nd	nd	2.61	0.72	nd	6.17	nd	1.44
%Pb	3.95	nd	0.30	0.16	0.65	nd	nd	nd	nd	0.42	0.13	nd	nd	nd	0.13	nd
%Zn	nd	nd	nd	-	0.21	nd	0.23	nd	nd	nd	-	nd	nd	nd	nd	nd
%S	52.93	53.17	53.12	52.84	51.72	52.97	53.03	51.22	52.99	52.62	53.19	53.06	53.37	52.91	53.14	53.28
%As	0.26	0.28	0.35	0.79	0.82	nd	0.23	1.81	0.27	0.71	0.26	0.35	nd	0.36	0.26	nd
%Se	0.10	nd	nd	nd	nd	nd	nd	nd	0.17	nd	nd	nd	nd	nd	nd	nd
Total	99.64	99.85	99.81	99.60	99.43	99.57	99.60	99.39	99.92	99.64	99.67	99.99	99.99	99.82	99.55	99.83

BRAVOITE (Fe, Co, Ni)S_2 AND ZONED PYRITE

DDH/m	21/64.2				49/62.4		9/23.8	4/62.4		7/27.2		19/40.1		21/64.2	
								core	rim	core	rim	core	rim	core	rim
%Fe	37.33	41.72	44.32	45.13	43.08	44.51	44.93	46.51	46.81	43.37	45.55	42.29	46.52	46.45	46.55
%Co	7.28	3.57	2.05	1.28	0.21	nd	0.10	nd	0.10	0.34	0.16	nd	nd	0.11	0.12
%Ni	2.33	1.33	0.16	0.10	3.28	1.57	1.39	nd	nd	2.59	nd	nd	nd	nd	nd
%Cu	0.44	0.16	nd	nd	0.18	nd	nd	nd	nd	nd	0.29	3.91	nd	nd	nd
%Pb	nd	nd	0.28	nd	nd	nd	nd	nd	nd	nd	0.31	0.11	nd	nd	nd
%Zn	nd	-	-	-	nd	nd	nd	nd	nd	nd	nd	nd	nd	nd	nd
%S	52.22	52.90	53.19	53.15	52.94	53.09	53.37	52.92	51.79	53.34	53.38	53.13	53.12	52.81	52.07
%As	nd	nd	nd	0.27	nd	nd	nd	0.35	1.17	nd	nd	0.26	0.31	0.50	1.14
%Se	0.40	0.27	nd	nd	0.24	0.35	nd	nd	nd	nd	nd	nd	nd	nd	nd
Total	100.00	99.95	99.80	99.93	99.93	99.52	99.79	99.78	99.87	99.64	99.51	99.90	99.95	99.87	99.88

DDH/m	21/64.2										9/23.8			
	core	rim	core	rim	core	rim	core	rim	core	rim	core	rim	core	rim
%Fe	45.70	45.39	45.90	44.07	44.89	42.13	45.02	43.84	44.97	45.11	44.46	45.16	44.34	45.58
%Co	0.46	1.15	0.47	2.06	1.34	3.45	1.13	2.02	1.12	0.87	nd	nd	nd	nd
%Ni	nd	0.12	nd	0.77	0.12	0.43	0.13	0.23	0.16	0.12	2.04	1.25	1.94	0.88
%Cu	nd	nd	nd	0.17	nd	nd	nd	nd	nd	nd	0.11	0.17	0.13	0.11
%Pb	0.15	0.13	nd	nd	nd	nd	0.15	0.25	0.15	0.15	nd	nd	nd	nd
%S	53.15	53.25	53.11	52.87	53.24	52.95	52.99	52.88	53.29	53.39	53.28	53.36	53.25	53.31
%As	nd	nd	0.30	nd	nd	nd	0.16	0.28	nd	nd	nd	nd	nd	nd
%Se	nd	nd	nd	nd	nd	nd	0.15	0.25	nd	nd	nd	nd	nd	nd
Total	99.56	99.94	99.78	99.94	99.59	99.96	99.78	99.73	99.69	99.64	99.89	99.94	99.66	99.88

GERSDORFFITE (Co, Ni, Fe) AsS

Weight %

DDH/m	58/31.0		58/31.0	87/63.9
	core	rim		
Co	28.28	25.41	27.67	22.47
Ni	5.82	9.44	6.50	5.95
Fe	1.14	0.31	0.97	6.77
As	44.96	45.07	44.99	45.40
S	19.06	19.45	19.15	19.40
Se	0.75	0.30	0.65	-
Total	100.01	99.98	99.93	99.99

Cation %

Co	80.27	72.25	78.79	63.85
Ni	16.49	26.84	18.48	16.91
Fe	3.24	0.91	2.73	19.24

* nd denotes "not detected"

* - denotes "not measured"

APPENDIX 4

BULK DRILL CORE ASSAYS (Noranda, unpublished data, 1971)

DDH No.	Depth		Core Length	Rock Type	U_3O_8 ppm	Cu ppm	Pb ppm	Zn ppm	Ag ppm	Au ppm	Co ppm	Ni ppm	Mo ppm	Mn ppm	Bi ppm	V ppm	K %	Na %	Mg %	Ca %	CO_2 %	As ppm	Se ppm	Ti %	Y ppm
	From	To																							
4	65.5m	88.4m	22.9m	Hanging wall and graphitic schists	60	90	430	82	13	nd	42	68	0.5	470	15	110	1.00	nd	5.10	0.17	0.08	10	-	0.30	nd
	88.4m	103.6 m	15.2m	Ore horizon (waste)	165	46	381	56	0.7	nd	30	34	0.75	550	15	30	1.83	nd	3.98	0.10	0.43	nd	-	0.17	36
	103.6m	115.8 m	12.2m	Ore horizon (waste)	90	24	38	84	0.9	0.0	40	50	1.0	700	15	50	1.66	nd	5.46	0.13	0.29	nd	-	0.24	26
	115.8m	125m	9.2m	Ore horizon (waste)	1475	8	120	80	1.2	0.60	36	76	0.75	550	20	100	1.91	nd	5.94	0.33	0.43	nd	-	0.29	nd
	125m	137.2 m	12.2m	Ore horizon (waste)	45	8	34	54	0.9	0.04	34	62	1.0	340	20	40	2.24	nd	5.10	0.15	0.17	nd	-	0.32	20
	137.2m	146.3 m	9.1m	Faulted zone	15	6	26	40	0.7	nd	16	42	0.75	200	20	20	2.74	nd	3.66	0.32	0.41	nd	-	0.20	22
5	1.5m	33.5m	32m	Weathered zone (dispersed)	890	230	100	110	0.8	nd	58	98	7.0	550	10	100	2.08	0.052	2.10	0.05	1.83	nd	-	0.47	25
	33.5m	*54.9m*	*21.4m*	*Main upper ore zone*	*3.8%*	*160*	*6200*	*96*	*1.8*	*2.8*	*50*	*110*	*18*	*500*	*30*	*350*	*1.33*	*0.052*	*5.16*	*0.25*	*1.06*	*20*	-	*0.23*	*146*
	54.9m	64m	9.1m	Ore zone	275	26	74	62	2.0	0.16	34	40	0.75	500	20	50	2.16	nd	4.38	0.15	0.45	nd	-	0.27	23
	64m	65.5m	1.5m	Ore zone	9490	190	720	130	5.5	5.6	50	56	0.75	1200	45	150	0.66	nd	4.08	0.07	0.24	5.0	-	0.14	21
	65.5m	79.2m	13.7m	Ore zone	910	12	140	110	1.4	4.1	32	54	0.75	550	20	90	1.99	0.052	4.56	0.13	0.28	nd	-	0.23	25
	79.2m	82.3m	3.1m	Ore zone	205	6	58	30	0.8	0.76	24	40	0.5	500	15	50	2.32	0.059	4.08	0.07	0.53	nd	-	0.17	25
	82.3m	85.3m	3m	Ore zone	1850	14	150	60	1.9	2.4	28	56	0.75	390	20	100	1.99	0.052	4.56	0.10	0.45	nd	-	0.21	28
	85.3m	*91.4m*	*6.1m*	*Ore zone*	*255*	*4*	*60*	*44*	*1.0*	*0.16*	*26*	*56*	*0.75*	*310*	*25*	*70*	*2.49*	*nd*	*4.86*	*0.15*	*0.55*	*nd*	-	*0.30*	*nd*
8	4.9m	19.8m	14.9m	Weathered zone (dispersed)	1295	54	70	220	1.0	0.08	56	190	3.0	240	15	130	2.16	nd	0.54	0.04	2.44	5.0	-	0.27	nd
	19.8m	22.7m	2.9m	Weathered zone (leached primary)	4955	-	-	-	-	-	-	-	-	-	-	-	-	-	-	-	-	-	-	-	-

DDH No.	Depth		Core Length	Rock Type	U_3O_8 ppm	Cu ppm	Pb ppm	Zn ppm	Ag ppm	Au ppm	Co ppm	Ni ppm	Mo ppm	Mn ppm	Bi ppm	V ppm	K %	Na %	Mg %	Ca %	CO_2 %	As ppm	Se ppm	Ti %	Y ppm
	From	To																							
	22.7m	30.2m	7.5m	Weathered zone (leached primary)	360	52	92	98	1.1	0.12	44	90	1.0	450	20	60	0.56	nd	5.94	0.10	0.42	nd	-	0.14	nd
8	30.2m	54.9m	24.7m	Partially weathered zone; Barren ore schists	80	24	40	30	1.2	0.04	46	86	0.75	490	15	40	0.78	nd	7.14	0.10	0.19	nd	-	0.14	nd
	54.9m	84.4m	29.5m	Partially weathered zone; Barren ore schists	10	12	40	92	1.3	nd	56	82	0.75	380	15	40	0.43	nd	8.28	0.15	0.32	nd	-	0.21	nd
9	3.1m	27.4m	24.3m	Weathered zone dispersed	1165	350	430	140	1.0	nd	80	94	40	1000	10	70	1.58	0.052	0.64	0.05	1.38	nd	-	0.07	nd
	27.4m	51.5m	24.1m	Main upper ore zone including graphite	1.7%	680	2400	72	1.1	0.28	46	92	40	360	15	200	1.49	0.052	3.9	0.13	1.37	100	-	0.36	nd
	51.5m	61.4m	9.9m	Main upper ore zone	1295	24	88	50	0.9	0.48	36	76	1.0	340	15	50	1.41	nd	5.16	0.10	0.47	nd	-	0.20	25
11	3.1m	12.2m	9.1m	Weathered zone waste	40	68	34	68	0.7	nd	46	70	1.0	1050	15	60	1.58	0.052	1.50	0.05	0.47	nd	-	0.42	21
	12.2m	21.3m	9.1m	Weathered zone waste	85	260	46	80	0.8	nd	44	66	2.0	650	15	70	1.83	0.067	1.92	0.05	0.91	nd	-	0.42	30
	24.4m	35.1m	10.7m	Hanging wall schist including graphite schist	50	78	50	150	1.1	nd	50	84	2.0	850	15	80	2.82	0.081	4.68	0.10	0.21	nd	-	0.56	21
	36.6m	68.6m	32m	Hanging wall schist including graphite schist	75	56	44	94	1.2	0.08	60	76	2.0	550	15	110	0.62	nd	5.76	0.13	1.50	nd	-	0.45	nd
	68.6m	88.4m	19.8m	Ore zone (barren)	35	36	46	72	1.3	nd	50	78	0.75	310	20	70	0.45	nd	7.86	0.10	0.58	nd	-	0.32	nd
	88.4m	97.5m	9.1m	Ore zone (barren)	25	16	34	60	1.3	nd	44	74	1.0	390	15	40	0.57	nd	6.06	0.10	0.24	nd	-	0.17	nd
	97.5m	118.9 m	21.4m	Ore zone (barren)	75	20	40	54	1.0	0.28	40	72	1.0	270	15	50	1.16	nd	5.70	0.15	0.29	nd	-	0.17	22
	118.9m	123.4 m	4.5m	Faulted zone	125	6	34	68	1.0	0.24	36	82	0.75	200	10	70	0.09	nd	4.50	0.20	0.37	nd	-	0.09	-

DDH No.	Depth		Core Length	Rock Type	U_3O_8 ppm	Cu ppm	Pb ppm	Zn ppm	Ag ppm	Au ppm	Co ppm	Ni ppm	Mo ppm	Mn ppm	Bi ppm	V ppm	K %	Na %	Mg %	Ca %	CO_2 %	As ppm	Se ppm	Ti %	Y ppm
	From	To																							
13	6.1m	29m	22.9m	Weathered zone. Mixed waste and marginal ores (dispersed)	235	16	30	170	0.9	nd	64	70	2.0	550	20	140	0.35	nd	5.16	0.10	0.45	nd	-	0.84	nd
13	29m	42.7m	13.7m	Hanging wall schist (barren)	35	40	48	70	1.2	nd	40	66	2.0	320	15	80	0.41	nd	5.88	0.15	0.82	nd	-	0.39	nd
	42.7m	67.1m	24.4m	Hanging wall schist including graphite (barren)	25	40	42	86	1.1	nd	48	82	3.0	350	15	100	0.37	nd	6.18	0.17	<.07 3	nd	-	0.31	nd
	68.6m	79.2m	10.6m	Main ore zone (barren)	10	32	34	76	1.2	nd	40	68	1.0	600	15	30	0.99	nd	5.88	0.10	0.33	nd	-	0.17	33
	79.2m	97.5m	18.3m	Main ore zone (barren)	50	6	36	68	1.1	nd	42	66	1.0	550	15	50	0.68	nd	6.18	0.07	0.58	nd	-	0.19	26
	79.2m	123.4 m	44.2m	Main ore zone (barren)	10	8	30	86	1.4	0.04	50	82	1.0	420	15	50	0.71	nd	8.28	0.10	0.28	nd	-	0.29	nd
	123.4m	134.1 m	10.7m	Main ore zone (barren)	20	22	42	94	1.4	nd	54	100	1.0	410	15	70	0.29	nd	10.02	0.13	0.26	nd	-	0.30	nd
	134.1m	145.4 m	11.3m	?Faulted zone (barren)	5	10	40	72	1.3	nd	38	78	1.0	1000	20	40	0.34	nd	8.88	4.27	9.13	nd	-	0.16	nd
15	1.5m	16.8m	15.3m	Weathered zone (dispersed)	170	350	200	160	0.8	nd	54	110	3.0	410	15	90	0.99	nd	6.66	0.07	1.45	nd	-	0.35	nd
	18.3m	27.4m	9.1m	Ore zone leached primary (waste)	65	230	56	72	1.2	nd	46	80	4.0	280	10	110	0.29	nd	5.88	0.10	0.10	nd	-	0.29	nd
	29m	39.6m	10.6m	Main ore zone (barren)	10	16	30	62	1.0	nd	36	44	1.0	260	10	30	0.78	nd	5.76	0.07	0.33	nd	-	0.20	nd
	41.1m	50.3m	9.2m	Main ore zone (barren)	20	14	34	42	0.8	nd	32	28	0.75	360	15	20	1.49	nd	4.38	0.10	0.54	nd	-	0.18	-
	51.8m	64m	12.2m	Main ore zone (barren)	15	16	28	50	0.7	nd	30	48	1.0	240	10	30	1.91	0.052	4.56	0.07	0.48	nd	-	0.17	28
	64m	68.6m	4.6m	Main ore zone (barren)	10	6	30	60	0.9	nd	40	56	1.0	380	10	30	1.16	nd	5.10	0.10	0.32	nd	-	0.16	25

DDH No.	Depth		Core Length	Rock Type	U_3O_8 ppm	Cu ppm	Pb ppm	Zn ppm	Ag ppm	Au ppm	Co ppm	Ni ppm	Mo ppm	Mn ppm	Bi ppm	V ppm	K %	Na %	Mg %	Ca %	CO_2 %	As ppm	Se ppm	Ti %	Y ppm
	From	To																							
	68.6m	76.2m	7.6m	Main ore zone (barren)	10	4	30	110	1.2	nd	54	110	1.0	220	15	60	0.08	nd	7.74	0.13	0.33	nd	-	0.14	nd
	80.7m	82.3m	1.6m	Faulted zone (barren)	5	4	26	90	0.8	nd	30	50	0.75	300	10	30	0.83	nd	4.50	0.30	0.46	nd	-	0.15	nd
21	77.7m	80.8m	3.1m	Hanging wall schist (barren)	10	16	46	100	1.2	nd	44	50	3.0	450	15	80	1.58	nd	4.80	0.15	0.073	nd	-	0.36	nd
	80.8m	96m	15.2m	Main ore zone including graphitic section	1090	270	1120	170	1.4	nd	60	100	7.0	390	20	140	0.34	nd	6.36	0.25	0.073	nd	-	0.21	nd
	96m	115.8m	19.8m	Main ore zone; Mineralised waste	205	14	38	66	1.0	nd	38	50	0.75	470	10	20	1.49	nd	4.98	0.15	0.21	nd	-	0.19	26
	115.8m	123.4m	7.6m	Main ore zone; Mineralised waste	100	20	38	44	1.1	nd	40	84	0.75	360	15	30	1.25	nd	5.88	0.10	0.15	nd	-	0.27	nd
	123.4m	137.2m	13.8m	Main ore zone; Mineralised waste	145	16	42	58	1.2	nd	44	90	0.75	310	15	50	1.33	nd	6.78	0.15	0.20	nd	-	0.25	nd
	137.2m	144.8m	7.6m	Faulted zone; Mineralised waste	135	4	46	60	1.2	3.2	36	110	1.0	200	20	80	1.33	0.052	5.58	0.17	0.37	nd	-	0.24	nd
30	6.1m	27.4m	21.3m	Weathered zone (dispersed ore)	590	26	36	88	0.7	nd	40	84	2.0	370	10	60	0.99	0.052	1.38	0.02	1.34	nd	-	0.36	-
	27.4m	32m	4.6m	Hanging wall schist; Mineralised waste	85	12	42	68	1.0	nd	44	90	2.0	240	15	60	1.25	0.052	6.96	0.05	0.48	nd	-	0.35	nd
	32m	42.7m	10.7m	Main ore zone (graphite)	1.69%	470	4000	82	1.7	0.50	48	100	6.0	300	200	210	0.17	nd	4.86	0.20	0.10	100	-	0.20	39
	42.7m	54.9m	12.2m	Main ore zone; Mineralised waste	240	18	50	72	0.9	0.40	40	78	1.0	320	15	20	0.79	nd	5.88	0.07	0.32	nd	-	0.17	25
	54.9m	85.3m	30.4m	Main ore zone; Mineralised waste	125	20	50	86	1.2	nd	54	110	1.0	290	15	60	0.33	nd	7.86	0.10	0.33	nd	-	0.23	nd
	85.3m	93m	7.7m	Main ore zone (barren)	25	30	40	80	1.3	nd	56	120	1.0	270	20	50	0.44	nd	8.58	0.13	0.44	nd	-	0.32	nd

DDH No.	Depth		Core Length	Rock Type	U_3O_8 ppm	Cu ppm	Pb ppm	Zn ppm	Ag ppm	Au ppm	Co ppm	Ni ppm	Mo ppm	Mn ppm	Bi ppm	V ppm	K %	Na %	Mg %	Ca %	CO_2 %	As ppm	Se ppm	Ti %	Y ppm
	From	To																							
40	7.6m	13.7m	6.1m	Weathered zone; Leached primary waste	100	10	20	20	0.5	0.12	10	42	1.0	30	10	60	0.50	nd	0.15	nd	0.22	nd	0.5	0.11	nd
	13.7m	24.4m	10.7m	Weathered zone; Leached primary waste	295	12	28	150	0.6	0.06	34	200	0.5	150	10	60	0.50	nd	0.80	nd	0.33	nd	nd	0.15	54
40	24.4m	33.5m	9.1m	Leached primary low grade ore; Main ore zone (?marginal ore)	255	8	28	74	1.1	nd	46	120	1.0	360	15	50	0.15	nd	5.9	nd	0.12	nd	1.0	0.16	nd
	33.5m	56.4m	22.9m	Main ore zone (barren)	45	6	22	68	1.4	nd	50	120	1.0	210	20	80	0.55	nd	8.2	0.10	0.16	nd	nd	0.31	nd
	57.9m	64m	6.1m	Main ore zone (marginal ore)	305	6	24	52	1.3	0.30	48	120	1.0	150	15	110	0.30	nd	8.4	0.10	0.30	nd	nd	0.26	nd
	64m	69.3m	5.3m	Main ore zone (marginal ore)	310	6	30	40	0.6	0.32	26	50	1.0	220	10	60	nd	nd	0.85	0.10	0.37	nd	nd	0.06	nd
47	6.1m	30.5m	24.4m	Weathered zone dispersed low grade ore waste	335	28	18	160	1.1	nd	66	54	1.0	800	15	170	0.40	nd	2.8	nd	0.17	nd	0.5	1.23	nd
	30.5m	35.1m	4.6m	Transition; Weakly mineralised	85	18	42	86	1.4	0.20	52	78	2.0	600	20	130	0.65	nd	6.9	0.15	0.83	nd	nd	0.64	nd
	45.7m	57.9m	12.2m	Hanging wall schist; Weakly mineralised	155	86	32	66	1.3	0.04	44	60	3.0	370	15	130	1.15	nd	6.0	0.15	2.19	nd	1.0	0.50	nd
	59.4m	67.1m	7.7m	Hanging wall schist; Weakly mineralised	50	22	26	54	1.3	nd	40	86	2.0	210	15	100	1.10	0.05	6.7	0.05	1.61	nd	nd	0.42	nd
	67.1m	70.1m	3m	Graphitic zone ore	5210	600	4000	42	1.4	0.2	30	64	2.0	150	20	170	0.55	nd	3.4	0.15	4.43	5	12.0	0.24	nd
	70.1m	79.2m	9.1m	Main ore zone; Mineralised waste	110	62	78	58	1.2	0.04	34	68	1.0	290	20	30	0.65	nd	6.0	0.05	0.25	5	3.0	0.14	nd
	79.2m	100.6 m	21.4m	Main ore zone	695	20	42	54	1.1	nd	36	74	1.0	390	20	40	1.00	nd	5.8	0.10	0.39	5	0.5	0.21	nd
	100.6m	114.3 m	13.7m	Main ore zone; Mineralised waste	415	12	44	64	1.4	0.08	42	90	1.0	250	20	70	0.60	nd	7.4	0.10	0.28	5	nd	0.29	nd

DDH No.	Depth		Core Length	Rock Type	U_3O_8 ppm	Cu ppm	Pb ppm	Zn ppm	Ag ppm	Au ppm	Co ppm	Ni ppm	Mo ppm	Mn ppm	Bi ppm	V ppm	K %	Na %	Mg %	Ca %	CO_2 %	As ppm	Se ppm	Ti %	Y ppm
	From	To																							
	114.3m	121.9 m	7.6m	Main ore zone; Lower section	6940	24	880	90	1.6	2.0	54	100	1.0	340	25	110	0.25	nd	8.3	0.15	0.50	5	1.0	0.28	169
	121.9m	128m	6.1m	Faulted zone (ore)	3460	16	340	94	2.6	2.0	58	100	1.0	440	25	140	0.35	nd	10.7	0.75	1.07	5	nd	0.31	302
	128m	129.5 m	1.5m	Faulted zone (ore)	1730	18	76	72	1.6	3.2	50	100	1.0	220	25	150	0.10	nd	9.0	0.30	0.30	5	nd	0.26	147
49	79.2m	94.5m	15.3m	Graphitic and main ore zone (marginal)	380	120	210	76	1.3	nd	42	76	3.0	340	150	100	0.45	nd	6.2	0.15	4.77	5	0.5	0.29	nd
	94.5m	112.8 m	18.3m	Main ore zone; Mineralised waste	150	12	26	52	1.3	0.12	40	84	1.0	340	15	40	0.50	nd	69	0.10	0.09	5	nd	0.26	nd
	112.8m	121.9 m	9.1m	Main ore zone; Mineralised waste	125	12	52	80	1.6	0.06	58	130	0.5	300	25	60	0.50	nd	9.6	0.15	0.15	5	nd	0.37	nd
	121.9m	132.6 m	10.7m	Main ore zone; Mineralised waste	195	12	34	48	1.2	0.28	44	94	0.5	220	15	70	0.80	0.05	7.4	0.10	0.11	5	1.5	0.23	45
	132.6m	134.1 m	1.5m	Main ore zone; Mineralised waste	145	10	32	46	1.1	0.40	42	110	1.0	130	15	80	0.45	nd	7.4	0.05	0.15	5	nd	0.20	nd
	134.1m	146m	11.9m	Faulted zone; Mineralised waste	245	8	42	26	0.7	2.0	18	120	1.0	110	20	120	180	nd	3.5	0.30	0.23	nd	1.0	0.29	nd
50	103.6m	109.7 m	6.1m	Graphite and ore zone weak	200	110	180	70	0.9	nd	40	76	3.0	180	200	140	nd	nd	4.7	0.25	3.76	nd	6.0	0.16	nd
	109.7m	114.3 m	4.6m	Main ore zone	1.27%	1240	2800	62	1.5	1.3	50	130	5.0	390	20	250	0.05	nd	6.9	0.25	4.59	5	6.0	0.32	125
	114.3m	118.9 m	4.6m	Main ore zone; Mineralised waste	210	40	32	54	0.8	nd	30	54	1.0	390	20	30	0.55	nd	5.6	0.10	0.42	nd	1.0	0.13	47
51	3m	25.9m	22.9m	Weathered zone; Low grade leached primary	380	22	210	70	0.7	0.6	62	72	1.0	500	150	110	0.40	nd	0.75	nd	0.19	nd	0.5	0.18	135
	25.9m	30.5m	4.6m	Main ore zone; Partially weathered leached primary	480	10	60	60	1.1	0.22	38	64	1.0	250	20	80	0.75	nd	6.6	0.15	0.14	nd	0.5	0.26	nd

DDH No.	Depth		Core Length	Rock Type	U_3O_8 ppm	Cu ppm	Pb ppm	Zn ppm	Ag ppm	Au ppm	Co ppm	Ni ppm	Mo ppm	Mn ppm	Bi ppm	V ppm	K %	Na %	Mg %	Ca %	CO_2 %	As ppm	Se ppm	Ti %	Y ppm
	From	To																							
	30.5m	44.2m	13.7m	Main ore zone; Partially weathered leached primary	125	10	32	52	1.1	0.22	44	86	1.0	280	20	80	0.70	nd	7.0	0.10	0.16	nd	1.57	0.27	52
	44.2m	56.4m	9.2m	Main ore zone; Partially weathered leached primary	255	6	40	48	0.9	0.08	34	76	1.0	200	15	100	0.35	nd	5.9	0.15	0.21	nd	nd	0.14	71
54	3m	25.9m	22.9m	Weathered zone dispersed ore	595	40	26	100	0.6	nd	46	60	1.0	390	15	150	0.45	nd	1.3	0.05	0.74	nd	nd	0.74	242
54	47.2m	56.4m	9.2m	Main ore zone including graphitic schist	275	24	86	80	1.0	nd	40	86	2.0	410	20	130	0.10	nd	6.2	0.15	3.52	nd	2.0	0.33	50
	79.2m	82.3m	3.1m	Main ore zone; Mineralised waste	95	12	28	80	1.0	0.04	48	74	1.0	700	20	60	0.35	nd	8.9	0.75	1.72	nd	1.0	0.21	54
57	24.4m	36.6m	12.2m	Weathered zone (Leached primary?)	140	28	40	88	0.7	0.40	48	120	0.5	300	20	110	0.45	nd	2.2	0.15	0.13	nd	nd	0.16	54

Notes:-

* nd denotes "not detected" * - denotes "not measured"
* limits of detection were:-

0.02ppm Au, Tl	0.01ppm Ag	2ppm Cu, Pb, Zn, Co, Ni	10ppm Mn, V
0.05ppm K, Na, Mg, Ca, Se	0.25ppm Mo	5ppm Bi, As	40ppm Y

APPENDIX 5

REPRESENTATIVE ANALYSES OF KOONGARRA URANIUM-LEAD OXIDES AND URANYL SILICATES (Snelling, 1980a)

PART I. Uranium-Lead Oxides (DDH 58, 31.2m) VANDENDRIESSCHEITE, FOURMARIERITE, CURITE

Mineral	Vandendriesscheite ($PbO.7UO_3.12H_2O$)		Fourmarierite ($PbO.4UO_3.4H_2O$)			Curite ($2PbO.5UO_3.4H_2O$)		
$\%UO_2$	84.12	83.57	78.48	76.26	77.84	75.26	74.87	73.55
% PbO	11.78	12.36	17.01	15.11	12.64	20.49	19.24	18.18
%CaO	1.07	0.61	0.13	0.22	0.40	0.09	nd	0.13
$\%SiO_2$	0.34	0.38	0.16	0.52	0.45	0.62	1.46	1.01
%ΣFe(FeO)	0.36	0.26	0.09	0.34	0.39	0.45	0.25	0.39
%MgO	0.22	0.21	nd	0.24	0.25	0.16	0.51	0.48
$\%P_2O_5$	0.14	0.13	0.12	0.14	nd	nd	nd	0.11
Total	98.39	97.75	95.99	92.83	91.97	97.07	96.33	93.85

PART II. Uranyl Silicates KASOLITE - $Pb(UO_2)SiO_4.H_2O$

DDH/m	62/14.7	19/53.9	47/92.9	58/36.0	18/27.5	2/63.7		47/92.9		3/67.9	18/27.5
$\%UO_2$	51.84	57.20	52.95	51.76	53.87	50.85	53.31	51.05	54.03	59.02	56.05
%PbO	33.63	29.61	29.94	34.52	31.64	34.55	32.01	34.24	28.10	23.17	27.29
%CaO	nd	0.58	0.93	nd	0.22	0.32	0.17	0.51	2.13	1.76	0.13
$\%SiO_2$	8.83	9.14	10.43	9.75	9.30	9.87	9.79	10.32	11.25	10.79	9.62
%ΣFe(FeO)	nd	0.23	1.81	nd	0.26	0.10	0.13	0.49	1.26	0.32	0.69
%MgO	nd	0.29	0.53	0.23	0.41	0.17	0.27	0.11	0.26	0.42	0.53
$\%P_2O_5$	1.04	0.20	0.40	nd	0.93	0.34	0.28	0.34	0.37	0.16	0.88
$\%V_2O_3$	-	0.52	-	-	-	-	-	-	-	0.14	-
Total	95.34	97.77	97.21	96.26	96.63	96.20	95.96	97.06	97.40	95.78	95.19

SKLODOWSKITE - Mg $(UO_2)_2$ $Si_2O_7.6H_2O$

DDH/m	9/49.9	62/30.5	2/54.9	5/51.4		27/33.0	47/92.9		37/107.6	58/31.2			9/35.2
$\%UO_2$	67.10	67.50	67.15	67.46	64.99	67.44	67.28	66.69	67.27	67.25	68.58	67.11	67.47
%PbO	nd	0.26	0.38	nd	0.13	0.37	0.48	0.54	0.16	0.40	0.40	0.21	nd
%CaO	0.09	0.15	0.11	nd	0.19	0.09	0.10	0.24	0.11	nd	0.18	0.23	nd
$\%SiO_2$	15.86	13.45	14.87	14.47	16.18	13.03	14.20	14.94	13.49	15.58	13.13	14.61	12.85
%ΣFe(FeO)	0.24	nd	0.33	0.23	3.53	nd	1.15	0.22	0.20	0.35	nd	0.31	0.13
%MgO	5.47	4.42	5.23	5.28	6.33	4.29	5.20	4.82	4.89	5.03	4.64	5.14	4.41
$\%P_2O_5$	0.49	0.42	0.23	0.49	1.30	1.11	0.38	0.24	0.17	0.30	0.64	0.34	-
$\%V_2O_3$	-	0.13	0.09	-	-	nd	0.10	-	-	-	-	-	-
$\%As_2O_5$	0.35	-	-	-	-	-	0.31	-	-	-	-	-	0.42
$\%Ce_2O_3$	-	-	-	-	-	-	-	-	-	-	-	-	0.23
Total	89.60	86.33	88.39	87.93	92.65	86.33	89.10	87.69	86.29	88.91	87.57	87.95	85.51

DDH/m	9/35.2	58/36.0		18/27.5	3/67.9		2/63.7			2/50.9	2/52.6	2/58.1	
$\%UO_2$	67.72	66.05	66.34	67.01	66.49	67.42	66.75	68.18	66.72	66.95	66.92	66.86	67.41
%PbO	0.22	0.41	0.56	0.48	nd	0.21	1.07	0.19	nd	0.56	nd	0.37	nd
%CaO	0.14	0.09	0.21	0.14	nd	nd	0.69	0.13	0.13	0.21	0.07	0.16	0.10
$\%SiO_2$	13.78	13.88	14.18	14.49	14.56	14.90	14.47	13.85	14.85	14.79	13.47	14.21	13.09
%ΣFe(FeO)	nd	0.10	0.32	1.17	nd	0.91	nd	nd	nd	nd	0.27	nd	nd
%MgO	4.70	4.94	4.47	5.24	4.71	4.06	4.63	4.10	4.83	4.75	5.13	4.44	4.43
$\%P_2O_5$	0.21	nd	0.24	0.77	0.14	0.52	0.21	nd	0.33	0.72	0.16	0.55	1.45
$\%V_2O_3$	-	-	-	-	nd	-	-	-	-	-	nd	-	-
$\%As_2O_5$	-	-	-	0.12	-	-	-	0.43	-	-	-	-	-
Total	86.77	86.07	86.32	87.42	85.90	88.02	87.82	86.88	86.86	87.98	85.62	86.59	86.48

URANOPHANE - $Ca(UO_2)_2Si_2O_7.6H_2O$

DDH/m	47/92.9					19/53.9		47/92.9		
$\%UO_3$	66.04	66.93	65.44	66.65	66.36	67.32	69.58	66.51	66.80	66.37
%PbO	1.25	nd	nd	0.13	1.87	0.27	1.05	3.06	1.92	0.36
%CaO	3.82	7.46	7.14	6.60	5.28	7.47	4.89	6.14	6.60	7.06
$\%SiO_2$	11.53	13.35	14.10	11.97	12.69	11.96	12.06	12.88	13.22	14.70
%ΣFe(FeO)	nd	nd	1.93	0.08	0.38	0.08	0.70	0.39	0.59	0.10
%MgO	nd	nd	0.12	0.10	1.29	0.14	1.16	0.54	0.27	nd
$\%P_2O_5$	1.67	0.40	0.42	1.75	0.37	2.02	0.35	0.45	0.30	0.19
$\%V_2O_3$	-	-	-	3.01	0.91	0.20	0.31	-	-	nd
$\%As_2O_5$	-	-	-	-	-	-	-	nd	nd	-
Total	86.31	88.14	89.15	90.29	89.15	89.46	90.10	89.97	89.70	88.80

DDH/m	47/92.9		3/67.9	2/63.7	2/50.9		2/52.6		2/58.1
$\%UO_2$	66.43	64.64	66.95	66.21	66.01	65.98	65.96	65.79	66.02
%PbO	0.41	1.36	2.01	1.57	nd	nd	nd	nd	nd
%CaO	4.61	7.57	5.94	7.24	5.79	5.22	7.03	6.37	7.21
$\%SiO_2$	14.29	14.60	12.57	12.28	14.84	13.56	14.92	13.21	14.98
%ΣFe(FeO)	0.37	2.07	0.23	0.35	nd	0.31	0.27	0.54	0.14
%MgO	0.24	0.15	0.63	0.28	nd	0.76	0.46	1.22	0.34
$\%P_2O_5$	0.38	0.57	0.24	0.63	1.73	1.61	0.26	0.31	0.81
$\%V_2O_5$	-	-	0.11	-	-	-	0.09	nd	-
Total	86.73	90.96	88.68	88.56	88.37	87.44	88.99	87.44	89.50

SKLODOWSKITE-URANOPHANE (Mg,Ca) $(UO_2)_2$ $Si_2O_7.6H_2O$

DDH/m	19/53.9		19/53.9		47/92.9	
%UO_2	65.49	65.06	69.58	66.45	65.79	66.53
%PbO	1.24	0.87	1.05	0.15	1.00	1.91
%CaO	4.39	2.40	4.89	3.86	5.50	2.34
%SiO_2	15.00	13.09	12.06	14.83	16.11	14.35
%ΣFe(FeO)	0.73	0.60	0.70	nd	1.68	0.39
%MgO	2.65	3.70	1.16	4.76	2.34	3.62
%P_2O_5	0.42	0.31	0.35	0.34	0.40	0.40
%V_2O_3	1.64	0.34	0.31	nd	-	-
%As_2O_5	-	-	-	-	nd	-
Total	91.56	86.37	90.10	90.39	92.82	89.54

DDH/m	3/67.9	2/63.7		2/50.9		2/58.1	
%UO_2	66.88	67.04	66.83	66.88	67.24	66.76	66.65
%PbO	1.09	0.54	nd	0.36	0.27	nd	nd
%CaO	1.16	2.53	3.61	3.66	1.19	1.17	2.53
%SiO_2	12.25	13.69	14.95	14.44	14.61	13.97	14.18
%ΣFe(FeO)	0.24	0.18	nd	nd	0.67	nd	0.12
%MgO	3.28	2.83	2.20	1.64	2.44	4.31	3.99
%P_2O_5	0.11	-	0.31	1.17	1.22	1.52	0.51
%V_2O_3	nd	-	-	-	-	-	-
Total	85.01	86.81	87.90	88.15	87.64	87.73	87.98

APPENDIX 6

REPRESENTATIVE ANALYSES OF KOONGARRA URANYL PHOSPHATES (Snelling, 1980a)

SALEEITE - $Mg(UO_2)_2(PO_4)_2.8H_2O$

DDH/m	62/16.7	18/12.8	18/26.0	27/25.9	38/23.8	43/30.0	5/26.6
$\%UO_2$	63.53	63.94	63.44	64.37	65.15	63.24	64.82
%PbO	0.11	nd	-	nd	0.11	-	nd
%CaO	nd	nd	0.22	nd	nd	0.12	0.06
$\%SiO_2$	0.13	nd	0.27	0.14	0.29	0.28	0.22
%ΣFe(FeO)	0.11	nd	0.22	0.08	nd	0.46	3.52
%MgO	4.62	4.35	1.30	1.70	2.70	1.74	3.52
$\%P_2O_5$	15.93	17.19	16.34	17.47	16.32	14.40	14.40
$\%V_2O_3$	nd	nd	nd	-	-	-	-
$\%As_2O_5$	-	-	0.39	0.45	-	0.56	-
Total	84.43	85.48	82.18	84.21	84.19	84.72	83.72

SABUGALITE - $HAl(UO_2)_4(PO_4)_4.16H_2O$

Location	surface rubble	
$\%UO_2$	65.01	65.54
%PbO	nd	nd
%CaO	nd	nd
$\%SiO_2$	nd	nd
%ΣFe(FeO)	nd	nd
%MgO	nd	nd
$\%P_2O_5$	14.65	15.74
$\%Al_2O_3$	4.27	4.59
$\%V_2O_3$	nd	nd
$\%As_2O_5$	nd	nd
Total	83.93	85.87

RENARDITE - $Pb(UO_2)_4 (PO_4)_2.(OH)_4.7H_2O$
DEWINDTITE - $Pb(UO_2)_2 (PO_4)_2.3H_2O$

DDH/m	62/14.7m					surface rubble	
$\%UO_2$	66.51	64.08	58.31	59.80	60.06	73.51	73.31
%PbO	9.59	15.97	18.17	18.46	19.58	8.25	6.45
%CaO	0.64	0.33	0.31	0.16	0.18	nd	nd
$\%SiO_2$	0.63	0.27	3.35	1.71	0.81	nd	nd
%ΣFe(FeO)	0.17	nd	0.48	0.19	0.20	nd	nd
%MgO	0.10	nd	0.30	0.22	0.11	nd	nd
$\%P_2O_5$	11.46	9.07	9.19	9.97	9.86	8.75	9.35
$\%As_2O_5$	0.27	0.19	0.29	0.28	0.26	-	-
Total	89.37	89.91	90.40	90.79	91.06	90.51	89.11

TORBERNITE - $Cu(UO_2)_2 (PO_4)_4.8H_2O$
METATORBERNITE - $Cu(UO_2)_2 (PO_4)_4.8H_2O$

Location	surface rubble			
$\%UO_2$	59.97	59.40	63.40	63.25
%PbO	nd	nd	nd	nd
%CaO	nd	nd	nd	nd
$\%SiO_2$	nd	nd	nd	nd
%ΣFe(FeO)	nd	nd	nd	nd
%MgO	nd	nd	nd	nd
%CuO	2.18	2.98	4.78	5.45
$\%P_2O_5$	16.17	16.22	17.96	18.02
$\%As_2O_5$	-	-	nd	nd
Total	78.32	78.60	85.14	85.72

* nd denotes "not detected"
* - denotes "not measured"

APPENDIX 7

LOGS OF ARAP DRILL HOLES

Hole M1

- Geology

0-3m	Surface sand and gravel, then weathered schist
3-21m	Weathered schist; bleached clay at first, but iron-staining increasing with depth until complete; schistosity still evident, marked by residual quartz grains; tiny mica (sericite) flakes occasionally visible; saleeite (?) in fractures at 19-19.2m.
21-24m	Partly weathered, fine-grained quartz-chlorite schist±sericite. Transitional zone.
24-50m	Fresh, fine-grained quartz-chlorite schist with quartz segregations. Minor iron oxides along fractures and occasional minor saleeite(?) too.

- Drilling and Sampling

0-22m	Cable tool drilling; 0.25m of core every 1m beginning at 3m (sample nos. M1-3 to M1-21)
22-50m	Rotary percussion drilling; drill chips collected over 2 m intervals beginning at 22-24m (sample nos. M1-23 to M1-49).

Hole M2

- Geology

0-2.8m	Surface sand and gravel, then clay (weathered schist)
2.8-11.9m	Weathered schist; clay with quartz grains embedded in it and defining the original schistosity. Some sericite and saleeite (?) flakes. Variable iron oxides.
11.9-22.9m	Partially weathered quartz-chlorite schist±sericite; 22.9m still some clay with patchy iron oxide staining; quartz bands and segregations. Some uranium phosphates (saleeite ?) along fractures and the schistosity.
22.9-27m	Fairly fresh quartz-chlorite schist (transitional zone), with iron oxides along fractures. Some flakes of saleeite visible.
27-37m	Fresh quartz-chlorite schist, with occasional pyrite and quartz veins/segregations. Some fracturing at 31-33m.
37-45m	Graphitic quartz-chlorite schist with quartz segregations and minor pyrite (hanging wall graphitic schist unit)
45-50m	Quartz-chlorite schist (ore zone, so possibly contains some uraninite).

- Drilling and Sampling

0.25.1m	Cable tool drilling; 0.25m of core every 1m beginning at 2.8m (sample nos. M2-3 to M2-25)
25.1-50m	Rotary percussion drilling; drill chips collected over 2m intervals beginning at 25.1-27m (sample nos. M2-26 to M2-48.5)

Casing set to 35m.

- *Water*

25m	5 litres/second, good quality
39m	3 litres/second, good quality

Hole M3

- *Geology*

0-3.8m	Surface sand and gravel, then weathered schist
3.8-15m	Weathered schist; clay with quartz grains and fragments embedded in it and defining the schistosity. Variable iron staining; complete in places. Fractures visible at 10m because they are lined with manganese and iron oxides.
15-25m	Partly weathered quartz-chlorite mica (sericite) schist with some quartz segregations and iron (and sometimes manganese) oxides along fractures.
25-27m	Fairly fresh quartz-chlorite mica (sericite) schist but still some goethite-stained grain and fracture surfaces (transitional zone).
27-40m	Fresh quartz-chlorite mica schist

- *Drilling and Sampling*

0-15.2m	Cable tool drilling; 0.25m of core every 1m beginning at 3.8m (sample nos. M3-4 to M3-15)
15.2-40m	Rotary percussion drilling; drill chips collected over 2m intervals beginning at 15.2-17m (sample nos. M3-16 to M3-38.5)

- *Water*

20.31m	3 litres/second, good quality

Hole M4

- *Geology*

0-4m	Surface sand and gravel, then weathered schist
4-24m	Weathered quartz-chlorite-mica (sericite) schist
24-28m	Almost fresh quartz-chlorite-mica (sericite) schist (transitional zone)
28-40m	Fresh quartz-chlorite-mica (sericite) schist

- *Drilling and Sampling*

0-40m	Rotary percussion drilling; drill chips collected over 2m intervals (sample nos. M4-2 to M4-39)

- *Water*

14m	Seepage, good quality
29.45m	5 litres/second, good quality

Hole M5

- Geology

0-2m	Surface sand
2-22m	Weathered quartz-chlorite-mica (sericite) schist; clay, quartz grains/fragments and mica flakes with variable amounts of iron oxides (goethite then hematite)
22-28m	Partially weathered to fairly fresh quartz-chlorite-mica (sericite) schist (transitional zone)
28-40m	Fresh quartz-chlorite-mica (sericite) schist

- Drilling and Sampling

0-40m	Rotary percussion drilling; drill chips collected over 2m intervals (samples nos. M5-1 to M5-39)

- Water

10.57m	3 litres/second, good quality

Hole W1

- Geology

0-3m	Surface sand, then weathered schist
3-24.1m	Weathered quartz-chlorite-mica (sericite) schist; bleached and decomposed to clay with quartz grains and segregations defining the schistosity, and variable amounts of goethite then hematite.

- Drilling and Sampling

0-24.1m	Cable tool drilling; 0.25m of core every 1m (sample nos. W1-3 to W1-24)

Hole W2

- Geology

0-3.1m	Surface sand, mixed with hematite-impregnated clay towards the bottom of the interval.
3.1-16.15m	Weathered and decomposed quartz-chlorite schist (goethite-stained clay with fine quartz grains). Heavily micaceous (sericite) at 14.0-14.2m.
16.15-25m	No samples recovered by drillers.

- Drilling and Sampling

0-16.15m	Cable tool drilling; 0.25m of core recovered every 1m beginning at 3m (sample nos. W2-3 to W2-16).
16.15-25m	Rotary percussion drilling; no drill chips collected by drillers.

Hole W3

- *Geology*

0-4m	Surface sand and ironstone fragments
4-16m	Weathered and decomposed quartz-chlorite mica schist
16-24m	Partially weathered quartz-chlorite mica schist
24-25m	Almost completely fresh quartz-chlorite mica schist

- *Drilling and Sampling*

0-25m	Rotary percussion drilling; drill chips collected over 2m intervals (sample nos. W3-1 to W3-11 and W3-17 to W3-21), but over 1m intervals in the water sampling zones (sample nos. W3-13 to W3-16 and W3-23 to W3-25)

- *Water*

14m	Seepage, good quality
24m	4 litres/second, good quality

Hole W4

- *Geology*

0-3.1m	Surface sand and gravel, then weathered schist
3.1-21m	Weathered and decomposed quartz-chlorite mica (sericite) schist; clay with quartz grains and segregations in part thoroughly impregnated by hematite. Saleeite (?) flakes in several cross-cutting fractures at 16.1-16.2m
21-25m	Partially weathered quartz-chlorite mica (sericite) schist; some saleeite (?) at 23-25m

- *Drilling and Sampling*

0-16.2m	Cable tool drilling; 0.25m of core every 1m (sample nos. W4-3 to W4-16)
16.2-25m	Rotary percussion drilling; drill chips collected over 2m intervals beginning at 16.2-19m (sample nos. W4-18 to W4-24)

- *Water*

17-25m	Seepage

Hole W5

- *Geology*

0-3.1m	Surface sand
3.1-12.1m	Weathered and decomposed quartz-chlorite-mica (muscovite) schist (variably goethite-stained and with occasional quartz segregations).
12.1-13.1m	Partially weathered quartz-chlorite-mica (muscovite) schist.
13.1-25m	No samples recovered by drillers.

- Drilling and Sampling

0-13.1m — Cable tool drilling; 0.25m of core recovered every 1m beginning at 3m (sample nos. W5-3 to W5-13).

13.1-25m — Rotary percussion drilling; no drill chips collected by drillers.

Hole W6

- Geology

0-25m — Kombolgie sandstone; iron-stained orthoquartzite

- Drilling and Sampling

0-25m — Rotary percussion drilling; samples were only collected at water sampling points; W6/13-15m and W6/23-25m

Hole W7

- Geology

0-4m — Surface sand; heavily impregnated with hematite towards the bottom of the interval.

4-15m — Weathered and decomposed quartz-chlorite-mica (muscovite) schist (variably goethite-stained and with occasional quartz segregations).

15-18.2m — Partially weathered quartz-chlorite-mica (muscovite) schist.

18.2-25m — No samples recovered by drillers.

- Drilling and Sampling

0-18.2m — Cable tool drilling; 0.25m of core recovered every 1m beginning at 3.9m (sample nos. W7-4 to W7-18).

18.2-25m — Rotary percussion drilling; no drill chips collected by drillers.

Hole C1

- Geology

0-4m — Surface sand and Kombolgie sandstone fragments

4-16m — Weathered and decomposed quartz-chlorite mica (sericite) schist; mainly goethite-stained clay with quartz grains and occasional sericite flakes.

16-20m — Partially weathered quartz-chlorite mica (sericite) schist; very little clay, mainly light grey schist with quartz segregations

20-26m — Almost fresh quartz-chlorite mica (sericite) schist with some goethite staining primarily along fractures and some quartz segregations (transitional zone)

26-29.5m — Fresh quartz-chlorite mica (sericite) schist

29.5-32m — Grey-white crystalline dolomite with minor chlorite

32-40m — Quartz-chlorite mica (sericite) schist; fairly uniform and fine-grained with a few thin dolomite layers

- *Drilling and Sampling*

0-40m Rotary percussion drilling; drill chips collected over 2m intervals (sample nos. C1-1 to C1-39)

- *Water*

3.8m Standing water level
10.37m Seepage, good quality

Hole C2

- *Geology*

0-4m Surface sand and Kombolgie sandstone fragments

4-20m Weathered and decomposed schist; clay with quartz grains and fragments increasingly stained by hematite

20-40m Fresh quartz-chlorite-sericite schist with some large quartz segregations and/or veins

- *Drilling and Sampling*

0-40m Rotary percussion drilling; drill chips collected over 2m intervals (sample nos. C2-1 to C2-39)

- *Water*

20m Seepage, good quality

Hole C3

- *Geology*

0-4m Surface sand and Kombolgie sandstone fragments

4-12m Weathered and decomposed schist; goethite-stained clay and quartz grains (and larger fragments from segregations), plus occasional mica flakes

12-20m Nearly fresh quartz-chlorite-mica schist, with only minor goethite along fracture surfaces

20-40m Fresh quartz-chlorite-mica schist with occasional quartz segregations and thin silicified dolomite (?) layers

- *Drilling and Sampling*

0-40m Rotary percussion drilling; drill chips collected over 2m intervals (sample nos. C3-1 to C3-39)

- *Water*

17m Seepage, good quality

Hole C4

- *Geology*

0-4m	Surface sand and Kombolgie sandstone fragments, then weathered schist
4-18m	Weathered and decomposed schist; both goethite and hematite staining clay with quartz grains and mica flakes defining the original schistosity
18-28m	Partially weathered to almost fresh quartz-chlorite-mica schist, with quartz segregations and goethite staining along fractures and schistosity planes
28-40m	Fresh quartz-chlorite-mica schist with quartz segregations

- *Drilling and Sampling*

0-40m	Rotary percussion drilling; drill chips collected over 2m intervals (sample nos. C4-1 to C4-39)

- *Water*

6.05m	Standing water level
18.75m	Seepage, good quality

Hole C5

- *Geology*

0-4m	Surface sand and Kombolgie sandstone fragments
4-10m	Weathered and decomposed schist; goethite and hematite stained clay with quartz grains and segregations
10-18m	Partially weathered quartz-chlorite schist
18-26m	Almost fresh quartz-chlorite schist with minor goethite along fractures (transitional zone)
26-40m	Fresh quartz-chlorite schist with only a few small quartz segregations

- *Drilling and Sampling*

0-40m	Rotary percussion drilling; drill chips collected over 2m intervals (sample nos. C5-1 to C5-39)

- *Water*

7m	Standing water level
17.3m	Seepage, good quality

Hole C6

- *Geology*

0-4m	Surface sand and Kombolgie sandstone fragments, then weathered schist
4-16m	Weathered and decomposed schist; hematite-stained clay with quartz grains and tiny sericite flakes
16-26m	Partially weathered to almost fresh quartz-mica-chlorite schist
26-40m	Fresh quartz-mica-chlorite schist; variable amounts of sericite and quartz

- *Drilling and Sampling*

0-40m Rotary percussion drilling; drill chips collected over 2m intervals (sample nos. C6-1 to C6-39)

- Water

6.45m Standing water level
10.57m Seepage, good quality
22m 2 litres/second, good quality

Hole C7

- Geology

0-4m Surface sand and Kombolgie sandstone fragments, then weathered schist.

4-18m Weathered and decomposed schist; clay with quartz grains and small fragments, progressively more stained by hematite.

18-22m Partially weathered quartz-mica-chlorite schist with quartz segregations

22-26m Almost fresh quartz-mica-chlorite schist with minor goethite staining along fractures

26-40m Fresh quartz-mica-chlorite schist; variable amounts of quartz and tiny sericite flakes, some pyrite grains and quartz segregations

- Drilling and Sampling

0-40m Rotary percussion drilling; drill chips collected over 2m intervals (sample nos. C7-1 to C7-39)

- Water

19.71m Seepage, good quality

Hole C8

- Geology

0-4m Surface sand

4-20m Weathered quartz-mica-chlorite schist; goethite and hematite staining and some impregnation; only minor clay, while quartz grains and muscovite flakes outline the original schistosity

20-26m Partially weathered to almost fresh quartz-muscovite-chlorite schist with some quartz segregations and goethite lining fractures (transitional zone).

26-40m Fresh quartz-muscovite-chlorite schist; dark green-grey colour with quartz segregations; muscovite content is high but chlorite predominates.

- Drilling and Sampling

0-40m Rotary percussion drilling; drill chips collected over 2m intervals (sample nos. C8-1 to C8-39)

- Water

15.14m Seepage, good quality

Hole C9

- *Geology*

0-4m	Surface sand and Kombolgie sandstone fragments, then weathered schist
4-22m	Weathered schist; bleached and goethite-stained clay with quartz grains, quartz segregations and mica flakes outlining the schistosity
22-26m	Partially weathered to almost fresh quartz-chlorite schist with minor goethite staining along fractures (transitional zone)
26-39.82m	Fresh quartz-chlorite schist with quartz veins and/or segregations and occasional pyrite.

- *Drilling and Sampling*

0-39.82m	Rotary percussion drilling; drill chips collected over 2m intervals (sample nos. C9-1 to C9-39)

Casing cemented in at 26m

- *Water*

19.5m	0.5 litres/second, good quality

Hole C10

- *Geology*

0-28m	Weathered Kombolgie sandstone; hematite-stained quartz grains and ferruginised sandstone with quartz veins becoming progressively decomposed with depth to bleached clay; hematite giving way to goethite to about 12m, then hematite gradually predominating again with depth.
28-40m	Kombolgie sandstone; ferruginous sandstone with minor quartz veins.

- *Drilling and Sampling*

0-40m	Rotary percussion drilling; drill chips collected over 2m intervals (sample nos. C10-1 to C10-39)

- *Water*

25.11m	Seepage, good quality